Aus der Klinik und Poliklinik für Innere Medizin A

(Kommisariche Leiterin OÄ Dr. Antje Steveling)

der Universitätsmedizin der Universität Greifswald

Role of DNA polymerase theta in the genesis of pancreatic ductal adenocarcinoma

Inaugural - Dissertation

zur

Erlangung des akademischen

Grades

Doktor der Wissenschaften in der Medizin
(Dr. rer. med.)

der
Universitätsmedizin
der
Universität Greifswald

2021

vorgelegt von:
Agnieszka Anna Smolinska
geb. am: 02.07.1989
in: Ciechanow, Poland

Dekan: Prof. Dr. med. Karlhans Endlich

1. Gutachter: Prof. Dr. Markus M. Lerch

2. Gutachter: Prof. Alexander Kleger

Ort, Raum: Greifswald, Seminar room, Department of Internal Medicine A

Tag der Disputation: 17.04.2023

- **To my beloved family** -

TABLE OF CONTENTS

Abbreviations

°C	Degree Celsius
µg	Microgram = 10^{-6} Gram
µl	Microliter = 10^{-6} Liter
3-MCA	3-methylcholanthrene
alt-EJ	Alternative end joining
ANOVA	Analysis of variance
BER	Base-excision repair
BLM	Bloom helicase
bp	Base pairs
BSA	Bovine serum albumin
cDNA	Complementary DNA
CIP	Calf Intestinal Alkaline Phosphatase
C-NHEJ	Canonical non-homologous end joining
COX-2	Cyclooxygenase-2
CSR	Class Switch Recombination
CtIP	CtBP Interacting Protein
DAB	3,3'-diaminobenzidine
DFS	Disease-free survival
D-loop	Displacement-loop
DMEM	Dulbecco's Modified Eagle Medium
DMSO	Dimethylsulfoxid
DNA	Deoxyribonucleic acid
DNA-PKcs	DNA-dependent protein kinase catalytic subunit
DSB	Double-strand break
dsDNA	Double-stranded DNA
EDTA	Ethylenediaminetetraacetic acid
EMT	Epithelial-mesenchymal transition
Exo1	Exonuclease 1
FACS	Fluorescence-activated cell sorting
FBS	Fetal bovine serum

FI	Fatty infiltration
GAPDH	Glyceraldehyde 3-phosphate dehydrogenase
GAPs	GTPase-activating proteins
gDNA	Genomic DNA
GDP	Guanosine diphosphate
GEFs	Guanine nucleotide exchange factors
GEMM	Genetically engineered mouse model
GFP	Green fluorescent protein
GSEA	Gene Set Enrichment Analysis
GTP	Guanosine-5'-triphosphate
H	Hours
H&E	Hematoxylin and eosin
HEPES	Hydroxyethyl piperazine N'-2-ethane sulfonic acid
HR	Homologous recombination
ICL	Interstrand DNA crosslink
IHC	Immunohistochemistry
IPA	Ingenuity Pathway Analysis
IPMN	Intraductal papillary mucinous neoplasms
IR	Ionizing radiation
KC	p48$^{+/Cre}$; LSL-Kras$^{G12D/+}$
KrasMT	KRAS mutant; G12D
KrasWT	KRAS wild-type
LIG3	DNA ligase 3
LIG4	DNA ligase 4
LigD	DNA Ligase IV homolog
MAPK	Mitogen-activated protein kinase
MCN	Mucinous cystic neoplasms
Min	Minutes
ml	Milliliter = 10^{-3} Liter
mm	Millimeter = 10^{-3} Meter
MMEJ	Microhomology-mediated end joining
mRNA	Messenger RNA

MT	Mutant
NHEJ	Non-homologous end joining
nm	Nanometer = 10-9 Meter
nt	Nucleotide
OS	Overall survival
PALB2	Partner and Localizer of BRCA2
PanIN	Pancreatic intraepithelial neoplasia
PARP1	Poly (ADP-ribose) polymerase 1
PBS	Phosphate buffer saline
PC	Pancreatic cancer
PCNA	Proliferating cell nuclear antigen
PCR	Polymerase chain reaction
PDAC	Pancreatic ductal adenocarcinoma
PI	Propidium iodide
PI3K	Phosphoinositide 3-kinase
PIKK	Phosphatidylinositol 3-kinase-related kinase
PNKP	Polynucleotide kinase 3' phosphatase
Polθ	DNA polymerase theta; PolQ
qKC	p48$^{+/Cre}$; LSL-Kras$^{G12D/+}$; Polq^{tm1Jcs}
qKO	Polq-deficient mice
qPCR	Quantitative PCR
RIN	RNA integrity number
RMA	Robust Multi-array Average
RNA	Ribonucleic acid
ROS	Reactive oxygen species
RPA	Replication protein A
rpm	Revolutions per minute
rRNA	Ribosomal RNA
RT	Room temperature
SD	Standard deviation
SDS	Sodium dodecyl sulfate
Sec	Seconds

SEM	Standard error of the mean
ssDNA	Single-stranded DNA
TBS	Tris buffered saline
TBST	Tris buffered saline Tween 20
TCGA	The Cancer Genome Atlas
TEMED	N,N,N',N'-Tetramethylethylenediamine
TGF-β	Transforming growth factor-beta
TLR	Traffic Light Reporter
TLS	Translesion synthesis
TRIS	Tris(hydroxymethyl)aminomethan
USFDA	United States Food and Drug Administration; FDA
UV	Ultraviolet light
V	Volt
WT	Wild-type
XLF	XRCC4-like factor; Cernunnos
XRCC4	X-ray repair cross-complementing protein 4
XRCC5	X-Ray Repair Cross Complementing 5
XRCC6	X-Ray Repair Cross Complementing 6

List of Figures

List of Tables

1. INTRODUCTION

1.1 Pancreatic cancer

Pancreatic cancer (PC) is one of the deadliest human malignancies in the world with an extremely poor prognosis that remains unchanged for many decades. The most common type of pancreatic cancer is pancreatic ductal adenocarcinoma (PDAC) which is predicted to be the second most common cause of death within the next 10 years, regardless of the age and gender [1-4]. According to the studies, individuals have a chance of about 1:64 to develop pancreatic cancer during their lifetime, and the 5-year overall survival is approximately 7% [1, 5]. The poor survival is attributed to high aggressiveness of this disease, intrinsic resistance to chemotherapy and lack of effective targeted therapies. However, the dismal prognosis is mainly caused by the late detection of the disease where usually is diagnosed at an advanced stage. It has been reported that more than 80% of patients diagnosed with pancreatic cancer had already locally advanced tumors and/or even metastases, due to the lack of specific symptoms and the presence of early markers for this disease [4, 6]. Moreover, genetic predisposition, obesity, comorbidities and lifestyle habits including smoking, alcohol consumption or poor diet have also influence the survival rates [7].

Despite the extensive molecular studies, diagnostic progress using high-resolution imaging such as endoscopic ultrasound with fine-needle aspiration biopsy (EUS-FNA), chemotherapeutic strategies using gemcitabine, gemcitabine plus nab-paclitaxel and FOLFIRINOX (folinic acid, 5-fluorouracil, irinotipecan, and oxaliplatin), there is still a lack of effective treatments for pancreatic cancer [8-10]. Even the surgical procedures that are considered the most effective and the only curative intervention are insufficient. Only 20% of patients diagnosed with PC are operable due to the stage of the disease, and up to 80% of these patients relapse [11]. Compared to other resected solid tumors, the worst results are observed usually in patients after pancreatic cancer resection [12]. Therefore, a better understanding of biological and molecular mechanisms driving initiation and development of pancreatic cancer is required.

1.1.1 Precursor lesions of PDAC

The development of pancreatic cancer is a stepwise process that arises from noninvasive, histologically distinct precursor lesions to invasive cancer. There are three major forms of noninvasive precursor lesions which include pancreatic intraepithelial neoplasia (PanIN), intraductal papillary mucinous neoplasms (IPMN) and mucinous cystic neoplasms (MCN) [13, 14]. PanINs are the most frequent and well-known PDAC precursors and, due to their nature, can be detected microscopically, while IPMN and MCN are macroscopic, clinically diagnosed as a cyst by radiological examination, and occur less common [15]. PanIN lesions initiate from the small, usually <5 mm, intralobular pancreatic ducts and are histologically subdivided into low-grade PanIN-1A and B, PanIN-2 and high-grade PanIN-3 referred to as carcinoma in situ [16, 17]. Clinical studies have been shown that PanIN with low-grade dysplasia is associated with a low risk of tumor progression and allows clinical observation. In contrast, high-grade dysplasia is associated with a high risk of progression to invasive cancer and requires surgical treatment [18-20].

Molecular studies of pancreatic cancer have indicated that tumor progression involves the activation of oncogenes, inactivation of tumor suppressor genes and deregulation of the cell cycle [21]. A comprehensive genome analysis of pancreatic cancer disclosed a high number of genetic aberrations, on average 63 in a single tumor affecting 12 core signaling pathways [22]. Waddell et al. reported even 119 genetic aberrations on average in a single tumor [23]. Moreover, the exome sequencing findings revealed that PanINs harbor the most frequent genomic alterations found in invasive PDAC [24-27].

The earliest alterations found in low-grade PanIN-1A lesions were associated with activating point mutations of the *KRAS* gene, occurring in over 90% of all pancreatic cancers, as well as with the presence of telomere shortening [27-30]. The oncogenic *KRAS* may not only drive pancreatic cancer precursor lesions, but is also essential for their progression and for the maintenance of invasive and metastatic disease [31]. Critical shortening of telomere can lead to progressive accumulation of additional chromosomal abnormalities and consequently to the development of invasive cancer [32].

Another early alteration associated with tumor progression is the inactivation of the tumor suppressor gene *CDKN2A* which occurs in PanIN-2 lesions. *CDKN2A* encodes protein p16

(INK4A) that plays a critical role in the cell cycle progression, differentiation, and apoptosis [33, 34]. Mutations of the *CDKN2A* gene lead to dysregulation of the cell cycle, contributing to carcinogenesis by increasing histological dysplasia [35, 36].

The other tumor suppressor genes that altered in PanIN lesions, including *TP53* and *SMAD4* have been found in the higher-grade PanINs. *TP53* is essential for DNA damage response and is commonly referred to as the "guardian of the genome" [37]. *SMAD4* gene encodes a protein involved in signal transduction of the transforming growth factor-beta (TGF-β) affecting cell differentiation, proliferation and apoptosis [38, 39]. According to the studies, these genetic alterations appeared after activated KRAS mutations and telomere sheltering supporting the hypothesis that PanINs are a precursor to invasive PDAC [19, 35, 40] (Figure 1).
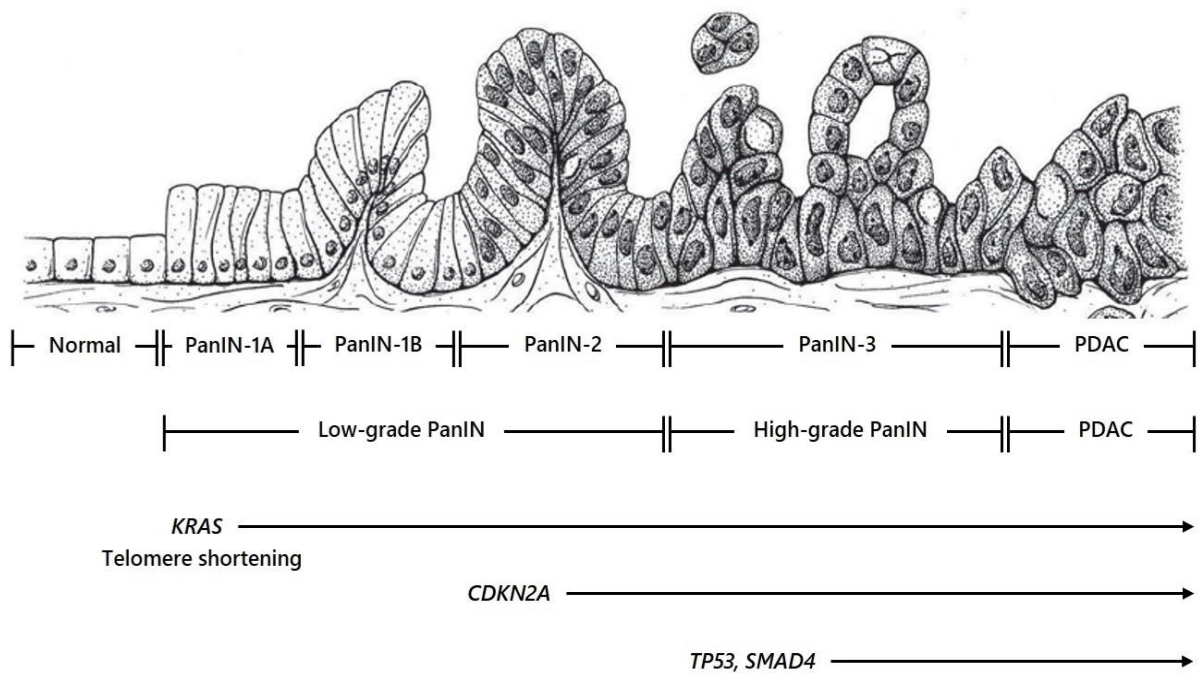
Figure 1. Genetic progression model of pancreatic ductal adenocarcinoma. Development from normal duct epithelium (left) to invasive carcinoma (right) have been shown. Adapted and modified from Maitra et al. [41].

1.1.2   Role of KRAS in pancreatic cancer

KRAS gene (Kirsten rat sarcoma viral oncogene homolog; Ki-ras 2) is a proto-oncogene that encodes a small GTPase transducer protein called KRAS belonging to the RAS family. KRAS acts as a molecular switch for various cellular processes by alternating between active GTP-bound and inactive GDP-bound states [42]. The activity of KRAS is regulated by guanine nucleotide exchange factors (GEFs) that stimulate nucleotide exchange, and by GTPase-activating proteins (GAPs) that accelerate the intrinsic GTP hydrolysis activity of KRAS [43, 44]. This switch mechanism plays an important role in enabling and disabling signals through KRAS because only active KRAS can bind to and trigger its downstream proteins [45]. Once the KRAS protein is bound to GTP, it interacts with more than 80 downstream effector proteins and signaling pathways such as mitogen-activated protein kinase (MAPK; also known as RAF-MEK-ERK), phosphoinositide 3-kinase (PI3K), and the Ral-GEF pathway, leading to cell survival, proliferation, migration, transformation, and cytokine secretion [44, 46] (Figure 2).
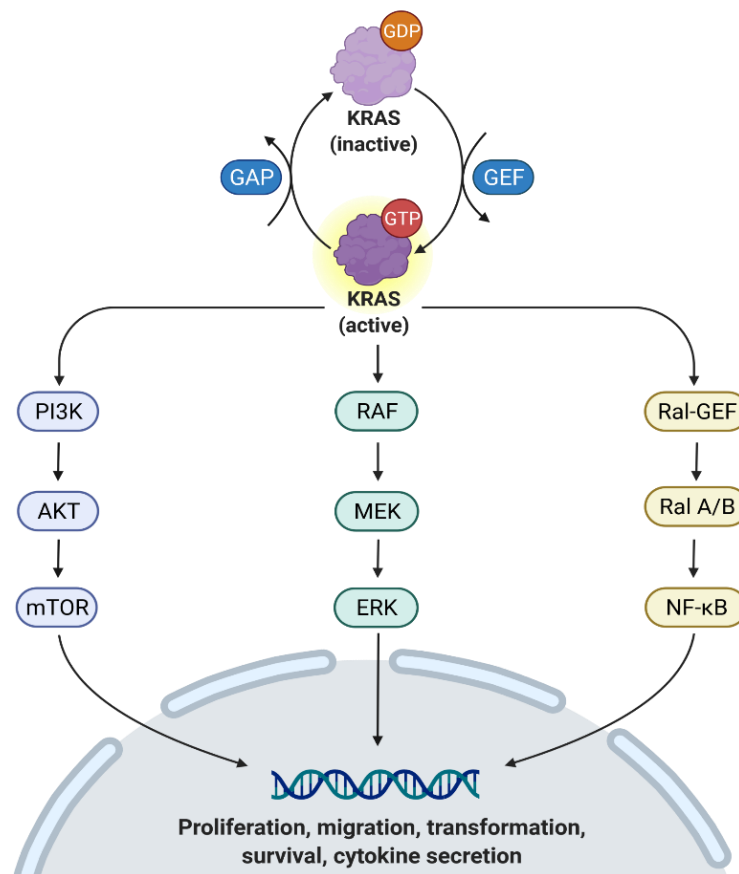
Figure 2. Activation of KRAS protein and its downstream intracellular pathways. The oncogenic KRAS activates intracellular PI3K, MAPK or Ral-GEF pathways to promote cell proliferation, migration, transformation, survival and cytokine secretion.

KRAS is one of the most frequently mutated oncogenes in human cancer, mostly in pancreatic (>90%), colorectal (40%) and lung (30%) cancers [47, 48]. Mutations in the *KRAS* gene are found mainly at codons G12, G13, or Q61 that are usually associated with its constitutively active state [49]. The most common mutation in PDAC is one amino-acid substitution in position 12 of the KRAS protein, leading to a glycine (G) to aspartic acid (D) substitution called G12D [31]. Next-generation sequencing analysis of 356 patients with resected PDAC revealed that patients with KRAS-mutant tumors had a worse disease-free survival (DFS) and overall survival (OS) than those who had KRAS wild-type tumors. Additionally, patients carrying the KRAS G12D mutation had particularly different outcomes and the worst DFS [50].

However, the acquisition of a single point mutation of the *KRAS* might not be sufficient to induce a malignant transformation. Numerous studies reported that KRAS mutations present in different organs, including pancreas, colon, and lungs are also frequently detected in healthy individuals [51-54]. As previously shown, KRAS-activating mutations can initiate PanIN formation, but to ultimately lead to carcinogenesis, the subsequent and combined inactivation of tumor suppressors (i.e., *CDK2NA*, *TP53*, and *SMAD4*) is also necessary [13, 44, 55]. Given that PDAC is likely initiated during adulthood by somatic mutations in the *KRAS* rather than during embryonic development, Guerra et al. demonstrated in a mouse model that adult pancreatic acinar cells are rather refractory to transformation by KRAS G12V mutation alone and no PanIN lesions or PDAC foci were observed [56]. Similarly, mice expressing oncogenic KRAS at endogenous levels showed that only a small fraction of the cells carrying the KRAS mutation were transformed [57]. These findings suggest that mutant KRAS alone may be insufficient to drive full-blown PDAC, and presence of additional genetic or environmental factors is necessary.

Apart from activating KRAS mutations involved in the development of many types of cancer, the association between wild-type and mutant KRAS also plays an important role in this process. Many studies have been shown that wild-type KRAS antagonizes oncogenic KRAS, leading to ineffective cell transformation and reduction of tumor burden in several malignancies. Thus, KRAS wild-type is considered as a tumor suppressor of KRAS-driven cancers [58-61]. However, this inhibitory effect is often overcome during tumor progression due to either loss of the wild-type KRAS allele or an increase in the copy number of the oncogenic form, leading to allele imbalance and the enhanced tumor [48, 62, 63]. Loss of the

wild-type KRAS allele has been observed in both human and mouse tumors [64]. Studies on the KrasG12D-driven mouse model of PDAC reported that loss of the wild-type KRAS allele has been associated with a higher incidence of metastasis [65]. Taken together, these observations suggest that the presence of the wild type KRAS allele in the presence of a mutant may have a significant effect on the efficiency of tumor development as well as on the function of KRAS downstream signaling pathway in various cancers types, including pancreatic ductal adenocarcinoma.

1.1.3 Mouse models of pancreatic ductal adenocarcinoma

A breakthrough in pancreatic cancer research was the development of genetically engineered mouse models (GEMMs) to better understand the PDAC carcinogenesis and molecular pathology of this disease. Over the years, numerous studies have established GEMMs by introducing specific mutations and inactivating different tumor suppressor genes. Since activating mutations in the *KRAS* gene are the most frequent in human pancreatic carcinoma, most of the GEMMs are based on oncogenic KRAS [66]. It has been shown that mouse models harboring KRAS mutation can mimic pancreatic tumorigenesis and oncogenic KRAS alone is sufficient to initiate PanIN [56, 67, 68]. Hingorani et al. demonstrated that the transgenic KrasG12D mouse model reproduces the full spectrum of human PanIN lesions in 100% of animals. However, progression to invasive pancreatic cancer in these animals occurs sporadically (10 to 20% of animals) and was usually seen in older animals [44, 67]. On the other hand, GEMM models that combine an oncogenic KRAS mutation with conditional loss of one or more tumor suppressor genes such as *TP53*, *CDKN2A* and *SMAD4* accelerate pancreatic tumor progression, often leading to metastasis [55, 68-71]. While ductal cells in the presence of oncogenic KRAS and TP53 deletions are more prone to form carcinoma in situ, acinar cells with the same mutational landscape require a prolonged period of transition or reprogramming to initiate PDAC [44, 72]. These findings confirm the essential role of the KRAS proto-oncogene in both pancreatic cancer initiation and progression. Furthermore, these mouse models can be also used to investigate the role of the signaling pathway and microenvironment in pancreatic cancer, as well as cofactors, such as inflammation [44, 56, 73].

1.2 Genome instability

The increased tendency of genomic changes and mutations associated with abnormal cell proliferation contributes to the damage of multiple genes regulating cell division or involved in repairing damaged DNA, as well as the formation of chromosome abnormalities. This process is known as genomic instability. The accumulation of genetic changes, from single nucleotide mutations to chromosome rearrangements, can predispose cells to malignancy [74]. Thus, genomic instability is believed to be a characteristic of most cancers and plays a pivotal role in both tumor initiation and progression [75]. Moreover, sustained genome instability enables cancer cells to survive under selective pressure and adapt to their microenvironments by evolving mechanisms that resist different types of therapies [74, 76].

1.2.1 DNA double-strand breaks

The maintenance of genome stability is crucial for cellular integrity to prevent endogenous and exogenous damage such as replication errors, reactive oxygen species (ROS), ionizing radiation (IR), ultraviolet light (UV), viruses, and chemical agents (e.g. nitrogen mustard, acrylamide) [77]. As a result of the above-mentioned DNA damage, one of the most dangerous is a double-strand break (DSB). Many of DSBs also arise from the collapse of the replication forks when they encounter DNA damage [78].

DNA double-strand breaks are generated when two complementary strands of the DNA double helix are broken simultaneously at a short distance (~10 base pairs, bp) that base-pairing and chromatin structure are insufficient to keep the two DNA ends juxtaposed. Consequently, these two DNA ends generated by a DSB are prone to physical dissociation from each other, making repair difficult and providing the opportunity for inappropriate recombination with other sites in the genome [79]. It has been estimated that DSBs are rarely formed, with estimates ranging from 10-50 DSBs per cell each day under normal conditions [80-82]. DSBs can result both in small local changes in the DNA sequence (e.g. gene mutations) and chromosomal rearrangements. Due to the severity of such damage, even a single unrepaired DSB can lead to cell death or cancer development [83, 84].

Although DNA DSBs pose a serious threat to genome integrity, several developmental and physiological processes require the generation of programmed site-specific DSBs. In mammals, through the VDJ recombination process, DSBs are generated at specific loci by

a site-specific endonuclease composed of the RAG1 and RAG2 proteins for assembling immunoglobulin antigen receptor genes, as well as T-cell receptor genes. DSBs also arise during immunoglobulin class switching [79, 85-87].

Moreover, DNA double strand breaks can be induced artificially using highly site-specific nucleases such as CRISPR/Cas9 to trigger the desired repair results. Thus, the engineered DNA cleavage and repair could be used as a potential therapeutic approach to repair mutations that cause disease.

Regardless of what causes the DSBs, the inability to repair these critical and dangerous types of DNA damage can have fatal consequences for cells. Thus, to maintain genome integrity and cell viability effective and immediate repair of DNA DSBs is required.

1.2.2   DNA double-strand break repair pathways

To ensure genome stability, cell homeostasis and prevent cancer formation, cells evolved various surveillance systems and DNA repair mechanisms. In mammalian cells, DNA double-strand breaks (DSBs) can be repaired by three main pathways: homologous recombination (HR), canonical (or classical) non-homologous end joining (c-NHEJ) and alternative end joining (alt-EJ), also known as alternative non-homologous end-joining (alt-NHEJ) or microhomology-mediated end joining (MMEJ) [88-90].

The pathway chosen for DSB repair is determined by several factors, including DSB complexity, cell cycle stage, and the extent of DNA end processing.

DSBs are mainly repaired by c-NHEJ pathway which religates the two broken DNA ends with little or no sequence homology and without extensive processing, frequently introducing small insertions and deletions at the repair junction [90, 91]. C-NHEJ operates throughout the cell cycle, but its activity is predominant in G1. Unlike c-NHEJ, HR takes place in S and G2 phases of the cell cycle and employs sister chromatid as a template to promote high fidelity and error-free repair. In addition, HR requires DNA resection, where nucleolytic degradation of a DSB generates a 3' single-stranded DNA (ssDNA) overhang [92-94]. Finally, alt-EJ is a mutagenic mechanism that is most active during the S and G2 phases of the cell cycle and is associated with the presence of HR- and c-NHEJ-independent proteins [95-99]. DSB repair via alt-EJ is driven by the annealing of microhomologous sequences (5-25 bp) flanking the DNA

ends which always results in large deletions and other sequence alterations at the junctions [92, 95]. Importantly, a limited DNA end resection is required to initiate alt-EJ, which is sufficient to expose the microhomological region close to the break site. The initial end resection step in alt-EJ is shared with HR [92, 100, 101]. While alt-EJ was initially considered as a backup DNA repair pathway, recent studies have shown that alt-EJ also functions in the presence of c-NHEJ and HR, which confirms that it may be the only available repair pathway for specific types of DNA damage [90, 92, 95, 102-105] (Figure 3).
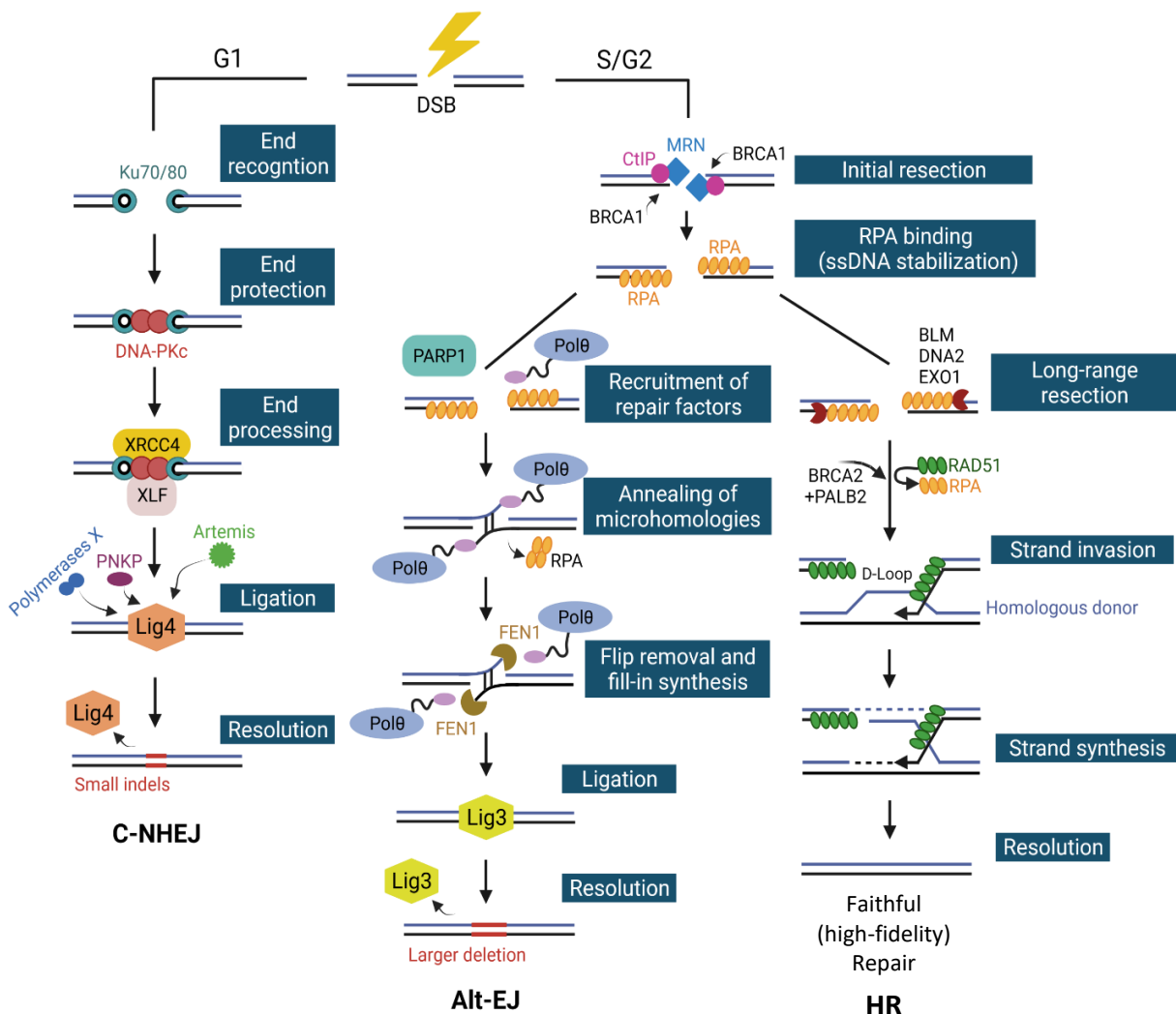
Figure 3. Major DNA double-strand break repair pathways. Canonical non-homologous end joining (C-NHEJ), homologous recombination (HR) and alternative end joining (alt-EJ) determinated by cell cycle are described.

1.2.3 Canonical non-homologous end joining

The canonical non-homologous end joining (c-NHEJ) pathway is initiated by binding Ku70/80, also known as XRCC6/XRCC5 heterodimer to DSB ends, followed by recruitment of the DNA-dependent protein kinase catalytic subunit (DNA-PKcs). The binding of the Ku heterodimer is essential to protect broken ends from extensive resection and inhibit their degradation [106]. The DNA-PKcs is a nuclear serine/threonine kinase that belongs to the phosphatidylinositol 3-kinase-related kinase (PIKK) family [107]. This large kinase, together with the Ku heterodimer, forms a DNA-PK complex that bridges and aligns broken ends of the DSB. In addition, the DNA-PK complex stimulates the DNA-PKcs catalytic activity and phosphorylates numerous c-NHEJ downstream factors such as X-ray repair cross-complementing protein 4 (XRCC4) and XLF (also called Cernunnos) to promote end joining by DNA Ligase 4 (Lig4) [92, 108, 109]. Interestingly, DNA-PKcs has been only identified in eukaryotic cells [110, 111]. In prokaryotes, c-NHEJ requires only a Ku homodimer in a complex with DNA Ligase IV homolog (LigD) [112, 113]. If the ends of DSB are not compatible for ligation, c-NHEJ employs additional end-processing enzymes, including nuclease Artemis, polynucleotide kinase 3' phosphatase (PNKP) and two family X polymerases, Pol λ and Pol μ that are necessary for joining chemically incompatible ends [92, 114, 115]. Finally, the ligation of the broken DNA ends is executed by Ligase 4 [116] (Figure 3). Despite the incredible flexibility of end processing and ligation, the repair of DNA DSBs via the c-NHEJ pathway is error-prone and results in the appearance of small indels or chromosomal translocations [117]. Nevertheless, c-NHEJ is generally considered essential for the maintenance of genomic stability [118, 119].

1.2.4 Homologous recombination

Homologous recombination (HR) is considered the most accurate and error-free pathway for DSB repair. It plays a crucial role for organismal development and is also the most frequently used pathway for DSB repair in Saccharomyces cerevisiae [78, 120, 121]. HR is activated by the 5' to 3' resection of the 5' DNA strand on the DSB ends, leaving a 3' ssDNA overhang [92]. In mammals, DNA end resection is a two-step process, where the initial phase involves the Mre11-Rad50-Nbs1 (MRN) complex, CtIP (CtBP Interacting Protein) and BRCA1 [122-124]. In this process the MRN complex recognizes and binds to the broken DNA ends, followed by

nicking of the dsDNA and 3'-5' degradation towards the break termini by endo- and exonuclease activity of Mre11 [125-127]. Additionally, CtIP is recruited to the MRN complex through Nbs1 protein, leading to an increase in Mre11 nuclease activity [108, 128, 129]. Finally, BRCA1 promotes the resection process by directly interacting with the resection factor CtIP [130, 131]. This initial processing results in relatively short 3' ssDNA overhangs (~20 nt) which are immediately coated by the (ssDNA-binding) replication protein A (RPA) [132]. Binding of RPA to ssDNA tail prevents secondary structure formation and protects them from degradation. [133]. In vitro studies have also implicated that RPA is important for promoting long-range resection by stimulating both Exo1- and Dna2-dependent pathways [134-136].

In the second step of end resection known as extensive, extended or long-range, other more processive nucleases such as Dna2 and Exonuclease 1 (Exo1) in conjunction with Bloom helicase (BLM) are recruited to form long 3' ssDNA tails [132, 137, 138]. Subsequently, RPA is exchanged for Rad51 recombinase through the action of BRCA2 and PALB2 (Partner And Localizer Of BRCA2) which bind Rad51 monomers and destabilize RPA affinity for ssDNA respectively. This exchange allows Rad51 to properly bind and nucleate a protein-DNA filament along resected 3' ends [92, 139-142]. The Rad51-coated nucleofilament performs strand invasion and homology search on the sister chromatid, leading to displacement-loop (D-loop) formation [142]. Ultimately, the invading 3'-end primes DNA synthesis which fills in the gaps and repair is completed with minimal alterations to the original sequence [92, 142] (Figure 3).

1.2.5   Alternative end joining

While c-NHEJ and HR are well characterized DSB repair pathways, alternative end joining (alt-EJ) is poorly studied. The existence of the alt-EJ pathway was first demonstrated in early studies of *S. cerevisiae* where inactivation of c-NHEJ caused cells to use an error-prone and microhomology-dependent alternative end joining pathway [143]. Alt-EJ activity has been also detected in bacteria, flies, worms, plants, and fish [104, 144-148]. In mammals, alt-EJ was found from the analysis of Class Switch Recombination (CSR) in c-NHEJ-deficient B cells [149]. Although alternative end-joining was initially viewed as a back-up canonical repair pathway, further research has shown that alt-EJ operates even when c-NHEJ and HR are proficient. For instance, alt-EJ has been found to be essential for DSB repair in developing zebrafish embryos or during V(D)J recombination in c-NHEJ-proficient B cells that carry mutations in the RAG

recombination genes [104, 105]. Additionally, most of the chromosomal translocations and rearrangements that occur during DSB repair are catalyzed by alt-EJ.

The alternative end joining begins with DNA end resection mediated by MRN-CtIP complex which is shared with homologous recombination. This step exposes a relatively small single-strand microhomologous sequences (~20 nt) on either side of the DSB and allows for further sequence alignment [132]. Reliance on microhomology at the breakpoint is a hallmark of alt-EJ and therefore the term microhomology-mediated end joining (MMEJ) is often used synonymously with alt-EJ. Subsequently, poly(ADP-ribose) polymerase 1 (PARP1) both facilitates microhomology annealing and mediates the recruitment of DNA polymerase theta (Polθ) which displaces RPA to promote DSB synapsis [150-152]. Following the synapsis, the single-strand gaps flanking the annealed microhomology are filled by the low-fidelity polymerase Polθ, which stabilizes the annealed intermediates. Finally, DNA Ligase 3 (Lig3) seals the remaining nicks to complete repair of DSB [152, 153]. The annealing process can also be driven by internal microhomologies that lead to ssDNA flaps formation, which then have to be removed before fill-in synthesis by Polθ and ligation. In this case, FEN1 endonuclease recognizes and cleaves these 5' ssDNA flaps [154-156] (Figure 3).

Obviously, after alt-EJ-mediated repair large deletions or more serious genomic alterations such as inversions and translocations often occur at the breakpoints [95]. Due to inappropriate repair, alt-EJ may also promote tumorigenesis by increasing genomic instability. Thus, it is important to discover all protein factors or specific enzymes that only function in the alt-EJ repair pathway, to better understand the alt-EJ mechanism and its unique role both in DSB repair and cancer development.

1.2.6 DNA polymerase theta

DNA polymerase theta (Polθ) also known as PolQ is encoded by the *POLQ* gene and belongs to the A-family DNA polymerases. In contrast to other eukaryotic polymerases, Polθ contains both C-terminal polymerase domain and N-terminal helicase-like domain which are linked by a long unstructured central region [88, 156, 157]. Coordinated interaction between all domains is necessary to enable the implementation of Polθ activities [90].

The polymerase domain exhibits highly promiscuous enzyme activity. For instance, it is responsible for DNA synthesis using its terminal transferase or templated extension activity

[90]. This domain is also fundamental for the Polθ functions in alt-EJ. In vitro studies implicated that Polθ polymerase domain can join DNA ends using microhomology and mediate the alignment of internal and terminal microhomologous sequences [151, 158]. In addition, it is essential for interstrand DNA crosslink (ICL) repair [151, 159]. On the other hand, the Polθ helicase domain contains both DNA-dependent ATPase and DNA unwinding activity which can act independently of each other [90, 91]. This domain uses its ATPase activity to promote alt-EJ and restrict HR by removing RPA from resected DNA ends and subsequent strand annealing [92, 160]. Moreover, it has been shown that inhibition of Polθ helicase leading to reduced microhomology at repair junctions and impaired chromosomal translocation [92, 146, 160]. Finally, the central region of the polymerase theta contains three predicted RAD51 binding motifs which are involved in HR suppression by inhibiting the formation of RAD51 nucleofilament [92]. Furthermore, it plays an important role in the regulation of Polθ substrate selection [90].

DNA polymerase theta was first identified in Drosophila melanogaster through the analysis of mus308 mutants that displayed hypersensitivity to a variety of interstrand crosslinks inducing agents (e.g. nitrogen mustard) [92, 161, 162]. Other studies in flies indicated that Polθ activity was linked to alt-EJ during the repair of DSBs induced by P-element transposition [146]. Since then, the role of Polθ in alt-EJ has been demonstrated in several multicellular organisms, including worms, fish, plants, and mammals [92]. In mammalian cells, Polθ stimulates alt-EJ in response to endonuclease-mediated cleavage of reporter constructs, drives the fusion of dysfunctional telomeres, and promotes chromosomal translocations [160, 163, 164]. Other studies have shown that inhibition of Polθ sensitizes cells to DSB inducers such as topoisomerase inhibitors and radiation [165, 166]. Moreover, the knockout of Polθ suppresses alt-EJ in mammalian cells [151, 167]. Notably, the alt-EJ activity driven by Polθ also found to be essential during the random integration of foreign DNA into the host genomes in both plants and mammals [92, 148, 168, 169]. In addition to its role in alt-EJ, polymerase theta has also been implicated in translesion synthesis (TLS), base-excision repair (BER), and replication repair [92]. Overall, due to its ability to promote alternative end joining, polymerase theta plays a key role in DNA repair and may have a major impact on genome stability in a variety of biological contexts associated with DNA double-strand breaks.

1.2.7 DNA polymerase theta and cancer

Expression of polymerase theta is generally repressed in somatic cells but is significantly upregulated in several types of cancers, including ovarian, breast, lung, stomach, pancreas, and colon cancers [170-172]. High levels of Polθ especially in breast, and lung cancers are linked to poor prognosis and shorter relapse-free survival of patients [172, 173]. The upregulation of Polθ is also associated with the HR genes depletion [164]. Comprehensive analysis of the cancer genomes has revealed that Polθ-mediated repair translates into a specific mutational signature which is increased in frequency in HR-deficient breast, ovarian, and pancreatic cancers [174, 175]. Thus, it appears that cancer cells lacking the HR pathway use Polθ-dependent repair as a compensatory mechanism to maintain genome stability and for survival. Interestingly, Ceccaldi et al. reported that knockdown of polymerase theta in HR-deficient cells leading to cell death, which demonstrates a synthetic lethal relationship between Polθ and HR factors [164]. Synthetic lethality has been also observed in cells deficient in c-NHEJ, where depletion of Polθ reduces cell survival [167]. In contrast, loss of Polθ does not affect embryonic viability, development, and growth in normal cells, indicating that Polθ is not essential for the survival of healthy cells [176].

Since polymerase theta activity plays a critical role in HR- and c-NHEJ-deficient cells, inhibition of Polθ can be a promising cancer treatment strategy. To date, HR-deficient cancers, due to the BRCA1/2 mutation, have been shown to be very sensitive to PARP inhibitors, which promote replication-dependent DSBs and suppress alt-EJ repair pathway [155, 164, 177, 178]. Thus, PARP inhibitors including olaparib and rucaparib have been approved by The United States Food and Drug Administration (USFDA or FDA) for the treatment of BRCA-deficient breast and ovarian cancer patients [178].

As BRCA-deficient breast and ovarian cancer is very sensitive to PARP inhibitors, it is necessary to find further biomarkers for HR deficient tumors [179]. Additionally, cellular resistance to PARP inhibitors is becoming a major clinical problem, and therefore ongoing identification and development of alternative drug targets for BRCA-deficient tumors are required [155, 180]. Beyond HR-deficient cancers, there are cancers with competent HR repair that also require effective treatment. Recent reports have shown that combined inhibition of DNA-PK, a key component of the c-NHEJ pathway, and Polθ restores therapeutic DNA damage sensitivity in p53-deficient cells [181]. These findings reveal the high potential of polymerase theta as a new

therapeutic candidate for the treatment of HR-deficient and other cancers and highlight the need for a complete understanding of Polθ and its contribution to the alt-EJ repair pathway.

2. OBJECTIVES

The occurrence of oncogenic KRAS mutations is a signature event in pancreatic ductal adenocarcinoma (PDAC) leading to genomic instability. The mechanism of genomic instability mediated by KRAS is still poorly understood, and the role of DNA repair in this process has not been fully investigated in pancreatic cancer. Thus, a better understanding of error-prone alt-EJ and its contribution to pancreatic tumorigenesis may reveal new diagnostic and therapeutic pathways in the treatment of the deadliest cancers. This study addressed the following objectives:

1. To estimate the interaction between (abberant) alt-EJ activation and genomic instability mediated by oncogenic KRAS.
2. To investigate the influence of oncogenic KRAS on the activity of alt-EJ repair pathway.
3. To determine the effect of alt-EJ inactivation on the development of premalignant PanIN lesions mediated by oncogenic KRAS and their malignant transformation to pancreatic cancer.

3. MATERIAL AND METHODS

3.1 Materials

3.1.1 Chemicals, reagents and buffers

Acetic acid	Fluka, Switzerland
Acetone	Roth, Germany
Acid-Phenol: $CHCl_3$	Thermo Fisher, USA
Agar	Roth, Germany
Agarose	Roth, Germany
Alkaline Phosphatase, Calf Intestinal (CIP)	New England Biolabs, UK
Ammonium peroxydisulphate	Roth, Germany
AMPure XP for PCR Purification	Beckman Coulter, USA
ATP solution	Illumina, USA
Aurion BSA-c^{TM} (10%)	Aurion, Netherlands
Bovine Serum Albumin	PAN-Biotech, Germany
Bradford Reagent	Sigma-Aldrich, Germany
Bromophenol Blue	Merck, Germany
Calcium chloride	Merck, Germany
Chloroform	Roth, Germany
Crystal violet	Roth, Germany
DEPC-Treated Water	Thermo Fisher, USA
DNA Gel Loading Dye (6X)	Thermo Fisher, USA
dNTP Mix	PAN-Biotech, Germany
Eosin Y solution	Sigma-Aldrich, Germany
Ethanol absolute	Th. Geyer, Germany
Ethidium bromide solution 0.025 %	Roth, Germany
Ethylenediaminetetraacetic acid	Th. Geyer, Germany
Formaldehyde solution 4.5%	Fischar, Germany
Gelatine	Roth, Germany
GeneRuler Low Range DNA Ladder	Thermo Fisher, USA
GeneRulerDNA Ladder Mix	Thermo Fisher, USA
Glycerol 86%	Roth, Germany

Hematoxylin Solution, Mayer's	Sigma-Aldrich, Germany
HEPES	Sigma-Aldrich, Germany
Hexadimethrine bromide	Sigma-Aldrich, Germany
Hydrogen peroxide 30%	Merck, Germany
Isopropanol	Sigma Aldrich, Germany
Magnesium chloride	Sigma-Aldrich, Germany
Methanol	J.T. Baker, Netherlands
Millipore water	in-house
Nonfat Dry Milk	Cell Signaling Technology, USA
Nuclease-Free Water	Thermo Fisher, USA
PageRuler^{TM} Plus Prestained Protein Ladder	Thermo Fisher, USA
PageRuler™ Prestained Protein Ladder	Thermo Fisher, USA
PCR Master Mix	Thermo Fisher, USA
PI/RNase Staining Buffer	BD Bioscence, USA
Pierce^{TM} RIPA Buffer	Thermo Fisher, USA
Ponceau S	Roth, Germany
Potassium chloride	Merck, Germany
Potassium dihydrogen phosphate	Merck, Germany
Protease inhibitor cocktail tablets	Roche, Germany
Puromycin	Sigma Aldrich, Germany
Q5® High-Fidelity DNA Polymerase	New England Biolabs, UK
Restriction Endonucleases	New England Biolabs, UK
RiboGuard™ RNase Inhibitor	Illumina, USA
RNAlater™ Stabilization Solution	Thermo Fisher, USA
Rotiphorese® Gel 30 (37.5:1)	Roth, Gemany
Sodium acetate	Merck, Germany
Sodium chloride	Roth, Germany
Sodium dodecyl sulfate	Sigma-Aldrich, Germany
Sodium phosphate dibasic	Merck, Germany
Sodium pyruvate	Sigma-Aldrich, Germany
SuperSignal™ West Femto Max Sensitivity Substrate	Thermo Fisher, USA
SuperSignal™ West Pico PLUS Chem. Substrate	Thermo Fisher, USA

SYBR® Select Master Mix	Thermo Fisher, USA
T4 DNA Ligase Buffer (10X)	Thermo Fisher, USA
T4 DNA Ligase	Thermo Fisher, USA
Taq DNA-Polymerase with buffer and $MgCl_2$	PAN-Biotech, Germany
Target Retrieval Solution (10x)	Dako, USA
TEMED	Sigma-Aldrich, Germany
Thiazolyl Blue Tetrazolium Bromide	Sigma-Aldrich, Germany
Tissue Freezing Medium	TBS Lab Products, USA
TriPure Isolation Reagent	Roche, Germany
TRIS	Roth, Germany
Triton X-100	Sigma-Aldrich, Germany
TRIzol Reagent	Thermo Fisher, USA
Trypan Blue	Roth, Germany
Tryptone/Peptone	Roth, Germany
Tween 20	Sigma-Aldrich, Germany
VectaMount® Permanent Mounting Medium	Vector laboratories, USA
Water, HPLC Gradient Grade	J.T. Baker, Netherlands
Xylene	Roth, Germany
Yeast Extract	Roth, Germany
β-Mercaptoethanol	Sigma-Aldrich, Germany

Western Blot:

<u>Laemmli Buffer (4x), pH 6.8</u>

125mM Tris-HCl, pH 6.8

2% SDS

10% Glycerol

0.5ml β-Mercaptoethanol

0.01% Bromophenol Blue

in distilled water

<u>Running Buffer/Tris-Glycine-SDS (10x)</u>

250mM Tris

1.92M Glycine

1% SDS

in distilled water

Towbin Transfer Buffer (10x), pH 6.8

25mM Tris

192mM Glycine

10% SDS

20% Methanol

in distilled water

Washing Buffer/TBST (10x)

165.9mM Tris-HCl

44.5mM Tris

1.5M NaCl

0.5% Tween 20

in distilled water

Ponceau S staining solution

0.5% (w/v) Ponceau S

3% Acetic acid

Stripping Buffer, pH 3.0

15g Glycine

1g SDS

10 ml Tween 20

Blocking Buffer

5% milk

in TBST (1x)

Immunocytochemistry:

Phosphate Buffer Saline (PBS), pH 7.4

137mM NaCl

2.7 mM KCl

1.5 mM KH_2PO_4

8.1 mM Na_2HPO_4

in distilled water

Primary Antibody Dilution Buffer

1% Aurion BSA

0.05% Tween 20

0.01% EDTA (0.5M, pH 8.0)

in PBS

Blocking Buffer

1% Aurion BSA

0.05% Tween 20

in PBS

3.1.2 Kits

Agencourt CleanSEQ Kit	Beckman Coulter, USA
Alcian Blue (pH 2.5) Stain Kit	Vector Laboratories, USA
BigDye™ Terminator v3.1 Cycle Sequencing Kit	Thermo Fisher, USA
CalPhos^TM Mammalian Transfection Kit	Takara Bio, Japan
DAB Substrate Peroxidase (HRP) Kit	Vector Laboratories, USA
GeneChip™ Human Gene 2.0 ST Assay	Thermo Fisher, USA
GeneChip™ Hybridization, Wash, and Stain Kit	Thermo Fisher, USA
GeneChip™ Mouse Gene 2.0 ST Assay	Thermo Fisher, USA
GeneChip™ WT PLUS Reagent Kit	Thermo Fisher, USA
Jetstar 2.0 Plasmid Maxiprep Kit	Genomed, Germany
KAPA Mouse Genotyping Kit	Peqlab, Germany
MMLV High Performance Reverse Transcriptase Kit	Illumina, USA
PEG Virus Precipitation Kit	BioVision, USA
PureLink™ Genomic DNA Mini Kit	Thermo Fisher, USA
PureLink™ HiPure Plasmid Maxiprep Kit	Thermo fisher, USA
QIAprep Spin Miniprep Kit	Qiagen, Germany
QIAquick Gel Extraction Kit	Qiagen, Germany
QIAquick PCR Purification Kit	Qiagen, Germany
RNA Clean-Up and Concentration Micro Kit	Norgen Biotek, Canada
RNeasy Mini Kit	Qiagen, Germany

3.1.3 Primers

Table 1. Primers used for genotyping.

Name	Sequence 5' → 3'
Polq wild type	F: TGCAGTGTACAGATGTTACTTTT
	R: TGGAGGTAGCATTTCTTCTC
Polq mutant	F: TCACTAGGTTGGGGTTCTC
	R: CATCAGAAGCTGACTCTAGAG
P48cre	F: GTCCAATTTACTGACCGTACACCAA
	R: CCTCGAAGGCGTCGTTGATGGACTGCA
KrasM	F: AGCTAGCCACCATGGCTTGAGTAAGTCTGCA
	R: CCTTTACAAGCGCACGCAGACTGTAGA

Table 2. Primers used for sequencing.

Name	Sequence 5' → 3'
KRAS mouse-S	TGACTGAGTATAAACTTGTGGTGG
KRAS mouse-AS	CCCAGTTCTCATGTACTGGTC
KRAS human-S	AGAACAGCAGTCTGGCTATTTAG
KRAS human-AS	TGGTCCTGCACCAGTAATATGC
Trp53 human-S	TGGGCTTCTTGCATTCTGGGA
Trp53 human-AS	ATAGGGCACCACCACACTATG
Trp53 mouse-S	AAACTTACCAGGGCAACTATGGC
Trp53 mouse-AS	AAAGTCTGCCTGTCTTCCAG
pLVX-DsRed-MonomerC1-F	ACACCGTGGTGGAGCAGTAC
pLVX-DsRed-MonomerC1-R	AGACTGCCTTGGGAAAAGC

Table 3. Primers used for PCR.

Name	Sequence 5' → 3'
Kras G12D human-F	AGTTAGCGCTCCATGACTGAATATAAACTTGTGGTAGTTGGA GCTGATGGCGTAGGCAAGAGTGCCTTGACG
Kras WT-AfeI mouse-F	AGTTAGCGCTCCATGACTGAGTATAAACTTGTGGTGGTTG
Kras WT-EcoRI mouse-R	GCGAATTCTCACATAACTGTACACCTTGTCCTT

Table 4. Primers used for qPCR.

Name	Sequence 5' → 3'
5S human/mouse-F	GCCCGATCTCGTCTGATCTC
5S human/mouse-R	GCCTACAGCACCCGGTATTC
Ku70 human-F	ACTGCAACACTTGAAGTCAAATCAAAG
Ku70 human-R	GATTTTCAACTCAGGAGGCAGTTC
Ku70 mouse-F	GGCCCTCTCTGTTCGTGTACC
Ku70 mouse-R	CCTCCTTCTCCACACACTTGGT
Ku80 human-F	GCTGGAGGACATTGAAAGCAA
Ku80 human-R	GCATCCAGGAAGTCAGCCTG

Ku80 mouse-F	AAGGGTACCGCTACGGAAGTG
Ku80 mouse-R	ACAGAGAAGCACTTCCCCTCAG
LIG4 human-F	CTT GCG TTT TCC ACG AAT TGA
LIG4 human-R	TCC AGG GTC ATG CAC TCA TG
LIG4 mouse-F	AGGAAGGCTCTCTCACCCCA
LIG4 mouse-R	CAAACTTGACCCCCTTCTGC
LIG3 human-F	GAGCCCCACCCCTAAGAGAAG
LIG3 human-R	CGAAACTCCCGTAGCAGACAG
LIG3 mouse-F	GCC GAG AAG GCA GCT ATA TG
LIG3 mouse-R	CAA GGG CAC AAA GGT TTC TC
MRE11 human-F	AACAGTACTTTCAAACCGCAGAGA
MRE11 human-R	CCCATCCCTCTTTCTGTTAGCA
MRE11 mouse-F	TGTTGAGACCAAAGGAAGATGAGA
MRE11 mouse-R	CCCAGATAACGAGGTCGATGA
PARP1 human-F	CCCAGGGTCTTCGGATAGC
PARP1 human-R	CCATGTCAGCGAAATAGATCCC
PARP1 mouse-F	GCAGCCGTTGATCCTGACTC
PARP1 mouse-R	ACAATGTCCACCAGGCCAAG
POLQ human-F	CGGAAATCAGCATCTTGTCAGG
POLQ human-R	ACTCATGCCAACGATTTGCAC
POLQ mouse-F	AAGGTTTCATTCGGGTCTTGG
POLQ mouse-R	CGAGCAGGAAGATTCACTCCA

3.1.4 Antibodies

Table 5. Antibodies used for Western blot and Immunohistochemistry.

Name	Application	Dilution	Catalog number	Company
Anti-Cox2 (D5H5)	IHC	1:200	12282	Cell Signaling Technology, USA
Anti-CyclinD1 (92G2)	IHC	1:50	2978	Cell Signaling Technology, USA

Anti-DNA Ligase III	Western blot	1:1000	611876	BD Transduction Laboratories, USA
Anti-DNA Ligase IV (H-300)	Western blot	1:1000	sc-28232	Santa Cruz Biotechnology, Germany
Anti-DNA Polymerase theta	Western blot	1:750	ab80906	Abcam, UK
Anti-DNA Polymerase theta	IHC	1:50	ab111218	Abcam, UK
Anti-GAPDH	Western blot	1:1000	H86504M	Meridian Life Science, USA
Anti-Ki67	IHC	1:200	IHC-00375	Bethyl Laboratories, USA
Anti-Ku70 (C-19)	Western blot	1:1000	sc-1486	Santa Cruz Biotechnology, Germany
Anti-Ku70 (C-19)	IHC	1:50	sc-1486	Santa Cruz Biotechnology, Germany
Anti-Ku86 (H-300)	Western blot	1:1000	sc-9034	Santa Cruz Biotechnology, Germany
Anti-Mre11	Western blot	1:1000	4895	Cell Signaling Technology, USA
Anti-Mre11	IHC	1:100	4895	Cell Signaling Technology, USA
Anti-PARP	Western blot	1:1000	9542	Cell Signaling Technology, USA
Anti-PARP1 (E102)	IHC	1:50	ab32138	Abcam, UK
Anti-PCNA (PC10)	IHC	1:1600	2586	Cell Signaling Technology, USA
Phospho-p44/42 MAPK (Erk1/2) (Thr202/Tyr204) (D13.14.4E)	IHC	1:100	4370	Cell Signaling Technology, USA

ECL™ Mouse IgG HRP-linked whole Ab (from sheep)	Western blot	1:3000	NA931	CiteAb, UK
ECL™ Rabbit IgG, HRP-linked whole Ab (from donkey)	Western blot	1:3000	NA934	CiteAb, UK
EnVision+System-HRP Labelled Polymer Anti-mouse	IHC	Undilited	K4001	Dako, USA
EnVision+System-HRP Labelled Polymer Anti-rabbit	IHC	Undiluted	K4003	Dako, USA
m-IgGκ BP-HRP	IHC	1:200	sc-516102	Santa Cruz Biotechnology, Germany
Peroxidase AffiniPure Rabbit Anti-Goat IgG (H+L)	Western blot	1:3000	305-035-003	Jackson ImmunoResearch, UK
Peroxidase AffiniPure Rabbit Anti-Goat IgG (H+L)	IHC	1:200	305-035-003	Jackson ImmunoResearch, UK

3.1.5 Cell culture media and reagents

Dimethylsulfoxid (DMSO)	Roth, Germany
Fetal bovine serum (FBS)	PAN-Biotech, Germany
Gibco™ DMEM, high glucose, GlutaMAX™, pyruvate	Thermo Fisher, USA
Gibco™ Penicillin-Streptomycin (100x)	Thermo Fisher, USA
Gibco™ RPMI Medium 1640 [+] L-Glutamine	Thermo Fisher, USA
Gibco™ Trypsin-EDTA (0.5%)	Thermo Fisher, USA
Water, sterile-filtered for cell culture	Sigma-Aldrich, Germany

Panc02 medium	BxPC3 medium
10% FBS	10% FBS
100U/ml penicylin	100U/ml penicylin
100µg/ml streptomicin	100µg/ml streptomicin
in DMEM	in RPMI 1640

NIH/3T3 medium

10% FBS

100U/ml penicylin

100µg/ml streptomycin

in DMEM

Plastic materials for cell culture experiments were purchased from BD Biosecence (USA), Biozym (Germany), Corning (USA), Eppendorf (Germany), Greiner Bio-One (Germany), Roth (Germany) or Sarstedt (Germany).

3.1.6 Cell lines and animals

BxPC3	Dr. Giese, UKH, Germany
Panc02 PDA	Prof. Tuveson Laboratory, USA
NIH/3T3	ATCC, USA
C57/BL6 mice	Charles River, Germany
LSL-Kras^{G12D}	Prof. Tuveson Laboratory, USA
P48$^{+/Cre}$ mice	Prof. Tuveson Laboratory, USA
B6.Cg-Polq^{tm1Jcs}/J	The Jackson Laboratory, USA

3.1.7 Scientific Labwares and glasswares

96-well Microplates	Greiner Bio-One, Germany
Centrifuge tubes (15ml, 50ml)	Corning, USA
Counting chambers	Marienfeld Superior, Germany
Eppendorf tubes (0.5ml, 1.5ml, 2ml)	Eppendorf, Germany
Falcon^{TM} Polystyrene tubes with cell strainer cap	Corning, USA

Glass coverslips	R. Langenbrinck, Germany
Glass slides	R. Langenbrinck
MicroAmp™ Optical Adhesive Film	Thermo Fisher, USA
Microscope cover glasses	Marienfeld Superior, Germany
Microscope slides	Thermo Fisher, USA
Nitrocellulose Blotting Mambrane (0.2µ, 0.45µ)	GE Healthcare, Germany
Petri dishes	Sarstedt, Germany
RNase-free Microfuge Tubes (1.5 ml)	Thermo Fisher, USA
Sapphire 384 well PCR plates	Greiner Bio-One, Germany
Sapphire 96 well PCR plates	Greiner Bio-One, Germany
Scalpel	Dahlhausen, Germany
Syringe filters (0.22µm, 0.45µm)	Sarstedt, Germany
Tissue-Tek® Cryomold Biopsy Molds	Sakura Finetek, Germany
Transfer pipettes	Sarstedt, Germany
Vacutainer® blood collection tubes	BD Bioscence, USA

3.1.8 Instruments

Affymetrix GeneChip® Instrument System	Thermo Fisher, USA
Applied Biosystems® 3130xl Genetic Analyzer	Thermo Fisher, USA
Autoclave	Systec, Germany
Bioanalyzer 2100	Agilent Technologies, USA
Biological safety cabinets	Thermo Fisher, Germany
Biomek® 3000 Laboratory Automation Workstation	Beckman Coulter, USA
Biophotometer	Eppendorf, Germany
Blotting system	Bio-Rad, Germany
Cell culture CO_2 incubator	Binder, Germany
Centrifuge (5702R and 5424R)	Eppendorf, Germany
Centrifuge (Megafuge 16R)	Thermo Fisher, USA
FluorChem SP Gel Imaging System	Alpha Innotec, Germany
Fusion FX	Vilber Lourmat, Germany
Gel electrophoresis system	Peqlab, Germany
GFL® Shaking Water Bath	Lauda, Germany

LSR II Flow Cytometer	BD Bioscence, USA
MasterCycler EP Gradient Thermal Cycler 96 Well	Eppendorf, Germany
MaxQ™ 4000 Benchtop Orbital Shaker	Thermo Fisher, USA
Microscope Axiophot	Zeiss, Germany
Milli-Q® Water Purification System	Merck, Germany
MS3 Minishaker Vortexer	IKA, Germany
Olympus FLUOVIEW FV1000	Olympus, Japan
Pannoramic Midi II	3DHISTECH, Hungary
pH Meter	Hanna Instruments, Italy
QuantStudio 7 Flex Real-Time PCR Systems	Thermo Fisher, USA
Rotary Microtome	Leica, Germany
Scale Adventure	Ohaus, USA
Shaker ROCKER 2D digital	IKA, Germany
SpectraMax Plus 384 Microplate Reader	Molecular Devices, USA
Thermocycler peqSTAR	Peqlab, Germany
Thermomixer Compact	Eppendorf, Germany
TissueLyser II	Qiagen, Germany
Trans-Blot Turbo Transfer System	Bio-Rad, Germany
Ultrasonic homogeniser	Bandelin, Germany

3.1.9 Software

CaseViewer	3DHISTECH, Hungary
CellSens imaging software	Olympus, Japan
FACSDiva	BD Bioscience, USA
FlowJo v10.7.1	BD Bioscience, USA
GraphPad Prism v.5.04	GraphPad Software, USA
ImageJ	National Institutes of Health, USA
Ingenuity Pathway Analysis software	Ingenuity Systems, USA
MS Office (Word, Excel, PowerPoint)	Microsoft Corporation, USA
Oligo Package Bioconductor	Bioconductor, USA
PrimerExpress 3.0.1	Thermo Fisher, USA
Quant Center	3DHISTECH, Hungary

Rosetta Resolver Software	Rosetta Bio software, USA
Sequencing Analysis v5.2 software	Applied Biosystems, USA
SnapGene	GSL Biotech LLC, USA
SoftMax Pro Software	Molecular Devices, USA

3.2 Methods

3.2.1 Cell lines

Panc02 cells provided by Prof. Tuveson (CSHL Cancer Center, USA) were derived from C57BL/6 mice after 3-methylcholanthrene (3-MCA) treatment as described previously (Corbett et al., 1984). The BxPC3, human pancreatic cancer cell line was a generous gift from Dr. Giese (University Hospital Heidelberg). Variants of Panc02 and BxPC3 cell lines with exogenous Kras wild-type expression or oncogenic Kras carrying G12D mutation, were generated by lentiviral transduction system. These cell lines were cultured in DMEM or RPMI respectively, supplemented with 10% (vol/vol) FBS, 100U/ml penicillin and 100 µg/ml streptomycin at 37°C and 5% CO_2.

3.2.2 DNA sequencing

Genomic DNA from the Panc02 and BxPC3 cell lines was extracted using PureLink™ Genomic DNA Mini Kit according to the manufacturer's protocol. The isolated gDNA was further used for PCR amplification of target sequence followed by standard protocol. Primers for the detection of desired mutations were included in Table 2. After PCR reaction, amplicons were purified using AMPure XP beads and then prepared for II PCR sequencing. In this step the BigDye Terminator v3.1 was used as mentioned by the manufacturer. Afterwards, the Agencourt CleanSEQ was used to remove unincorporated dyes, nucleotides, and other contaminants. Analysis of mutation of the genes of interest (KRAS, Trp53) was performed using the Applied Biosystems 3130xl Genetic Analyzer.

3.2.3   Generation of wild-type Kras and mutagenic Kras plasmid

3.2.3.1   Reverse transcription

One µg of RNA was isolated from NIH3T3 cells using trizol reagent according to the standard protocol and subsequently reverse transcribed into cDNA with the MMLV High Performance Reverse Transcriptase Kit and random primers according to the manufacturer's protocols. The reverse transcription was performed in a 20 µl of reaction.

3.2.3.2   Polymerase Chain Reaction (PCR)

To amplify a particular DNA sequence, in this case sequence for KRAS gene (wild-type Kras), 1 µl of cDNA was used. The PCR was carried out in 25 µl of reaction as shown below:

Component	Volume
cDNA	1 µl
5X Q5 Reaction Buffer	5 µl
10mM dNTPs	1 µl
Primer F (Kras WT-AfeI mouse)	0.5 µl
Primer R (Kras WT-EcoRI mouse)	0.5 µl
Q5 DNA Polymerase	0.1 µl
DEPC-treated H_2O	16.9 µl

The PCR reaction was run in the Eppendorf MasterCycler EP Gradient Thermal Cycler 96 Well using program as follow:

Step	Temperature	Time	Cycles
Initiation	98°C	30 sec	1
Denaturation	98°C	10 sec	
Annealing	55°C	15 sec	35
Extension	72°C	30 sec	
Final extension	72°C	2 min	1

After the PCR amplification samples were loaded on 2% agarose gel and electrophoresis at 100 V was performed. The PCR amplicon was visualized using FluorChem SP Gel Imaging System. Subsequently, the PCR product was excised with a scalpel under UV light and

extracted from the gel using the QIAquick Gel Extraction Kit according to the manufacturer's protocol.

The mutagenic Kras was generated by PCR amplification of the wild-type Kras plasmid using primers 'Kras G12D human-F' and 'Kras WT-EcoRI mouse-R' (see section 3.1.3, Table 3).

3.2.3.3   Restriction enzyme digestion

Restriction enzyme digestion was used to cut the DNA at the specific sites. For this purpose, pLVX-DsRed-Monomer-C1 vector purchased from Takara Bio, and PCR product containing wild-type or mutagenic Kras were digested with restriction enzymes (AfeI and EcoRI) followed by the manufacturer's instructions.

After digestion, calf intestinal alkaline phosphatase (CIP) was added to the vector to phosphorylate the 5 'and 3' ends of the vector DNA, preventing it from self-ligating. The dephosphorylation was performed in 37°C for 1h. Finally, sodium acetate/ethanol precipitation of digested vector and wild-type or mutagenic Kras PCR product was performed.

3.2.3.4   DNA Ligation and transformation

To ligate digested DNA fragments, wild-type Kras or mutagenic Kras was inserted into the EcoRI and AfeI site of pLVX-DsRed-Monomer-C1 vector following standard protocol. The ligation reaction containing linear digested DNA fragments, 10x T4 buffer, ATP, T4 DNA ligase and DEPC-treated H_2O was performed for 1h at room temperature.

3.2.3.5   Transformation of bacteria

10 μl of mixture ligation was transformed into 30 μl of *E. coli* DH5α competent cells by incubation on ice for 30 min, subjected to a heat shock at 42°C for 40 sec and followed by a second incubation on ice for 2 min. Afterwards, 150 μl of LB medium was added to induce cells recovery and incubated at 37°C with shaking in the Benchtop Orbital Shaker. After 1 hour, the mixture of transformed cells was spread onto LB agar plates with ampicillin (100μg/ml) and incubated overnight at 37°C. Next day, single colonies were picked and resuspended in 20 μl of DEPC-treated H_2O for PCR amplification as follows:

Component	Volume
Single colony in H_2O	1 µl
10X Buffer	2 µl
$MgCl_2$	1.6 µl
10mM dNTPs	0.5 µl
Primer F (Kras WT-AfeI mouse)	0.5 µl
Primer R (pLVX-DsRed-MonomerC1)	0.5 µl
Taq DNA-Polymerase	0.1 µl
DEPC-treated H_2O	14.8 µl

The PCR reaction was run in the Eppendorf MasterCycler EP Gradient Thermal Cycler 96 Well using program as follows:

Step	Temperature	Time	Cycles
Initiation	95°C	2 min	1
Denaturation	95°C	20 sec	
Annealing	55°C	20 sec	30
Extension	72°C	1 min	
Final extension	72°C	2 min	1

After the PCR amplification PCR products were separated on 3% agarose gel and visualized using FluorChem SP Gel Imaging System. Subsequently, chosen colonies carried the plasmid of interest were resuspended in 5 ml of LB medium supplemented with ampicillin (100µg/ml) and grown at 37°C with gentle shaking for 16 hours. The plasmids were subsequently isolated using QIAprep Spin Miniprep Kit according to the manufacturer's protocol and sequenced using primer "pLVX-DsRed-MonomerC1-R" as previously described (see section 3.2.2, Table 2).

3.2.4 Lentiviral production and infection

Lentiviral transduction is an effective method of delivering transgenes to mammalian cells. It combines simplicity of use and transient transfection speed with strong expression of stable cell lines. Used mainly in cases where the usual method of transfection does not give the desired effects. In this study lentiviral packaging plasmids (pCMV-dR8.91 and pMD2.G-VSVG), kindly provided by Dr. Piotr Grabarczyk (Univeristy Medicine Greifswald), and transfer

plasmids (pLVX-DsRed-Monomer-C1 expressing KrasWT or KrasG12D) were introduced into HEK293 LentiX cells using calcium phosphate precipitation kit in accordance with the manufacturer's protocol. After 48 hours the supernatant from transfected 293T cells containing the virus was filter sterilized and concentrated using PEG Virus Precipitation Kit according to the manufacturer's instructions. At the day of the infection, concentrated viruses were introduced in presence of 8 µg/ml polybrene into Panc02 or BxPC3 cells, respectively. After 24 hours of incubation, the media containing virus were changed and cells were left to recover. For selection of stable/infected cells, 1.5-2 µg/ml of puromycin was added for an additional 3 days. Transduction efficiency was checked on a BD LSR II Flow Cytometer.

3.2.5 Microarray analysis

Microarrays were performed and analyzed by our collaborators from the Interfaculty Institute for Genetics and Functional Genomics Department of Functional Genomics at University Medicine Greifswald.

Total RNA was isolated from all variants of Panc02 and BxPC3 cell lines using using the RNeasy Mini Kit according to the manufacturer's protocol. Obtained RNA samples were purified using the RNA Clean-Up and Concentration Micro Kit and quality was checked by the Agilent 2100 Bioanalyzer. For further microarray analysis, RNA samples with an RNA integrity number (RIN) ≥ 9.0 were used.

The microarray analysis was carried out using individual RNA samples (n=3) that were processed following the manufacturer's instructions of the GeneChip^{TM} WT PLUS Reagent Kit and hybridized with GeneChip™ Mouse Gene 2.0 ST Assay or GeneChip™ Human Gene 2.0 ST Assay respectively. The quality control of hybridizations and data analysis were conducted in Transcriptome Analysis Console. All data were normalized using Robust Multi-array Average (RMA) algorithm. The microarray data analysis was performed using the R/Bioconductor package oligo and Rosetta Resolver software system.

To identify significantly differentially expressed genes ($p < 0.05$, fold change ≥ 1.5-fold) One-way ANOVA and t-tests were performed. Significantly differentially expressed genes and common crucial pathways between experimental groups were subsequently identified by Ingenuity Pathway Analysis (IPA) and Gene Set Enrichment Analysis (GSEA).

3.2.6 Quantitative PCR (qPCR)

To investigate the mRNA expression by qPCR, total RNA was isolated from all variants of Panc02 and BxPC3 cell lines using the RNeasy Mini Kit and quality control was performed using an Agilent 2100 Bioanalyzer. 1 μg of RNA was further reverse transcribed into cDNA with MMLV High Performance Reverse Transcriptase Kit and gene specific primers according to the manufacturer's protocols. All primers were designed using PrimerExpress 3.0.1 software. The quantitative expression of the mRNA of desired genes (Table 4) was measured with QuantStudio 7 Flex Real-Time PCR using the SYBR Select Master Mix in accordance with the manufacturer's instructions. The relative expression of studied genes was normalized to the expression of the housekeeping/reference gene, 5S ribosomal RNA (5S rRNA).

3.2.7 Western Blot

For the lysate sample preparation, collected cells were lysed in an appropriate volume of RIPA buffer with protease inhibitors and sonicated on ice with 10 short cycles of 10 sec using 90% pulse mode. Samples were further centrifuged at 14 000 rpm for 15 min at 4°C and protein concentration from collected supernatant was determined by Bradford assay using standard laboratory protocol. After measurement, the samples were incubated in the presence of 4x Laemmli buffer at 70°C for 10 min. Prepared samples containing 30 μg of protein extract were loaded and separated on 8 or 10% SDS-PAGE gels, depending on the size of the protein of interest. After gel electrophoresis, proteins were transferred to nitrocellulose membranes in 1x Towbin transfer buffer using a semi-dry transfer device Bio-Rad. Transferred membranes were further stained with Ponceau S staining solution to check the transfer efficiency and protein loading. Subsequently, the membranes were washed with 1x TBST and blocked in 5% nonfat dry milk in 1x TBST for 1h at RT. After blocking, different primary antibodies against desired proteins (Table 5) diluted at 1:1000 in 1xTBST were added and incubated overnight at 4 °C with gentle shaking. To confirm equal protein loading for cell lysates, incubation with GAPDH was performed. The next day, blots were washed three times with 1x TBST for 10 min and then incubated with the appropriate secondary antibody diluted at 1:5000 in 1x TBST for 1h at RT. After incubation, the blots were washed again three times with 1x TBST for 10 min and developed using chemiluminescence substrate ECL in accordance with the manufacturer's

instructions. The signal of target proteins was visualized using the Fusion FX chemiluminescence imaging system.

3.2.8 Cell cycle analysis by flow cytometry

To discriminate cells in different phase of the cell cycle, 10^6 cells from all variants of Panc02 and BxPC3 cell lines were collected, centrifuged 4 min at 1300 rpm and washed twice with PBS. To obtain a single cell suspension, cells were resuspended in 300 µl of PBS and filtered using cell strained caps which were supplied with FACS tubes. Cell suspension was fixed by adding dropwise 700 µl of 100% cold ethanol and stored at -20°C. At the day of measurement, fixed cells were centrifuged 10 min at 3000 rpm, the supernatant containing 70% ethanol was removed and 1ml of PBS was added to the cell pellet. After 15 min of the incubation on the ice, 200 µl of PI solution was added to the cells and incubated for 30 min in the dark at room temperature. Finally, stained cells were analyzed using BD LSR II Flow Cytometer collecting $2.5x\ 10^3$ events per sample.

3.2.9 MTT assay

MTT assay is a colorimetric method commonly used to measure cellular metabolic activity as an indicator of cell viability, cytotoxicity and proliferation. The method is based on the ability of dehydrogenase enzymes from the metabolically active cells to cleave the tetrazolium rings of the yellow tetrazolium salt (MTT) and form purple insoluble formazan crystals. The crystals can be dissolved with a solubilization solution. The amount of viable cells is directly proportional to the level of the formed formazan, which can be measured via absorbance at 500-600 nm using a multi-well spectrophotometer.

To obtain growth curves of the generated variants of Panc02 and BxPC3 cells described above, $3.5x10^3$ of Panc02 and $5x10^3$ of BxPC3 cells were seeded in a 96-well plate containing 100 µl of DMEM or RPMI medium respectively. Cells were grown up to different time points, 24h, 48h and 72h. At the day of measurement, 10 µl of MTT was added to the cells and incubated for 3 hours. After the incubation time, the insoluble formazan was solubilized with 150 µl of acidic isopropanol (0.04 M HCl in absolute isopropanol. The quantity of formazan was measured at 570 nm in SpectraMax Plus 384 Microplate Reader. All assays were performed three times independently in triplicate.

3.2.10 The Traffic Light Reporter

The Traffic Light Reporter (TLR) published by Certo et al., allows for the simultaneous fluorescent measurement of homologous recombination (HR) and non-homologous end joining (NHEJ) activity in response to DNA damage. This reporter consists of a non-functional mutant eGFP gene with a unique recognition site for the endonuclease I-SceI, followed by a second mCherry gene shifted by 2 bp in a reading frame. Both fluorescent genes are separated by the T2A linker that enables the downstream-encoded mCherry to escape the degradation of the misfolded protein GFP encoded in this +3 reading frame of eGFP. Upon introducing the I-SceI endonuclease, a site--specific double strand break (DSB) is generated. Repair by homologous recombination (HR) restores the GFP with the help of the DNA donor template, resulting in a green fluorescent signal. If the DSB is repaired by the mutagenic non-homologous end joining (mutNHEJ), insertions and deletions will arise, thus shifting the mCherry sequence down the frame and causing a red fluorescent signal (mCherry) (Figure 4).
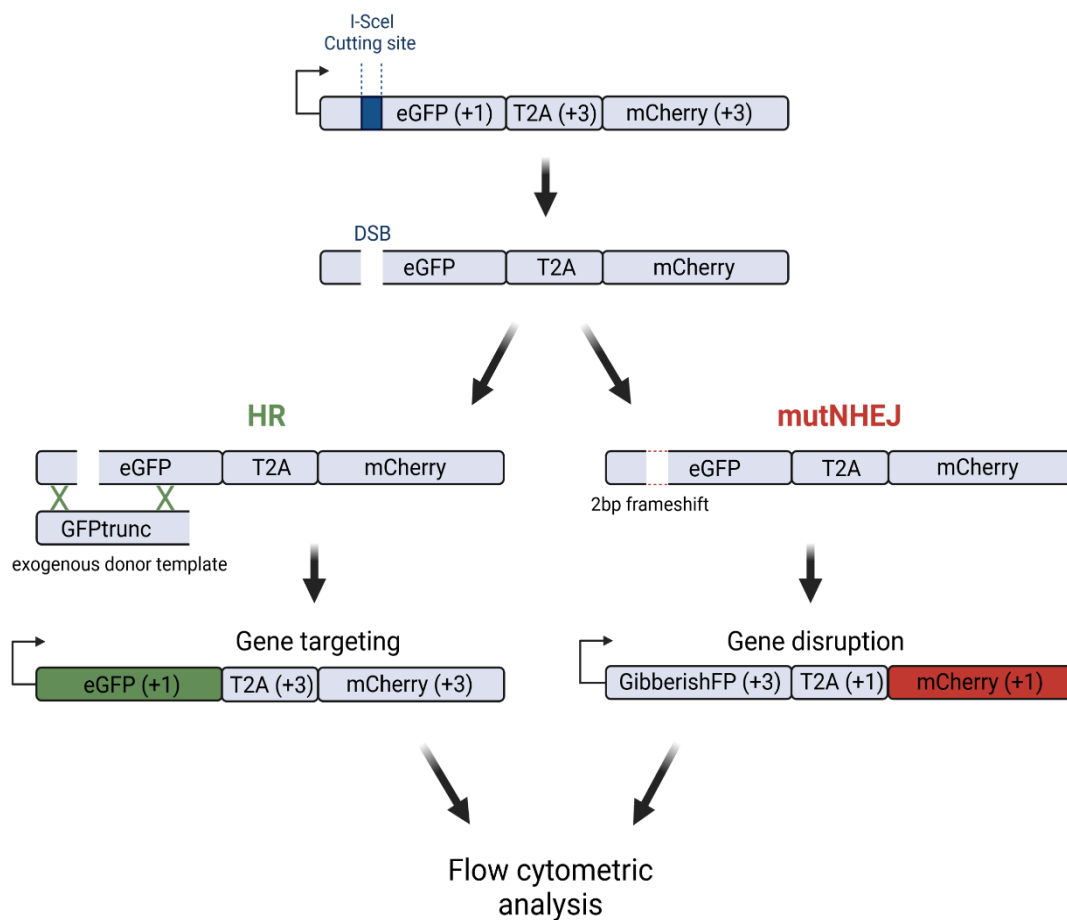

Figure 4. The Traffic Light Reporter System.

To measure the mutagenic alt-NHEJ activity in Panc02 and BxPC3 cell lines, a TLR reporter system was performed. First, the pCVL Traffic Light Reporter 1.1 Ef1a Puro plasmid (pCVL-TLR), together with lentiviral packaging plasmids (pCMV-dR8.91 and pMD2.G-VSVG) was introduced into HEK293 LentiX cells using the calcium phosphate transfection as described previously. Afterwards, 4×10^4 of Panc02 and 1×10^5 of BxPC3 cells (of all variants) were seeded in 12-well plate and infected with prepared viral plasmid (pCVL- TLR). Cells were transduced with 5-fold serial dilutions of the lentiviral stocks, followed by puro selection to estimate the lentivirus titer. Subsequently, Panc02 and BxPC3 cell lines containing single virus particles with TLR construct, were infected with the pCVL SFFV GFP EF1s HA NLS Sce (opt) viral plasmid (donor with I-SceI endonuclease) using lentiviral transduction as previously described (see section 3.2.5). Production of I-SceI lentiviral particles was performed using the calcium phosphate method. After 24 hours of incubation, the media containing the virus were changed and cells were left for an additional 48 hours to recover. Next day, activity of mutNHEJ (mCherry) and HR (GFP) was measured by flow cytometry. Plasmids used for TLR system were a generous gift from Prof. Sfeir (Skirball Institute of Biomolecular Medicine, New York).

3.2.11 Animal models

All experiments involving animals were performed and approved according to the regulations of Greifswald University. Animals were housed in standard specific-pathogen-free conditions and allowed food and water. Breeding and animal care was performed at the Central Core & Research facility of Laboratory Animals at the University Medicine Greifswald. For the animal studies p48[+/Cre]; LSL-Kras[G12D/+] (KC) mice and p48[+/Cre]; LSL-Kras[G12D/+]; Polq[tm1Jcs] (qKC) mice were used. In the KC mouse model, previously described by Hingorani et al. [31], LSL-Kras[G12D/+] animals were breed with p48[+/Cre] animals. Coexistance of p48Cre and Kras[G12D] locus results in expression of Cre recombinase and consecutive expression of KrasG12D mutant. To generate the qKC mouse model LSL-Kras[G12D/+] and p48[+/Cre] animals were crossed on PolQ deficient background using Polq[tm1Jcs] mice purchased from Jackson Laboratory. Progeny from these groups were further cross-breed to produce p48[+/Cre]; LSL-Kras[G12D/+]; Polq[tm1Jcs] (qKC) mice.

All genetically engineered mouse models were used to study the role of DNA polymerase theta (PolQ) in pancreatic cancer development. For this purpose, animals were euthanized with CO_2 for blood withdrawal and tissues collection. Tissues were collected from 1, 3, 4.5, 6, 9 and

12-month-old mice of each group and were subsequently analyzed for histological evaluation. Additionally, KC and qKC mice were monitored daily up to 440 days for survival.

3.2.12   Genotyping

To detect the presence or absence of desired DNA sequences, genotyping was performed. For this purpose, DNA was extracted from the tails using KAPA Mouse Genotyping Kit according to the manufacturer's protocol. Isolated DNA was further used for PCR genotype analysis. The PCR amplification program for Polq mice was performed in accordance to the Jackson laboratory protocol. Extracted DNA from p48Cre and LSL-Kras^{G12D} mice was amplified using program as follows:

Step	Temperature	Time	Cycles
Initiation	94°C	5 min	1
Denaturation	94°C	30 sec	
Annealing	60°C	30 sec	40
Extension	72°C	1 min	
Final extension	72°C	5 min	1

After the PCR reaction samples were loaded on 2% agarose gel and electrophoresis at 100V was performed. The PCR products were visualized using FluorChem SP Gel Imaging System.

*All primers used for genotyping are included in the section 3.1, Table 1.

3.2.13   Histology

For histological evaluation organs were fixed in 4.5% formaldehyde, store up to 48 h at 4°C and embedded in paraffin wax. Paraffin blocks were further cut in 2μm with a microtome for slide preparations and used for hematoxylin and eosin (H&E) and immunohistochemistry (IHC) staining. All slides used for histological analysis were scanned with the Pannoramic Midi II and evaluated with different magnification using Quant Center software.

3.2.13.1 Hematoxylin and Eosin staining

Slides with paraffin-embedded tissue sections were deparaffinized by two rinses with xylene for 10 min, washed in serial dilutions of ethanol (100%, 95%, and 70%) for 5 min in order to remove the toxic organic solvent, and finally rinsed with 1xPBS for 5 min. Afterwards, the sections were stained with Mayer's hematoxylin solution for 5 min, followed by a washing step under running tap water, and stained again with eosin Y solution with the addition of acetic acid for 1 min. The slides were subsequently dehydrated through graded ethanol (70%, 95%, and 100%) and rinsed in xylene for 10 min to clear the tissue and renders it completely transparent. Finally, the cleaned tissue sections were mounted with VectaMount Permament Mounting Media.

3.2.13.2 Immunochistochemistry

For immunohistochemical analysis, paraffin-embedded tissue sections were deparaffinized and rehydrated as mentioned before and incubated with Antigen retrieval buffer by cooking for 30 min in a pressure cooker. The slides were further blocked in 3% H_2O_2 for 20 min and incubated with PBS containing 5% Aurion BSA and 0.05% Tween 20 for 1 h to block non-specific staining. Subsequently, the sections were incubated with primary antibody against the protein of interest (Table 5) diluted at 1:50 or 1:100 in PBS containing 1% Aurion BSA and incubated overnight at 4°C. Incubation with anti-rabbit, anti-mouse and anti-goat secondary antibody was performed for 1h at room temperature. For chromogenic detection, 3,3'-diaminobenzidine (DAB) detection kit was used according to the manufacturer's protocol. After DAB staining slides were counterstained with Mayer's hematoxylin solution for 3 min and washed under running tap water. Afterwards, the sections were dehydrated in different dilution of ethanol, cleaned with xylene for 10 min and coverslipped using VectaMount mounting medium. Negative controls were prepared using the same procedure except that the primary antibody was replaced with 1% BSA in PBS.

3.2.13.3 Alcian Blue staining

Alcian Blue is a cationic dye that stains acidic carboxylated or sulfated mucins at the right pH and salt concentration. This staining was performed to detect acid mucin production, a characteristic feature of PanINs. The Paraffin-embedded tissue sections were deparaffinized

and rehydrated through graded ethanol solutions to distilled water. Staining with Alcian Blue solution was performed according to the manufacturer's protocol. Sections were subsequently washed with running tap water, dehydrated in serial increasing concentrations of ethanol and cleared with xylene. After dehydration to xylene, stained sections were mounted with VectaMount and submitted for histological analysis.

3.2.14   Statistical analysis

Statistical analysis was carried out with GraphPad Prism software v.5.04. Data from *in vivo* and *in vitro* experiments was plotted either with the mean value plus standard deviation (SD) or standard error of the mean (SEM). Significant differences were analyzed by unpaired student t-test to compare between two variables and one-way analysis of variance (ANOVA) for multiple comparison. Survival curves were analyzed with the Mantel-Cox test. A variance with a p-value < 0.05 was considered significant.

4. RESULTS

4.1 Oncogenic KRAS and its influence on the activity of the alt-EJ repair pathway

4.1.1 Generation of mouse and human pancreatic cancer cell lines expressing KRAS wild-type and oncogenic KRAS G12D

KRAS is considered to be the most frequently mutated oncogene in human cancers, mostly in pancreatic cancer (>90%) [48]. Numerous studies reported that mutations of the *KRAS* gene play an important role in PDAC development [31]. Furthermore, activation of oncogenic KRAS can affect DNA repair pathways causing abnormal repair and accumulation of genomic alterations. Therefore, we first investigated whether the mutagenic KRAS has effect on the alt-EJ repair pathway in pancreatic cancer. For this purpose, we used murine pancreatic cancer cell line Panc02 and human pancreatic cancer cell line BxPC3. Both of these cell lines do not harbor activating KRAS mutations. To confirm the absence of the KRAS G12D mutation, the most common mutation in PDAC we employed the Sanger sequencing in Panc02 and BxPC3 cell lines. In addition, we checked for the presence of another mutated gene *TP53*, frequently occurring in pancreatic cancer and associated with KRAS activation. *TP53* encodes a tumor suppressor transcription factor, p53, which mediates many antiproliferative effects in response to a variety of stresses, including DNA damage. Most known mutations are in the DNA binding domain and deactivate the suppressor by preventing DNA binding and transactivation [182]. Moreover, mutant TP53 causes loss of tumor suppressor function, leaving the mutant protein capable of driving additional oncogenic processes such as metastasis [183].

In this study, mutations in the *KRAS* exon 2 and *TP53* exon 5 were analyzed. As expected, no frequent point mutations were detected in the analyzed genes in the Panc02 and BxPC3 cell lines (Figure 5 and 6). However, a silent SNP was found at codon 32 (TAT to TAC) in Panc02 cells. Since this is a synonymous SNP, it does not affect protein expression and function (Figure 5).
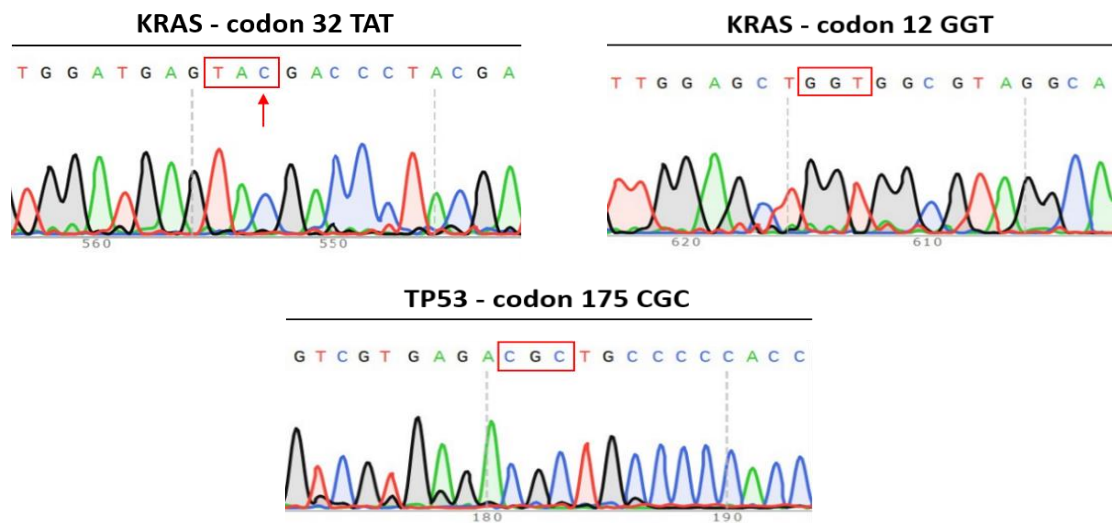
KRAS - codon 32 TAT

T G G A T G A G T A C G A C C C T A C G A

KRAS - codon 12 GGT

T T G G A G C T G G T G G C G T A G G C A

TP53 - codon 175 CGC

G T C G T G A G A C G C T G C C C C C A C C

Figure 5. Detection of mutations in *KRAS* exon 2, *TP53* exon 5 in Panc02 mouse pancreatic cancer cell line. The representative sequence analysis is shown for each case. The rectangle contains the codons in which hotspot mutations were expected. The arrow indicates the synonymous SNP in codon 32 of *KRAS* gene.
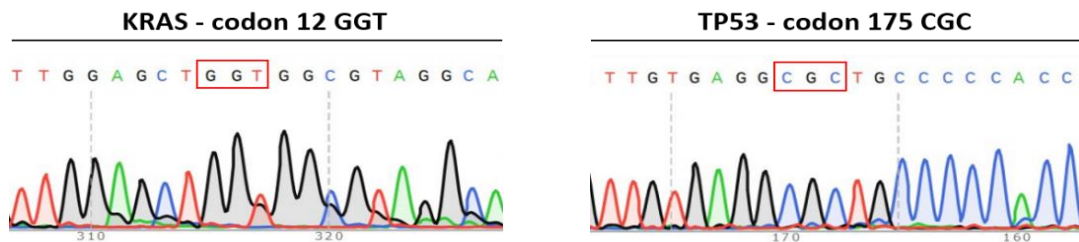

KRAS - codon 12 GGT

T T G G A G C T G G T G G C G T A G G C A

TP53 - codon 175 CGC

T T G T G A G G C G C T G C C C C C A C C

Figure 6. Detection of mutations in *KRAS* exon 2, *TP53* exon 5 in BxPC3 human pancreatic cancer cell line. The representative sequence analysis is shown for each case.

To enable observation of whether KRAS affects alt-EJ, we generated Panc02 and BxPC3 cells expressing wild-type or oncogenic KRAS with the G12D mutation. To achieve this, we used previously designed wild-type and mutagenic KRAS plasmids cloned into the pLVX-DsRed-Monomer-C1 vector and introduced them into cells. Since these cells are notoriously resistant to any kind of transfection reagents, we employed the lentiviral transduction system to express KRAS wild-type (KrasWT) and oncogenic KRAS (KrasG12D). To estimate the transduction efficiency, we transduced the cells in parallel with a control virus carrying the fluorescent DsRed protein (pLVX-DsRed-Monomer-C1), followed with fluorescence imaging and FACS measurement. We achieved a transduction efficiency of almost 100% for Panc02 and BxPC3 cells (Figure 7).
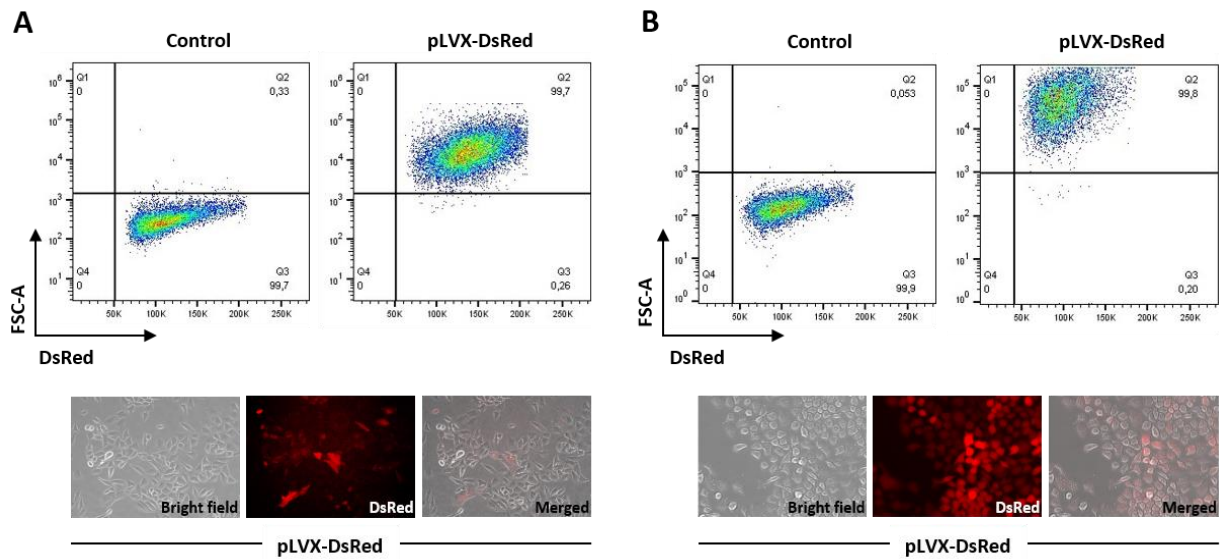
Figure 7. Lentiviral transduction of pLVX-DsRed, KRAS wild-type and mutagenic KRAS plasmids in Panc02 and BxPC3 cells. The transduction efficiency of pLVX-DsRed plasmid in (A) Panc02 and (B) BxPC3 cell lines was demonstrated by flow cytometry and microscopic analysis. Representative images of Panc02 and BxPC3 cells expressing pLVX-DsRed plasmid.

4.1.2 Oncogenic KRAS upregulates alt-EJ components at post-transcriptional level in pancreatic mouse and human cell lines

To investigate the effect of oncogenic KRAS on alt-EJ components activity, we used established Panc02 and BxPC3 cell lines expressing KrasWT and KrasG12D mutant (designated as KrasMT), and performed the immunoblot analysis. As shown in figure 8, exogenous expression of both KrasWT and the KrasMT clearly increased the expression level of Polθ, PARP1, Lig3 and Mre11, key factors of the alt-EJ pathway, in the mouse Panc02 cell line. As expected, the expression of the c-NHEJ components such as Ku80, Ku70 and Lig4 was not altered. In line, only the exogenous expression of KrasG12D in the human BxPC3 cell line increased the expression levels of Polθ, PARP1, Lig3 and Mre11, while the KrasWT did not significantly increase the expression of alt-EJ components in the same human cell line. The expression of all c-NHEJ factors in BxPC3 cells remained unchanged. These data strongly support that expression of the oncogenic KrasG12D mutant may result in enhanced activity of the alt-EJ pathway.
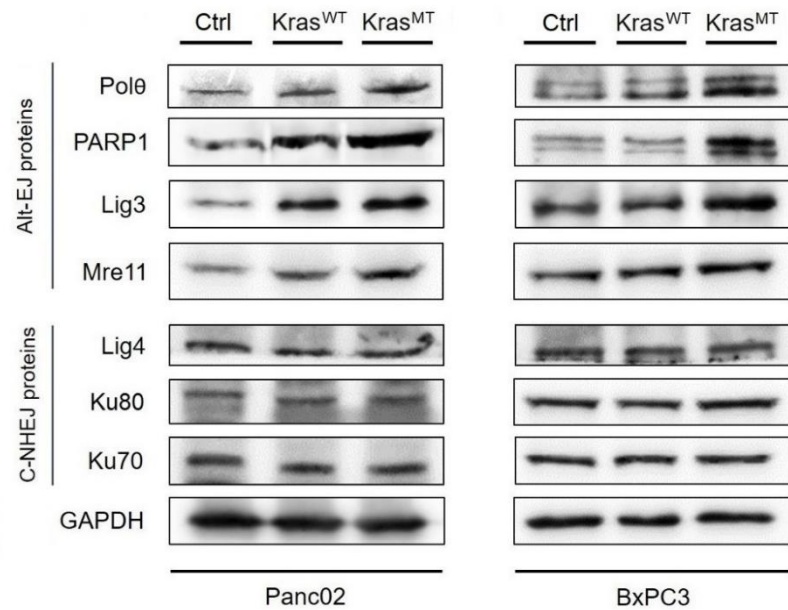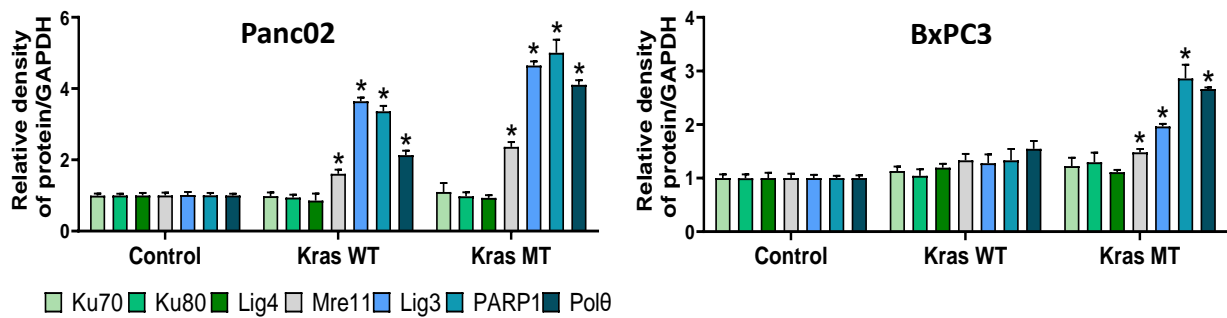
Figure 8. Impact of KrasWT and KrasG12D mutant on expression levels of alt-EJ components. (A) Protein expression of Polθ, PARP1, Lig3, Mre11, Lig4, Ku80 and Ku70 in cell extracts isolated from indicated Kras transduced Panc02 (left) and BxPC3 (right) cells. A representative immunoblot from three independent experiments is shown. (B) Bar graphs show protein expression levels relative to GAPDH in Panc02 and BxPC3 determined by the means of densitometry of three independent experiments (mean ± SD; *$P < 0.05$ is considered as significant; Student's t-test).

4.1.3 KRAS does not regulate the expression level of alt-EJ components at transcriptional level

Intracellular protein expression is precisely regulated at the transcriptional and/or translational levels, and its deregulation can have deleterious consequences. KRAS as a small GTPase transductor protein, transmits signals from extracellular receptors, mainly tyrosine kinase receptors, to the nucleus where it regulates the transcription of many proteins [184].

To address whether KRAS expression causes the transcriptional upregulation of DNA repair pathway components, in particular alt-EJ, we first conducted a microarray analysis of mouse Panc02 and human BxPC3 pancreatic cancer cell lines expressing either exogenous KrasWT or oncogenic KrasG12D (designated as KrasMT). Due to the discrepancy of one Panc02 control sample, it was excluded for further analysis. To our surprise, the overall gene set enrichment analysis (GSEA) of our microarrays did not identify any DNA repair pathways to be significantly enriched. In the additional targeted analysis of DNA double-strand break repair pathways, 10 genes of c-NHEJ and alt-EJ were upregulated in Panc02 cells. In BxPC3 cells, 9 genes of c-NHEJ and 10 genes of alt-EJ pathway were upregulated according to their signal-to-noise ratio. Although the GSEA analysis showed the upregulation of c-NHEJ and alt-EJ pathways in both Panc02 and BxPC3 cells, no significant enrichment was found (Figure 9).
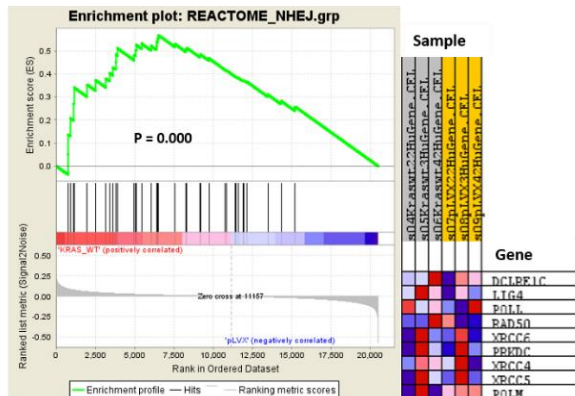
A

Kras WT vs Control
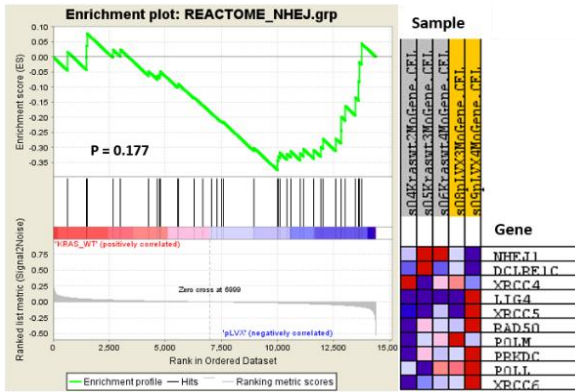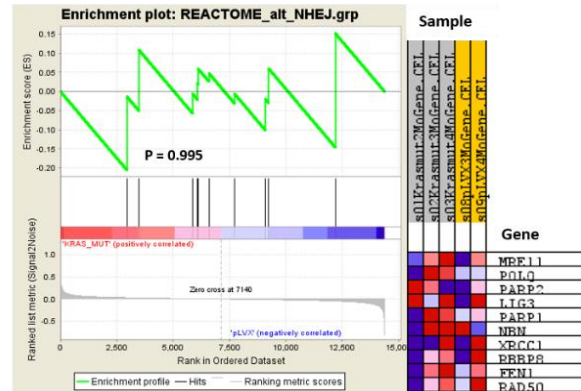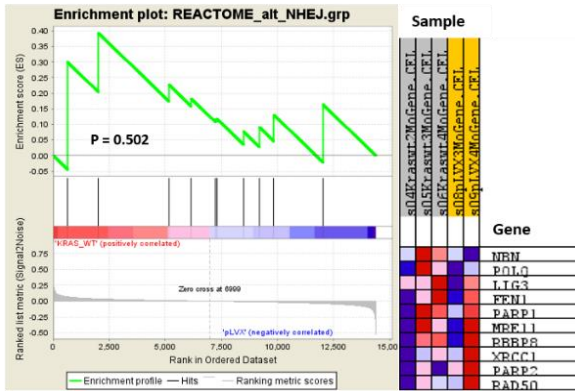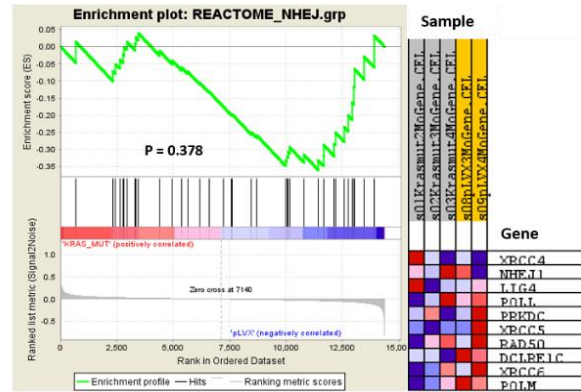
Kras MT vs Control

B

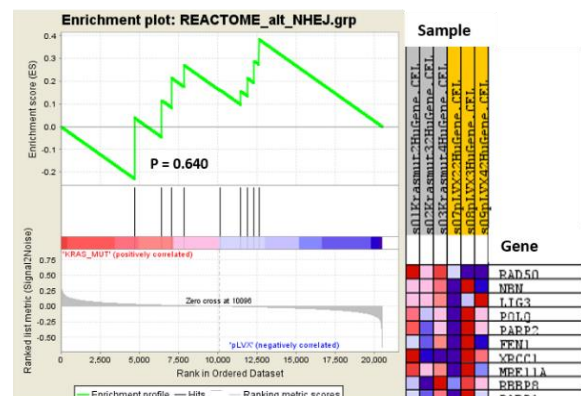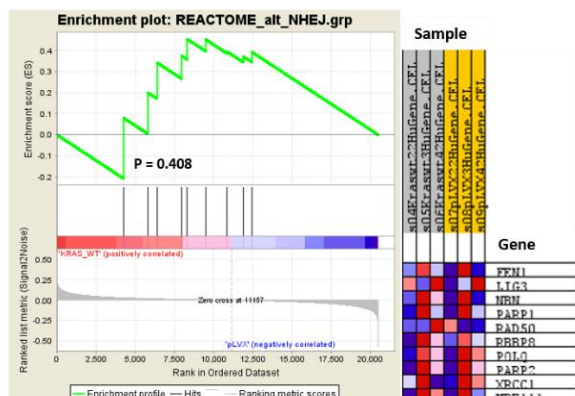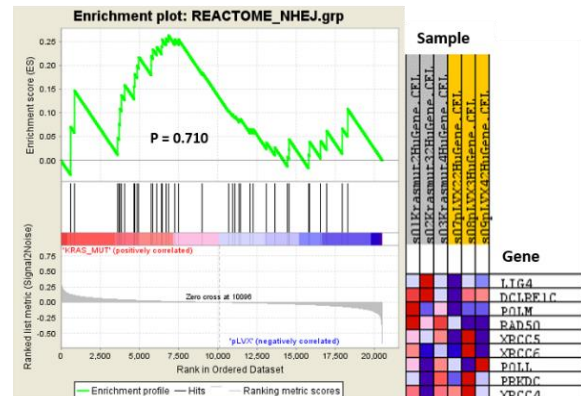**Kras WT vs Control**

Kras MT vs Control

Figure 9. Targeted GSEA in (A) mouse Panc02 and (B) human BxPC3 pancreatic cancer cell lines. Gene Set Enrichment Analysis plots for the Reactome NHEJ and alt-EJ are shown. The heatmap on the right side of each panel visualizes the genes contributing the most to the enriched pathway. The green curve corresponds to the ES (enrichment score) curve, the running sum of the weighted enrichment score in GSEA. P value are reported within each graph (Panc02 control, n=2; Panc02 KrasWT, KrasMT, n=3; BxPC3 control, KrasWT, KrasMT, n=3).

Next, we confirmed these results with qPCR analyzing mRNA expression of PolQ, PARP1, Lig3 and Mre11, which protein level was upregulated on the above immunoblots upon exogenous expression of oncogenic KrasG12D (Figure 10). According to the microarray analysis, mRNA level of the alt-EJ (PolQ, PARP1, Lig3 and Mre11) and c-NHEJ (Lig4, Ku80 and Ku70) core factors was also not altered. These data clearly indicate that Kras does not regulate the expression level of alt-EJ components at transcriptional level and thus, a post-transcriptional mechanism must be involved.

A

B

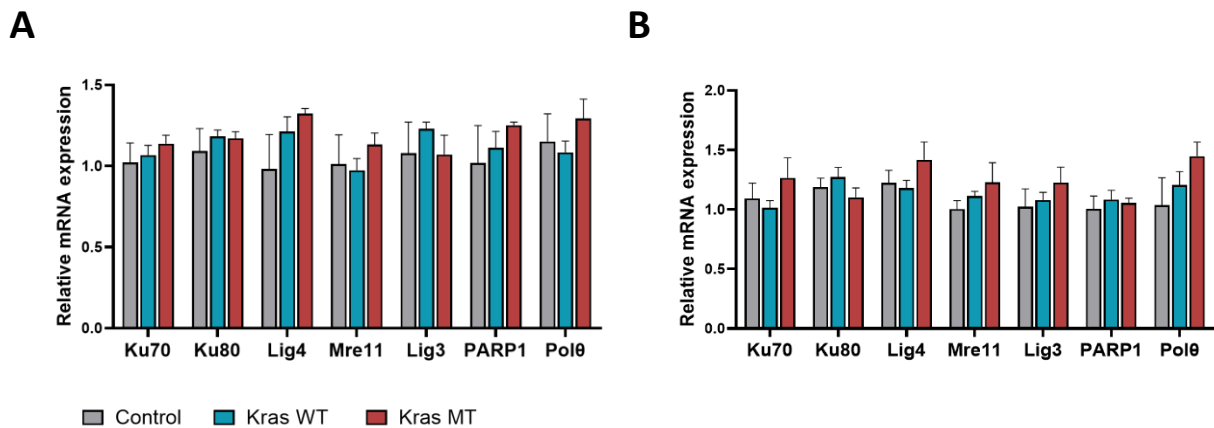☐ Control   ☐ Kras WT   ☐ Kras MT

Figure 10. mRNA expression of alt-EJ and c-NHEJ components in Panc02 and BxPC3 cells upon exogenous expression of KrasWT and mutagenic KrasG12D. Relative mRNA levels were normalized to 5S RNA of alt-EJ and c-NHEJ factors from three independent experiments (mean ± SD; *$P < 0.05$ is considered as significant; Student's t-test).

4.1.4 KRAS overexpression promotes proliferation of mouse and human pancreatic cancer cells *in vitro*

Cell proliferation is the process that results in an increase of cell number and is defined by the balance between cell division and cell loss through cell death or differentiation. This process is also an important part of cancer development and progression. Many studies have shown that cancer cells are characterized by increased proliferation [185, 186]. Given the well-known role of KRAS in the cell proliferation, we investigated whether activation of a point KRAS mutation results in different proliferation rate compare to cells carrying the wild-type KRAS. For this purpose, we employed MTT assay on murine Panc02 and human BxPC3 pancreatic cancer cells expressing pLVX vector, KrasWT or oncogenic KrasG12D. We used untransduced cells as a control. Measurements were made after 24, 48 and 72 hours. As shown in figure 11A, both murine Panc02 bearing oncogenic and wild-type KRAS showed increased proliferation compared to untransduced and pLVX cells throughout the measurement. Interestingly, Panc02 cells harboring wild-type KRAS exhibited higher proliferation rate than KRASmut-expressing Panc02 mainly after 24 and 48 hours. On the other hand, human cell lines did not show the same trend of cell growth (Figure 11B). In this case, BxPC3 cells carrying KRAS mutant also proliferated faster than pLVX and untransduced cells. However, the increase in the proliferation rate of BxPC3 KRAS wild-type cells was not higher than KRASmut-expressing BxPC3, as observed in the mouse cell line Panc02. Herein, cells harboring KRAS mutation proliferated significantly faster than cells with wild-type KRAS throughout the measurement. Our results revealed that both overexpression of KRAS wild-type and activation of KRAS mutations can influence the proliferation rate in murine and human pancreatic cancer cell lines resulting in an accelerated increase in cell number which is a common characteristic of tumor cells.
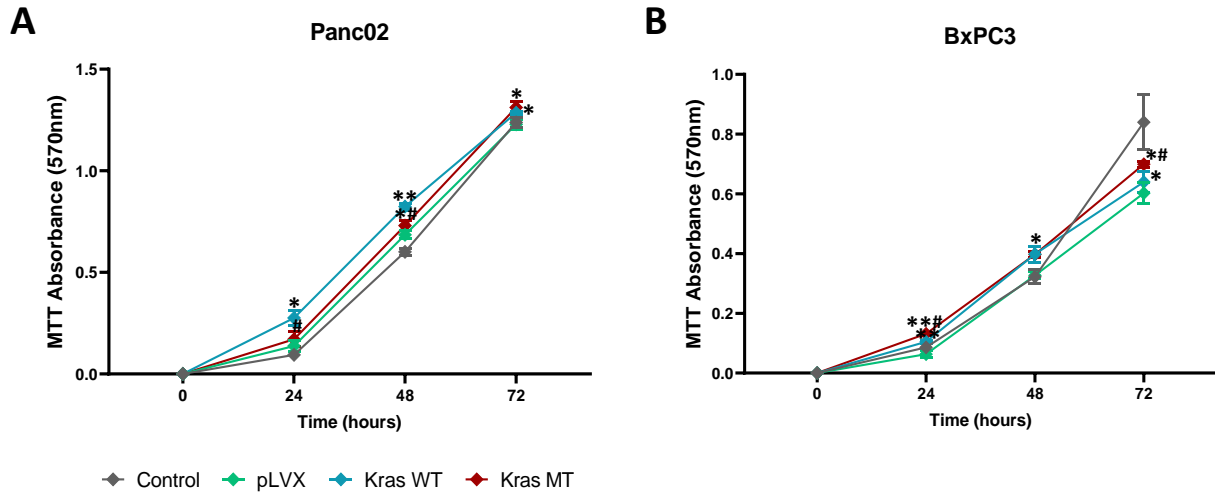
Figure 11. Effect of KRAS expression on proliferation of mouse Panc02 and human BxPC3 pancreatic cell lines. The MTT assay was performed for 72 hours and the absorbance of each well was read at 570 nm. A representative proliferation graph of (A) Panc02 and (B) BxPC3 cells from three independent experiments is shown. (mean ± SD; **$P < 0.01$, $P < 0.05$ compared to pLVX cells; #$P < 0.05$ compared to Kras WT cells; Multiple t-test).

4.1.5 Oncogenic KRAS G12D affects cell cycle progression in pancreatic cancer cells

Cell cycle phase is one of the main determinants of DNA DSB repair pathway choice. In eukaryotic cells, DSBs can be repaired by three main mechanisms: canonical nonhomologous end-joining (c-NHEJ), homologous recombination (HR) and alternative end joining (alt-EJ). While c-NHEJ operates throughout the cell cycle and its activity is predominant in G1, HR and alt-EJ take place in S and G2 phases of the cell cycle [88-90].

To investigate which DSB repair mechanism is activated in the cell cycle of pancreatic cancer cells depending on KRAS status, Panc02 and BxPC3 cells harboring wild-type or mutagenic KRAS (KrasG12D) were used and stained with propidium iodide (PI) followed by flow cytometry. This approach allows discriminating cells in different phases of the cell cycle based on their DNA content. Untransfected Panc02 and BxPC3 cells were used as a control. The FACS analysis showed a statistically significant increase in the number of cells in the S/G2-M phase in both Panco2 and BxPC3 cells with KRAS mutant (designated as Kras MT) compared to cells harboring KRAS wild-type (designated as Kras WT) and controls. In addition, the increased number of Panc02 and BxPC3 cells with oncogenic KRAS in the S/G2-M phase was accompanied to the same extent by a decrease in the G1 phase. No significant changes in the proportion of cells in the G1 and S/G2-M phases of the cell cycle were observed in both KRAS

wild-type Panc02 and BxPC3 cells, and in control cells (Figure 12). Since both HR and alt-EJ pathways operate in the S and G2 cell cycle phase, our results showed that presence of KRAS G12D mutation not only affects the cell cycle progression but also activates one of the DNA repair mechanisms mentioned above in murine and human pancreatic cancer cell lines.
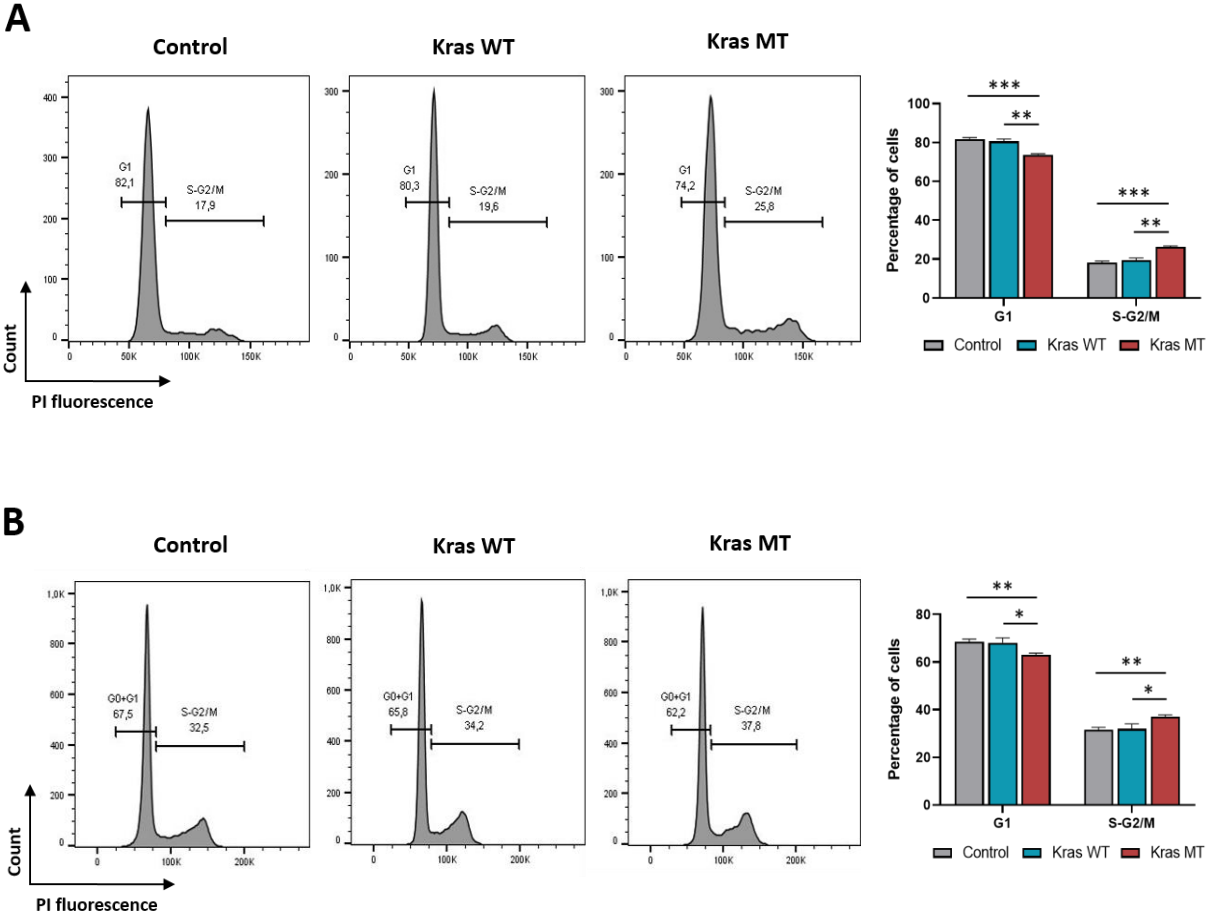
Figure 12. Oncogenic KRAS G12D alters cell cycle progression in (A) Panc02 and (B) BxPC3 cell line. Viable cells were collected by trypsynization, and DNA content was analyzed after PI staining. Representative flow cytometry histograms of cell cycle analysis from three independent experiments are shown. Quantification of data from Panc02 and BxPC3 cells is presented. Error bars represent mean ± SD; *$P < 0.05$, **$P < 0.01$, ***$P < 0.001$ (Student's t-test).

4.1.6 Activation of alt-EJ pathway due to the expression of exogenous KrasG12D in pancreatic cancer cells

As already shown in our previous studies in both murine and human pancreatic cancer cell lines, alt-EJ components are upregulated upon expression of the exogenous KrasG12D mutant. Based on the current understanding of cellular processes, we believe that upregulation of these key factors will reflect increased alt-EJ biological activity. Moreover, the analysis of the cell cycle in these cell lines showed an increased number of cells in the S/G2-M phase, which confirmed the activity of either the alt-EJ or HR pathway. For this purpose, the Traffic Light Reporter (TLR) assay was employed to measure and validate the mutagenic alt-EJ activity in Panc02 and BxPC3 cell lines. The TLR system developed by Certo et al. enables simultaneous monitoring of homologous recombination (HR) and mutagenic activity of non-homologous end joining (mutNHEJ) in response to DNA damage in single cells [187]. In this work, Panc02 and BxPC3 cell lines expressing Kras wild-type (KrasWT) or oncogenic KrasG12D were transduced with a lentiviral vector containing the fluorescent TRL system followed by flow cytometry. MCherry positive cells indicated a repair event induced by mutNHEJ and eGFP positive cells represented cells with the HR repair event. A detailed description of the conducted experiment can be found in section 3.2.10. As expected, Panc02 and BxPC3 cells transduced with I-Scel alone produced only mCherry positive cells, indicative of mutNHEJ at the reporter locus. On the other hand, both murine and human pancreatic cancer cells co-transduced with I-Scel and donor template produced either mCherry or eGFP positive cells (Figure 13 and 14). Further analysis showed a higher HR capacity in control Panc02 and BxPC3 cells (Figure 13A and 14A). BxPC3 KrasWT cells also exhibited an increasing fraction of events accounted for the HR pathway (Figure 14B). High mutNHEJ capacity was observed in both Panc02 and BxPC3 cell lines expressing the oncogenic KrasG12D (designated as Kras MT) (Figure 13C and 14C). In line, the ratio of HR to mutNHEJ was lower in murine and human KRASmut - expressing cells compare to control (Figure 13E and 14E). Moreover, increased mutNHEJ pathway events were also noted in KrasWT Panc02 cells (Figure 13B). However, the HR to mutNHEJ ratio in Panc02 cells between Kras wild-type and the Kras mutant was higher in Panc02 KrasWT cells, which is consistent with our results showing increased expression of alt-EJ proteins in these cells (Figure 13E and 8A). Of note, as the amount of virus is increased, we observed the expected dose-dependent increase in the

total number of repair events in all analyzed Panc02 and BxPC3 variants (Figure 13D and 14D). Taken together, these data clearly indicate that the oncogenic KrasG12D contributes to the activation of the alt-EJ pathway in pancreatic cancer cells.
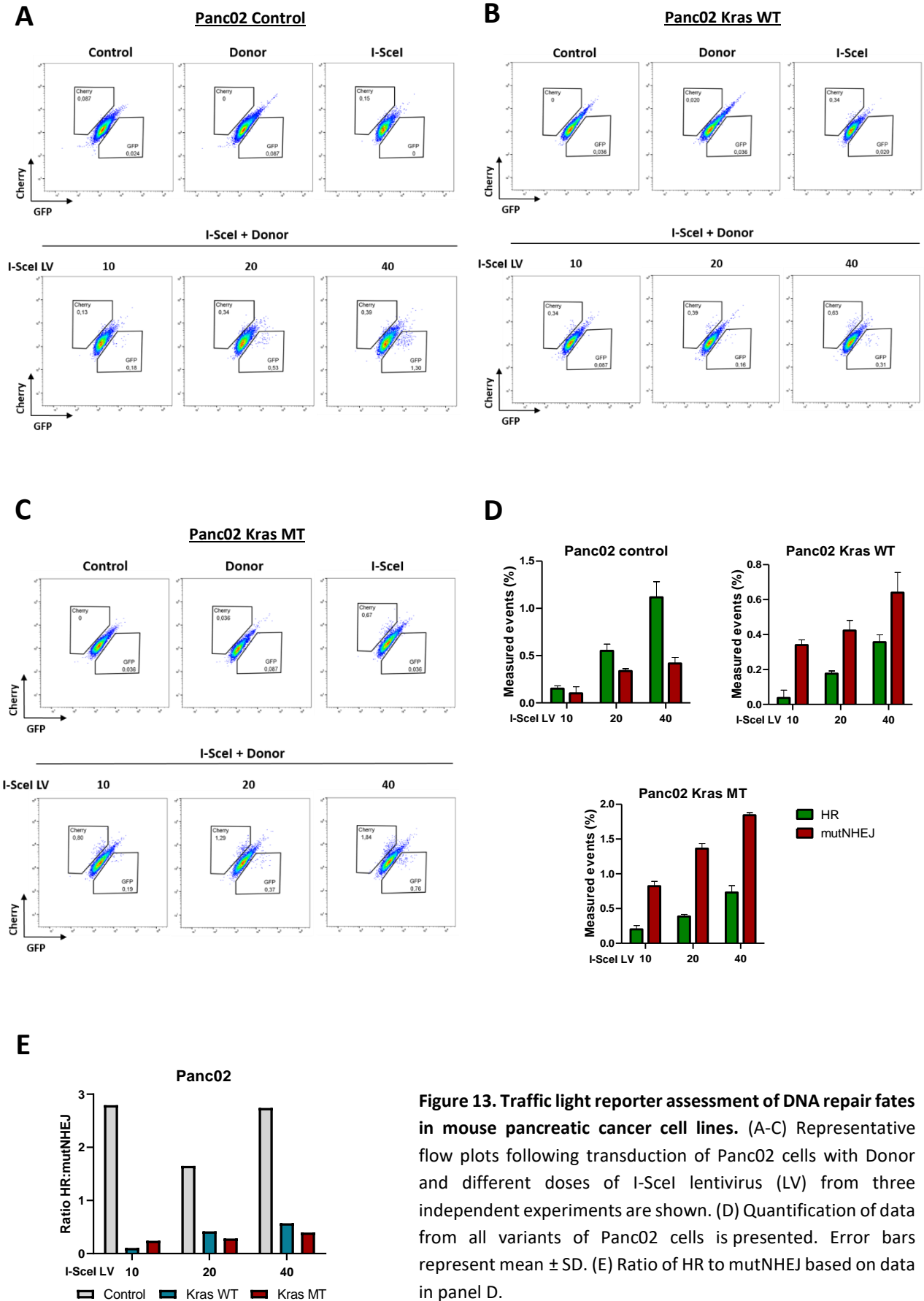
Figure 13. Traffic light reporter assessment of DNA repair fates in mouse pancreatic cancer cell lines. (A-C) Representative flow plots following transduction of Panc02 cells with Donor and different doses of I-SceI lentivirus (LV) from three independent experiments are shown. (D) Quantification of data from all variants of Panc02 cells is presented. Error bars represent mean ± SD. (E) Ratio of HR to mutNHEJ based on data in panel D.

Figure 14. Traffic light reporter assessment of DNA repair fates in human pancreatic cancer cell lines. (A-C) Representative flow plots following transduction of BxPC3 cells with Donor and different doses of I-SceI lentivirus (LV) from three independent experiments are shown. (D) Quantification of data from all variants of BxPC3 cells is presented. Error bars represent mean ± SD. (E) Ratio of HR to mutNHEJ based on data in panel D.
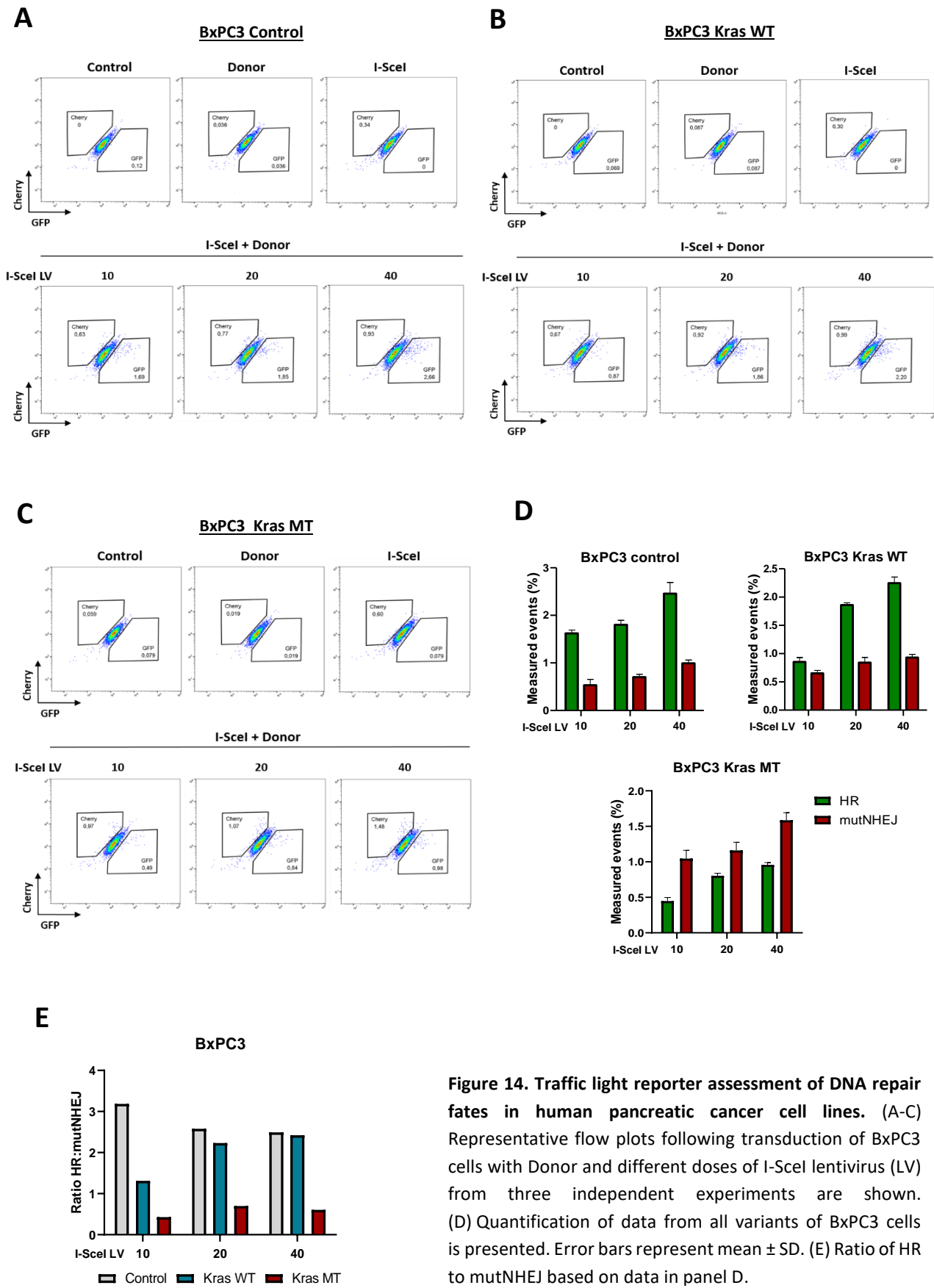
4.2 Effect of alt-EJ inactivation on the development of pancreatic ductal adenocarcinoma in a mouse model

4.2.1 PolQ deficiency delays pancreatic cancer progression

Genetically engineered mouse models (GEMMs) are an excellent research tool to study genetic mutations and their biological significance in a variety of cancers. Particularly, in the research of pancreatic cancer, several GEMMs have been over the past two decades engineered and provided new insights into its understanding [66]. Thus, to investigate *in vivo* KrasG12D role in the development of pancreatic intraepithelial neoplasia (PanINs) and their progression to pancreatic cancer, we used a KC mouse model. This pancreatic ductal adenocarcinoma mouse model is characterized by pancreas-specific expression of KrasG12D mutant and absence of suppressor mutations, leading to the formation of PanINs and ultimately invasive PDAC that bears striking resemblance to tumor progression in humans [67]. We believe that in the presence of oncogenic KRAS, the alt-EJ pathway is a key player in tumorigenesis, and loss of alt-EJ components may prevent or delay PanIN lesions development and ultimately pancreatic cancer progression.

As already mentioned above, polymerase theta plays an essential role in alt-EJ and its expression is generally repressed in healthy tissues but significantly increased in cancers [170-172]. In addition, it has been reported that Polq-null mice show no overt phenotype despite the elevated genomic instability in erythroblasts [176]. Accordingly, due to the well-established function of Polθ in the alt-EJ pathway and tumorigenesis, we decided to breed the Polq knockout mice on KC background (designated as qKC mice) to study the role of alt-EJ in development of PanIN lesions and transition to pancreatic cancer [164, 165]. We observed that the pancreas of KC and qKC mice, especially in older animals, is larger than in control and Polq-deficient mice (designated as qKO) showing focal nodular parenchyma or pancreatic cancer (Figure 15).
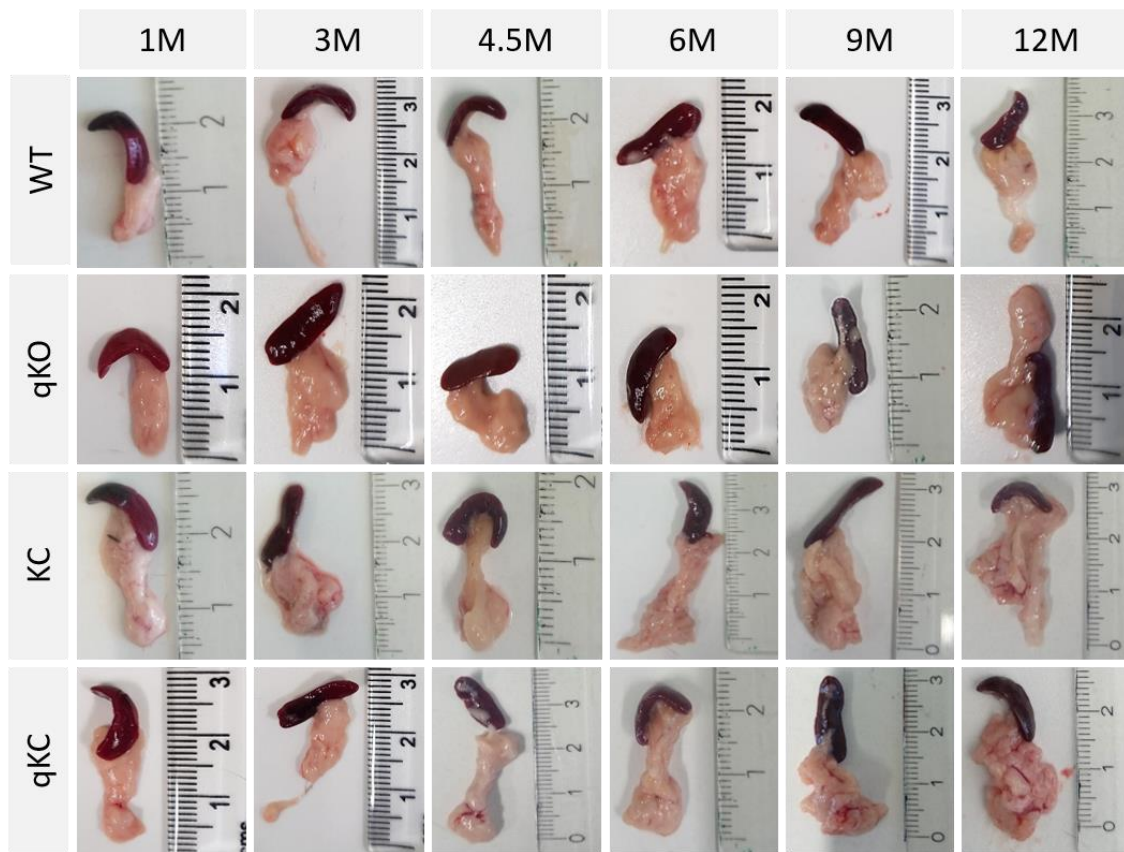
Figure 15. Representative pancreata from 1M, 3M, 4.5M, 6M, 9M and 12M WT, qKO, KC and qKC animals.

Further histopathological analysis of mouse pancreases revealed significant differences in the formation of PanIN lesions between KC and qKC mice (Figure 16A). While 3-month-old KC mice already showed 56% PanIN lesions, the same age qKC mice had 40% of PanINs. This tendency continued with the age of the mice, only in 9-month-old mice no significant changes were obderved. Interestingly, in both KC and qKC mice, one 4.5-month-old mouse did not show any PanIN lesions (Figure 16B). We also noticed that the KC mice also had an increased presence of high-grade PanINs compared to the qKC mice (Figure 16C). These results support the clear role of polymerase theta in the development of PanIN lesions in the mouse pancreas.

57
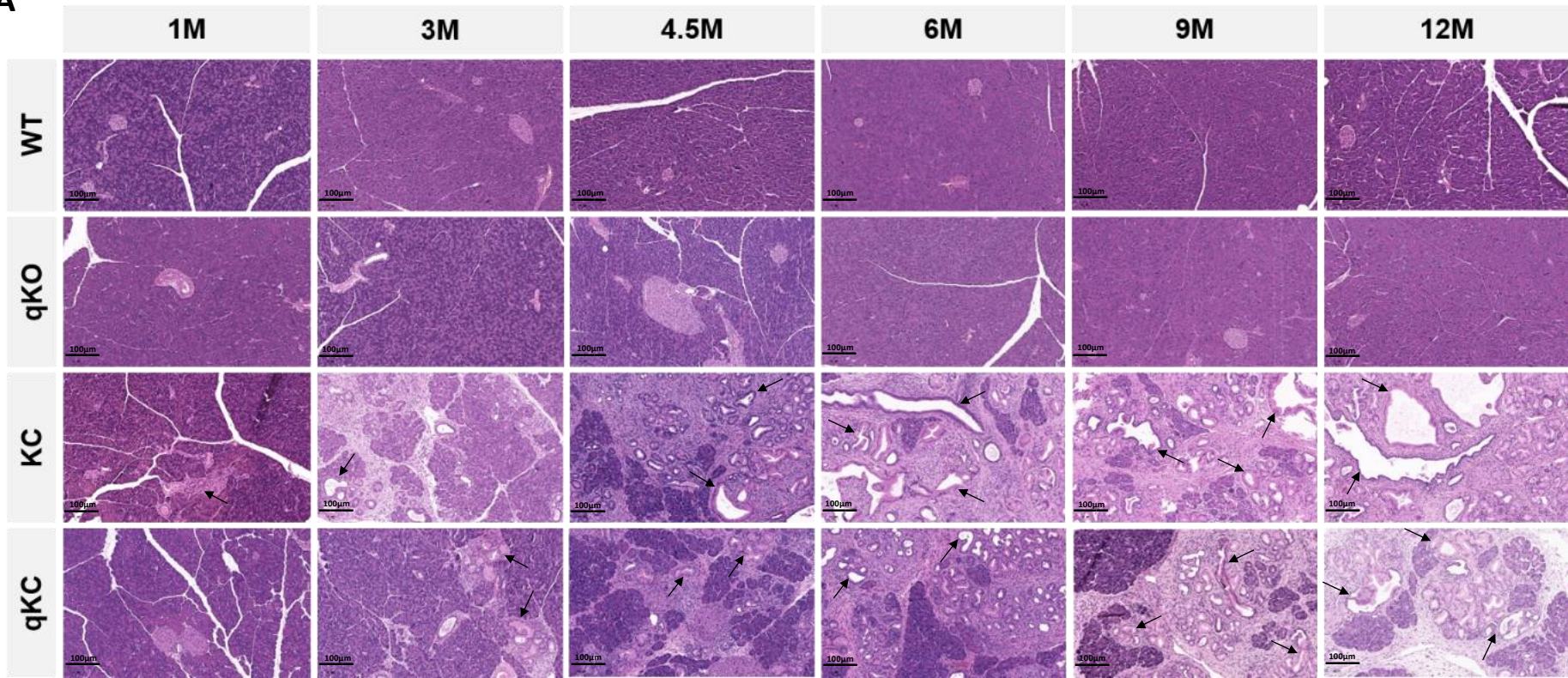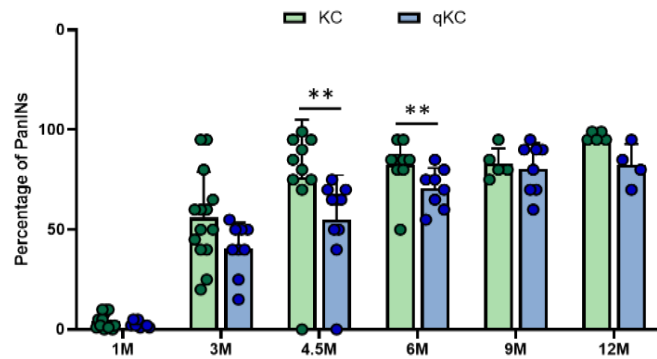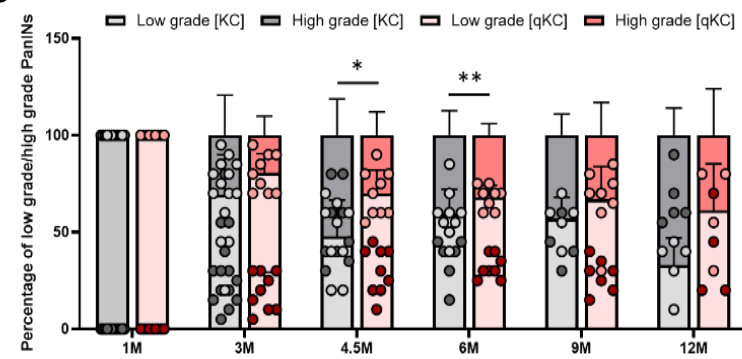
Figure 16. Knockout of polymerase theta delayes pancreatic intraepithelial neoplasia progression in qKC mice. (A) Representative images of the pancreas from age-matched wild-type, qKO, KC and qKC mice at 1, 3, 4.5, 6, 9, 12-month-old. Arrows indicate PanIN lesions (hematoxylin and eosin stain; scale bars represent 100μm). (B) Percentage content of PanIN lesions and (C) their histologic progression in KC and qKC mice at the age of 1 month (KC, n=14; qKC, n=9), 3 months (KC, n=14; qKC, n=9), 4.5 months (KC, n=10, qKC, n=10), 6 months (KC, n=9; qKC, n=8), 9 months (KC, n=5; qKC, n=8) and 12 months (KC, n=5; qKC, n=4). Error bars represent mean ± SD; *$P < 0.05$, **$P < 0.01$, (Student's t-test).

4.2.2 Differentiation of PanIN lesions in genetically engineered mouse models

PanINs are the most frequent and well-known PDAC precursors. These neoplastic lesions are characterized by conversion of the duct epithelial cells to a columnar phenotype with mucin accumulation [67, 69]. PanINs are histologically subdivided into low-grade PanIN-1A and B, PanIN-2 and high-grade PanIN-3 referred to as carcinoma in situ [16, 17]. Moreover, tumor differentiation is separated into three stages, from grade 1 well-differentiated (G1) to grade 3 poorly differentiated (G3) tumors. The mucin content decreases with decreasing differentiation status. To visualize PanIN changes in the KC and qKC mouse models, we performed an Alcian blue stain (Figure 17). The Alcian blue staining detects acidic mucins and has been used to accurately measure the frequency of PanIN lesions in similar transgenic mouse models of PDAC [188-191]. Our results revealed strong Alcian blue staining (acidic mucin stain) in both KC and qKC mice at 3, 4.5, 6, 9, and 12 months of age, both resembling grade 1 tumors. However, pancreatic tissue of KC mice at 3- and 6-month-old showed significantly more stained mucin-containing PanIN-like lesions with Alcian blue. Furthermore, significantly less cytoplasm was observed in KC mice at 3, 4.5, and 6 months of age compared with qKC mice of the same age. Because of very low number of PanIN foci in 1-month-old KC and qKC mice, there was little or no blue staining. As expected, less mucin-rich PanIN lesions and more cytoplasm were observed in qKC mice compared to KC mice, indicating a delay in tumor progression due to polymerase theta deletion.
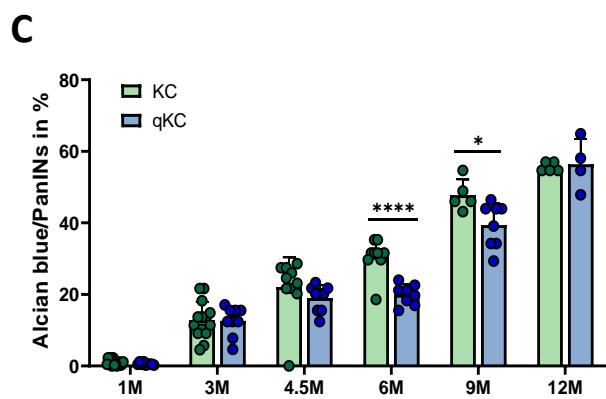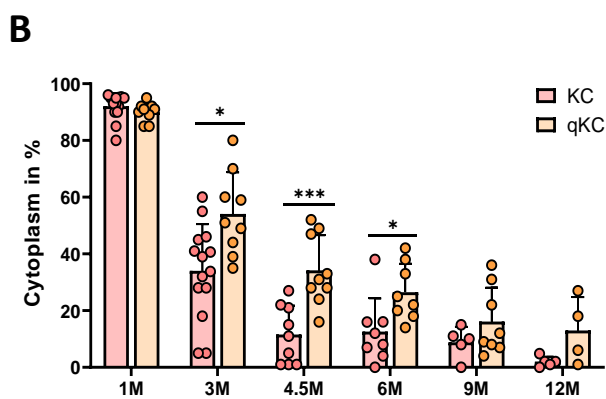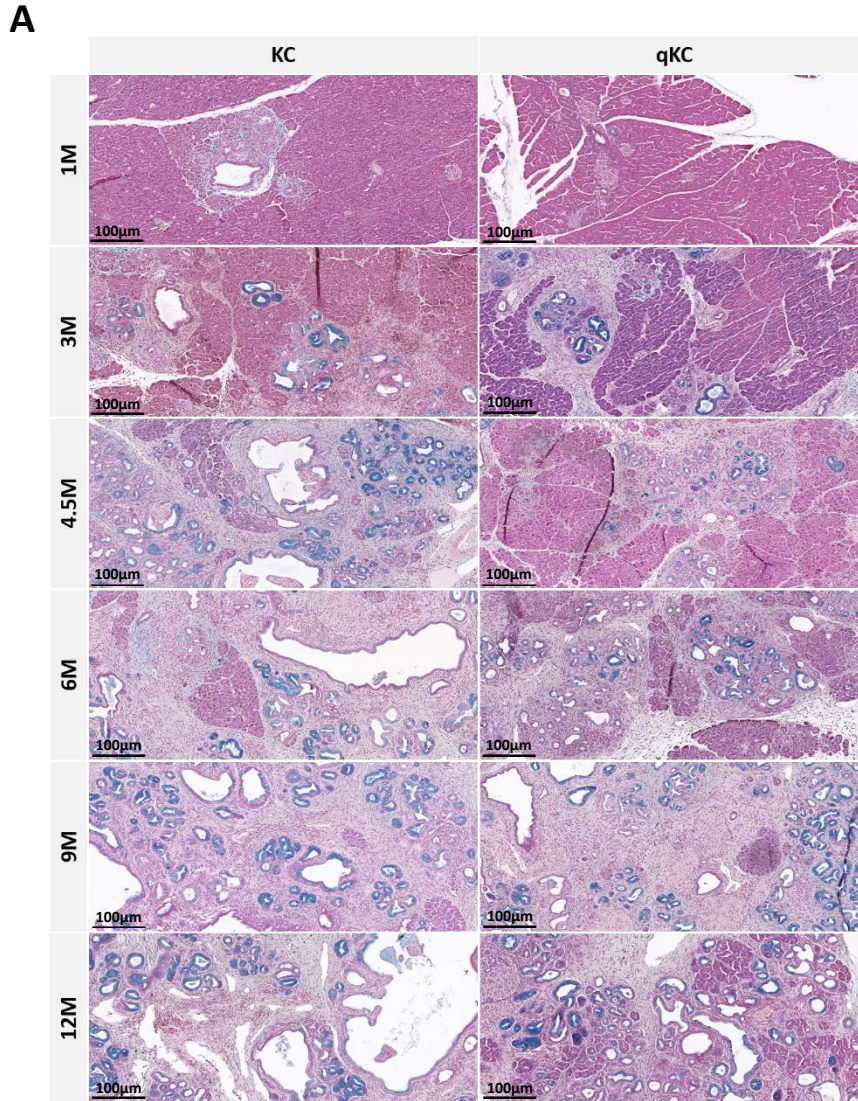
Figure 17. Differentiation status of pancreatic carcinoma in KC and qKC mice. Alcian blue staining was performed to visualize differentiation. (A) Mucin-rich PanINs lesions are depicted in blue, cytoplasm in light red, and nuclei in dark red. Representative images of the pancreas from age-matched KC and qKC mice at 1, 3, 4.5, 6, 9, and 12-month-old are shown. Scale bars represent 100 μm. Histological score of (B) cytoplasm and (C) PanINs in pancreas of KC and qKC animals at the age of 1 month (KC, n=14; qKC, n=9), 3 months (KC, n=14; qKC, n=9), 4.5 months (KC, n=10, qKC, n=10), 6 months (KC, n=9; qKC, n=8), 9 months (KC, n=5; qKC, n=8) and 12 months (KC, n=5; qKC, n=4). Error bars represent mean ± SD; *$P < 0.05$, **$P < 0.01$, ***$P = 0.0001$, ****$P < 0.0001$ (Student's t-test).

59

4.2.3 Deletion of polymerase theta leads to slower PDAC progression and extended overall survival

Because knockout of PolQ in the KC background delayed disease progression, we also evaluated the effect of loss PolQ on overall survival. Previous studies have reported that the survival rate of KC animals is higher than 450 days, and deaths of individuals begin after approximately 150 days [69]. Accordingly, in our research, we monitored the KC and qKC animals for 440 days. Survival studies conducted to explore the influence of PolQ deficiency in the oncogenic KrasG12D induced pancreatic cancer mouse model showed that KC mice began to die already after 96 days of observation. In contrast, qKC mice had longer lifespan, and the first deaths occurring only after 274 days (Figure 18A). Despite prolonged survival of qKC mice, histopathological analysis revealed that nearly 65% of animals (n=9/14) developed full-blown pancreatic tumors. Additionally, 30% of qKC mice with PDAC had liver (n=4/9) and lung metastases (n=2/9). Interestingly, two males had also abdominal distention (Figure 19). On the other hand, only 30% of KC mice (n=6/20) exhibited PDAC, and only one animal showing liver metastasis. Our results also showed no correlation between gender and cancer progression in either the KC or qKC mouse model (Table 6).
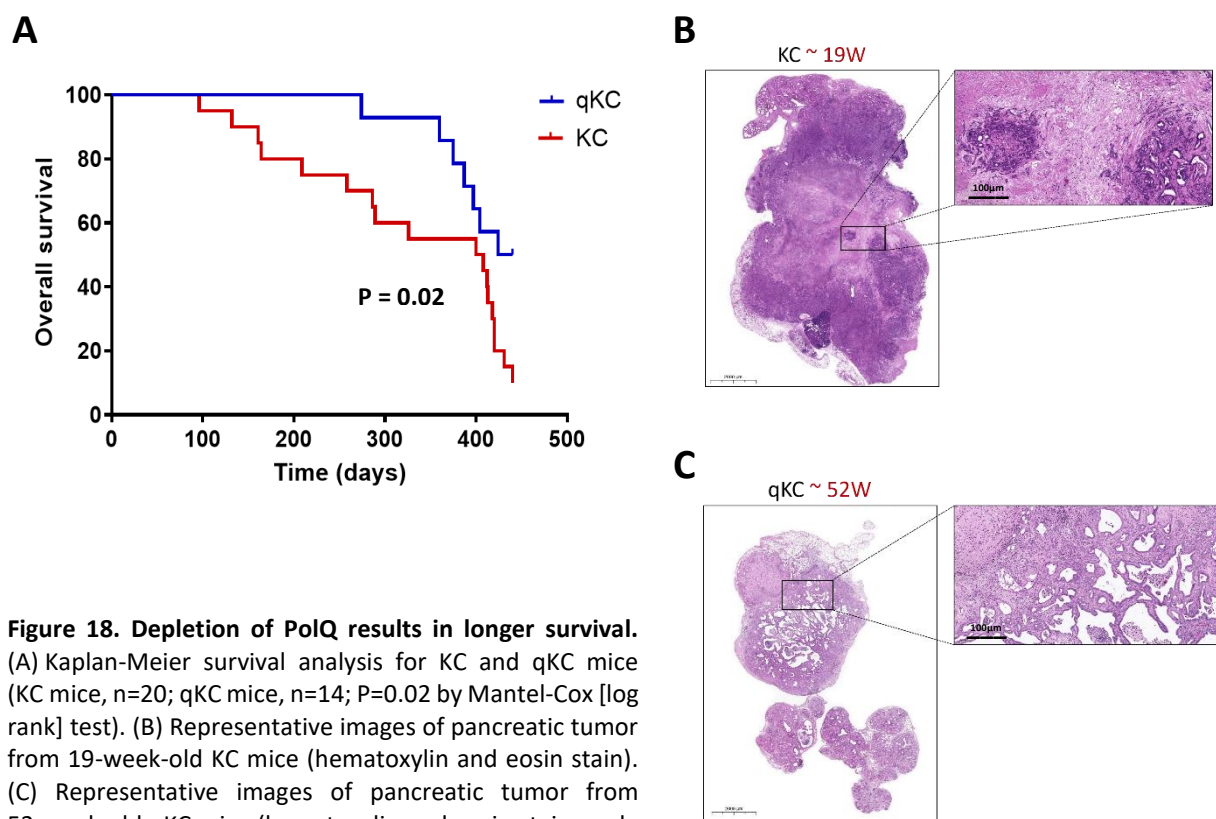
Figure 18. Depletion of PolQ results in longer survival. (A) Kaplan-Meier survival analysis for KC and qKC mice (KC mice, n=20; qKC mice, n=14; P=0.02 by Mantel-Cox [log rank] test). (B) Representative images of pancreatic tumor from 19-week-old KC mice (hematoxylin and eosin stain). (C) Representative images of pancreatic tumor from 52-week-old qKC mice (hematoxylin and eosin stain; scale bars of enlarged images represent 100 µm).

Table 6. Clinical spectrum of disease in KC and qKC mice. Histopathological analysis of animals used in the survival curve (N = no, Y = yes).

ID	Strain	Gender	Age (days)	PDA	Metastasis	Other
873	KC	F	289	N	N	
931	KC	F	164	N	N	
938	KC	M	96	N	N	
1034	KC	M	161	N	N	
1161	KC	M	132	Y	N	
872	KC	M	440	N	N	
878	KC	M	431	N	N	
916	KC	M	400	N	N	
1003	KC	M	326	Y	N	
251	KC	M	258	N	N	
208	KC	F	286	Y	Y' liver	Pancreatobiliary type IPMN
1151	KC	F	209	Y	N	Sarcomatoid dedifferentiation, Fatty Infiltration (FI)
957	KC	M	412	N	N	
967	KC	M	407	N	N	
994	KC	M	413	N	N	
1033	KC	F	440	Y	N	Sarcomatoid
1099	KC	M	440	Y	N	Serous microcystic adenoma
1116	KC	M	420	N	N	
1117	KC	M	420	N	N	
1126	KC	F	418	N	N	Serous microcystic adenoma
1050	qKC	F	274	Y	Y' liver, lung	Sarcomatoid, Fatty Infiltration (FI)
990	qKC	M	397	Y	N	
959	qKC	F	440	N	N	Serous microcystic adenoma
960	qKC	F	440	N	N	
1039	qKC	F	387	Y	Y' liver	Sarcomatoid, Fatty Inflltration (FI)
981	qKC	F	440	Y	N	
988	qKC	M	440	N	N	
1041	qKC	M	404	Y	N	
1080	qKC	F	360	Y	N	
1013	qKC	F	440	N	N	
1090	qKC	M	375	Y	Y' liver	
1046	qKC	F	446	N	N	
1086	qKC	F	440	Y	N	
1089	qKC	M	424	Y	Y' liver, Y' lung	Sarcomatoid, Fatty Infiltration (FI)
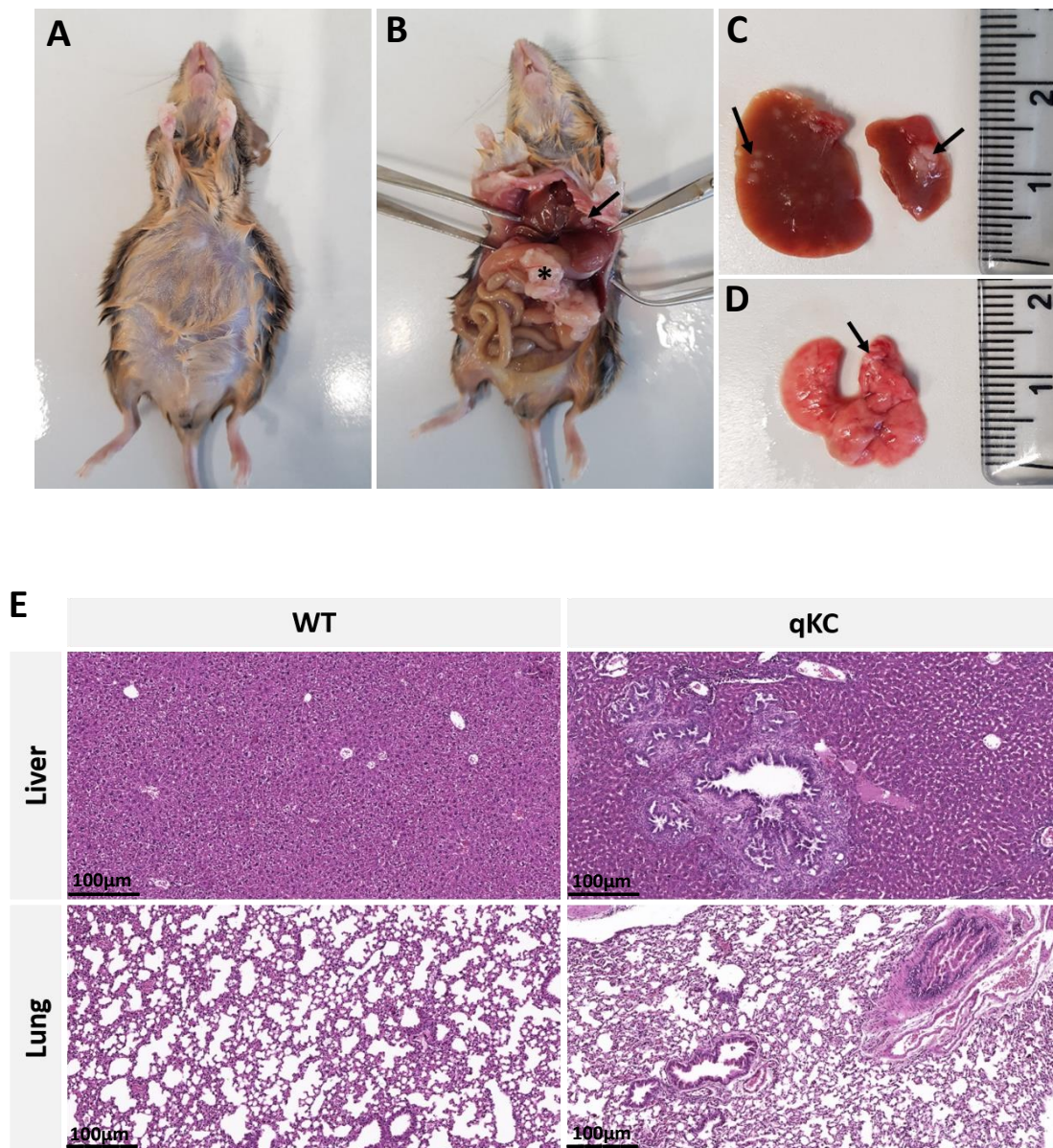
Figure 19. PolQ deficiency leads in the long term to the invasive and metastatic pancreatic cancer development. (A-D) Pathological photographs of metastatic PDAC in a representative qKC mouse. (A) Abdominal distention has been noted due to the accumulation of malignant ascites. (B) Primary PDAC in the pancreas (asterisk) and liver metastasis (black arrow). Tissue sample from the same mouse showing (C) multiple liver metastases and (D) lung metastasis marked with black arrowheads. (E) Representative images of healthy liver and lung of wild-type mouse and liver and lung metastases of qKC mouse are shown (hematoxylin and eosin stain). Scale bars represent 100 μm.

Further microscopic examination of KC and qKC tumors showed rare histologic variants of pancreatic ductal adenocarcinoma and extra-pancreatic pathologies such as sarcomatoid, fatty infiltration (FI), serous microcystic adenoma, and also pancreatobiliary type IPMN which was present only in one KC mouse (Figure 20). Sarcomatoid was observed in most qKC mice

with PDAC (Table 6). These findings suggest that despite delayed tumor progression and longer animal survival associated with loss of polymerase theta, most qKC mice eventually develop full-blown PDAC that can metastasize to other organs.
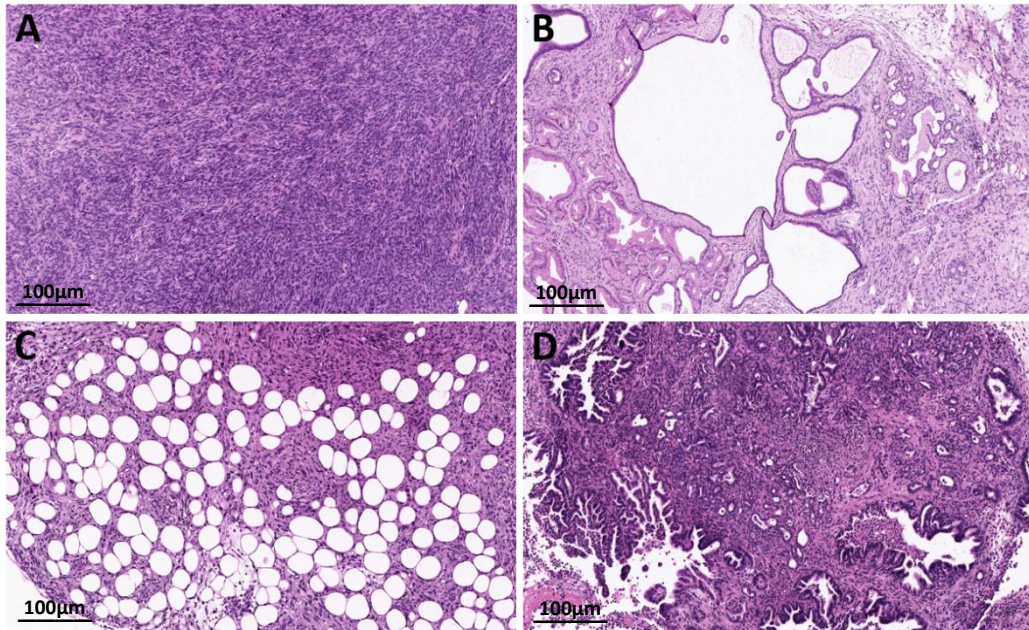
Figure 20. Uncommon histologic variants of pancreatic ductal adenocarcinoma occur infrequently in qKC and KC mice. Representative images of (A) sarcomatoid, (B) serous microcystic adenoma and (C) fatty infiltration in qKC mice. Representative image of (D) pancreatobiliary type IPMN in one KC mouse. Hematoxylin and eosin staining was performed. Scale bars represent 100 μm.

Next, we decided to check whether the absence of PolQ would also have an impact on clinical research. For this purpose, we used The Cancer Genome Atlas (TCGA) database of pancreatic adenocarcinoma patients with low and high expression of polymerase theta carrying KRAS wild-type or oncogenic KRAS to generate a survival curve. According to the mouse survival curve, patients harboring KRAS mutations and low expression of POLQ had a half longer median survival compared to patients with higher expression of POLQ. On the other hand, patients with KRAS wild-type tumor had a longer survival rate compared to the KRAS mutant patients, regardless of the POLQ expression level. Additionally, in the group of wild-type KRAS patients, individuals with lower POLQ expression showed long-term survival (Figure 21). These data clearly show that low expression of polymerase theta correlates with higher rate of survival and supports our data obtained with PDAC mouse model.
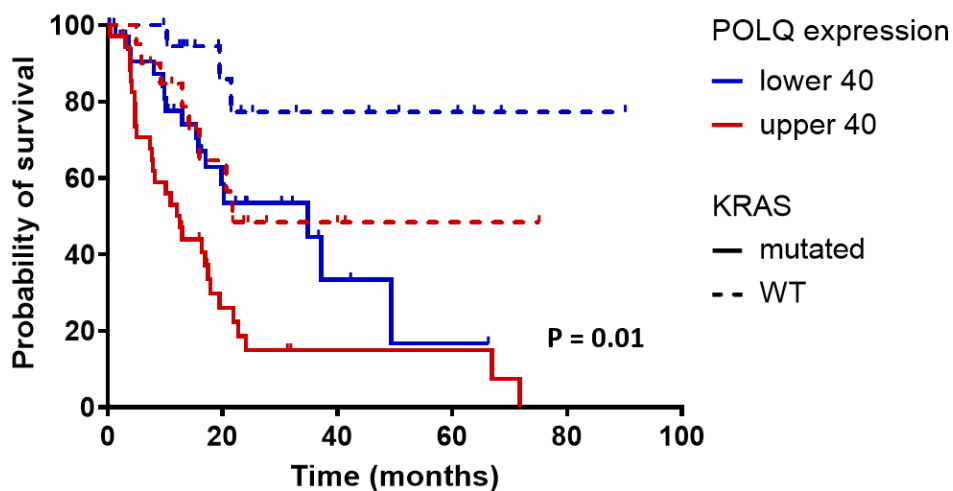
Figure 21. Polymerase theta expression correlates with longer survival in patients harboring KRAS mutations.
Kaplan-Meier survival analysis of TCGA PDA patients with low and high POLQ expression carrying KRAS wild-type or oncogenic KRAS (KRAS wild-type and lower POLQ expression, n=20; KRAS wild-type and higher POLQ expression, n=20; KRAS mutant and lower POLQ expression, n=36; KRAS mutant and higher POLQ expression, n=36; P value is indicated for comparison of patients with KRAS mutant and higher or lower POLQ expression using the Mantel-Cox [log rank] test.

4.2.4 Effect of polymerase theta deficiency on signaling pathways in oncogenic KRAS-driven mouse models

The oncogenic KRAS activates different intracellular pathways such as PI3K, MAPK or RAL-GEF to promote various cellular processes including proliferation, transformation and survival [44, 46]. To explore the effect of Polθ deficiency on cell signaling in murine KRAS models, we used immunohistochemistry for Ki67, Proliferating Cell Nuclear Antigen (PCNA), Cyclin D1, Cyclooxygenase-2 (COX-2) and the Extracellular Signal Regulated Kinases (ERK1/2) which are the major components of the greater MAPK cascade that transduce growth factor signaling in the cell membrane.

Ki67 and PCNA are antigens expressed in perinuclear or internal nuclear regions in all cell cycle phases except G0, making them excellent cellular markers for assessing cell proliferation in various tumors [192-195]. On the other hand, cyclin D1 is a proto-oncogene which acts as cell cycle regulator that controls transition from G1 to S phase in normal tissues. Its accumulation and mutations alter cell cycle progression, leading to increased cell proliferation and resulting in tumorigenesis. In addition, cyclin D1 is also involved in the regulation of cell migration and

invasion [196]. Immunohistochemical analysis showed a small amount of Ki67 and PCNA-labeled proliferative cells in the pancreas of control and qKO mice, while in KC and qKC mice the number of Ki67 and PCNA positive cells was significantly elevated. However, the observed increased Ki67 positivity was more pronounced in 9-month-old KC pancreas compared to qKC pancreas in the same age. In contrast, no expression of cyclin D1 was detected in control and qKO pancreata, but visible nuclear staining was observed in pancreas of KC and qKC mice. Similar to immunohistochemical labeling of Ki67 and PCNA, cyclin D1 expression was higher in the pancreases of KC mice than in qKC mice (Figure 22).

ERK1/2 similarly to cyclin D1 is considered a proto-oncogene that drives tumor cell proliferation, Epithelial-mesenchymal transition (EMT), migration and invasion [197]. Its activation has been reported in several tumors. Despite the established role of ERK in driving cell cycle progression, it is also associated with other cellular events such as senescence, autophagy, and apoptosis [197, 198]. Phosphorylation of ERK1/2 protein (p-ERK) as a mutant KRAS-activated signal is well-detected immunohistochemically. As shown in figure 22, nuclear and cytoplasmic localization of p-ERK was observed in the islets of control, qKO, KC and qKC pancreases. PanIN lesions were strongly stained in all KC and qKC animals. Additionally, expression of p-ERK was noted in stromal cells of younger and older KC and qKC mice. Although a higher level of p-ERK expression was observed in the pancreatic tissue of KC mice compared to qKC, it is not statistically significant. IHC analysis did not show positive staining for this protein in acinar cells of control, qKO, KC and qKC animals.

In the end, we evaluated the impact of PolQ absence on inflammatory response. For this purpose, we used a component of prostaglandin pathway, COX-2 whose synthesis can be upregulated by several cytokines, growth factors, and tumor promoters. In addition to its pro-inflammatory effects, up-regulation of COX-2 has been noted in many types of cancer, indicating its role in carcinogenesis [199, 200]. Immunohistochemical analysis for COX-2 demonstrated elevated expression in the cytoplasm of PanINs in KC and qKC mice, but not in the ductal cells, acini and islets of control and qKO animals. No differences were observed in the expression of this protein in younger animals between KC and qKC. Surprisingly, significantly increased expression levels of COX-2 were observed in the pancreases of 9-month-old qKC mice but not in the pancreases of KC mice (Figure 22).

In conclusion, histochemical analysis for Ki67, PCNA, cyclin D1, p-ERK, and COX-2 revealed increased expression of these proteins in both aged KC and qKC mice. In addition, it was noted that except for PCNA and COX-2, the rest of the analyzed proteins involved in KRAS-activated pathways showed significantly higher expression levels in KC mice compare to qKC mice. These reports demonstrate that theta polymerase deficiency may have an inhibitory effect on pancreatic cancer progression in early stages.
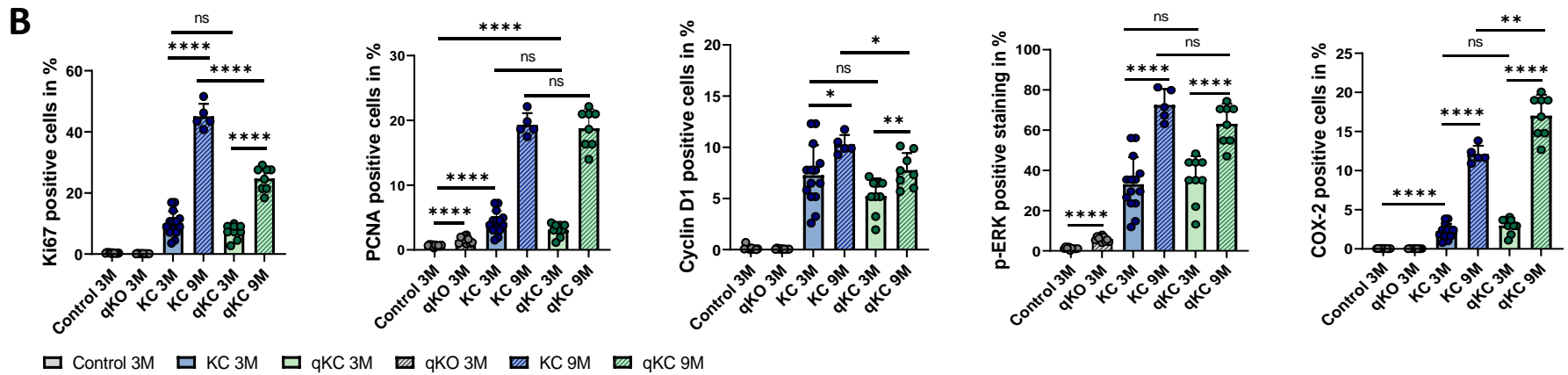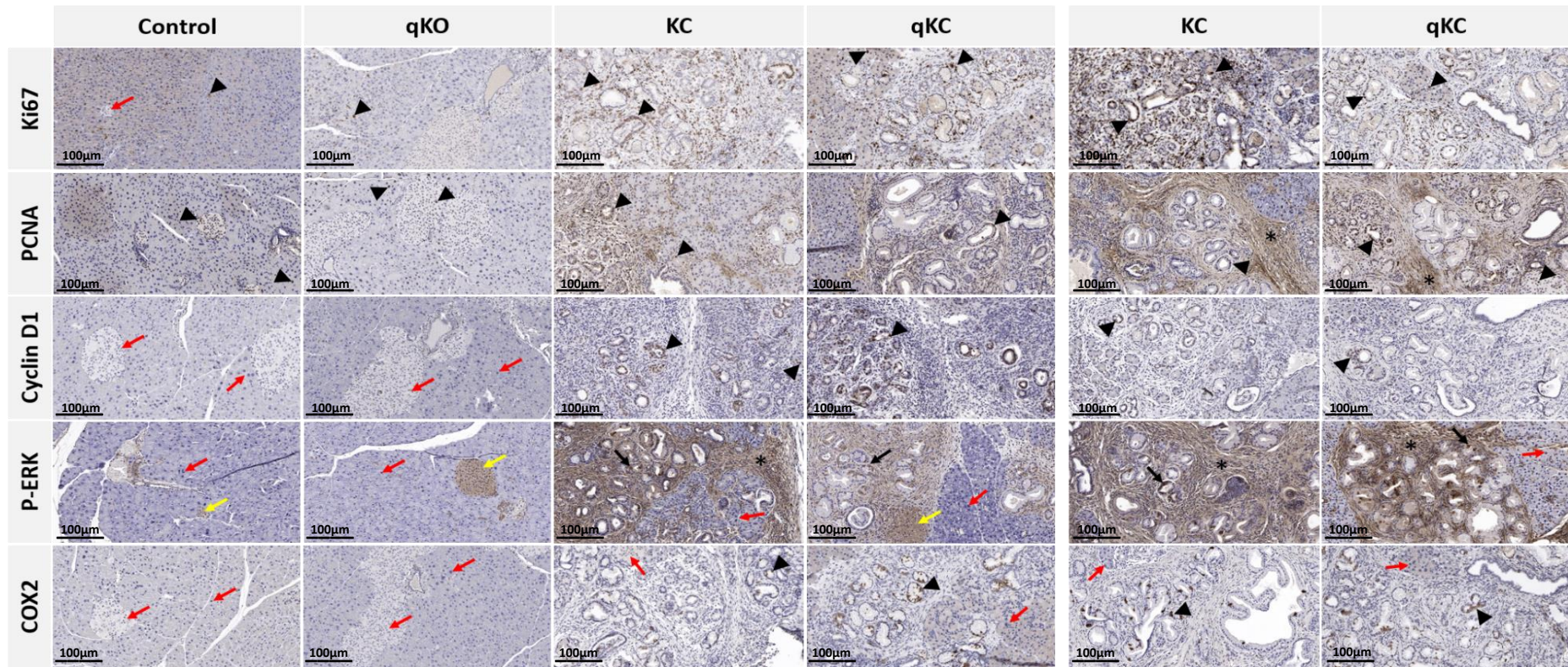
Figure 22. Signaling pathways in KC and qKC mice. (A) Representative immunohistochemical staining images for Ki67, PCNA, cyclinD1, p-ERK and COX-2 in the pancreas of control, qKO, KC and qKC mice at 3 months of age and 9-month-old KC and qKC mice. Strong nuclear staining of Ki67 detected in PanIN lesions of KC and qKC mice and acinar cells of control, qKO, KC and qKC animals (black arrowheads). No Ki67 expression in islets of control mice (red arrow). Positive staining of PCNA in acinar cells, islets, ducts in all experimental animals (black arrowheads). Absence of cyclin D1 immunoreactivity in control and qKO mice (red arrows). Strong nuclear labeling of cyclin D1 in all KC and qKC pancreata (black arrowheads). P-ERK expression visible in islets of control, qKO, KC and qKC animals (yellow arrows). In addition, strong positive staining of p-ERK noted in PanINs (black arrowheads) and stroma of KC and qKC mice (black asterisks). No expression of p-ERK in acinar cells of all experimental animals (red arrows). Cytoplasmic labeling of COX-2 detected only in PanIN lesions occurring in KC and qKC mice (black arrow). Absence of COX-2 immunoreactivity in control and qKO pancreata. Scale bars represent 100 µm. (B) Histological score of Ki67, PCNA, cyclin D1, p-ERK and COX-2 positive cells in pancreas of experimental mice groups (control mice, n=10; qKO mice, n=10; KC mice of age 3 months, n=14, 9 months, n=5; qKC mice of age 3 months, n=9, 9 months, n=8). Error bars represent mean ± SD; Error bars represent mean ± SD; *$P < 0.05$, **$P < 0.01$, ***$P = 0.0001$, ****$P < 0.0001$ (Student's t-test).

4.2.5 Impact of oncogenic KRAS on the expression of the DNA DSBs repair components in a mouse model of pancreatic ductal adenocarcinoma

According to the current understanding, pancreatic cancer develops through the continuous progression of PanIN lesions into neoplastic transformation. Many studies have shown that low-grade PanINs already harbor KRAS mutations in more than 90% of the lesions, which are considered to be site-directed mutations that can cause sequential inactivation of suppressor genes. Consequently, this leads to genomic instability, which is a hallmark of most cancers. Genome instability is also associated with error-prone DNA double-strand break repair. Assuming that expression of alt-EJ components correlates with the activity of the mutagenic pathway, we would expect increased expression of alt-EJ factors in the presence of oncogenic KRAS. For this purpose, we performed immunohistochemical (IHC) analysis for alt-EJ and c-NHEJ core components in KC and qKC mice.

As shown in figure 23, we found strong nuclear expression of Polθ, PARP1 and Mre11, all alt-EJ key factors, in PanIN lesions, acinar cells (acini) and islets of KC pancreata in 3- and 6-months old animals. Ku70, c-NHEJ factor, was also expressed in the same pancreas of KC mice. Interestingly, high expression of PARP1, Mre11 and Ku70 was also noted in 3- and 6-month-old qKC mice, with PARP1 being the highest. Additionally, we observed visible Ku70 immunoreactivity in the cytoplasm of low-grade PanINs in 3-month-old qKC mice. Positive immunohistochemical staining of Ku70 was also seen in islets and acini of control and qKO mice. In contrast, no expression of Polθ and Mre11 was detected in ducts, acinar cells and islets of 3-month-old pancreata of control and qKO animals. Negative staining for PARP1 was

also found in control mice. To our surprise, nuclear expression of PARP1 was noted in islets of qKO mice. Overall, we noticed that the development of PanIN lesions in qKC mice was similar to KC mice, accompanied by nuclear expression of the c-NHEJ and alt-EJ factors except for Polθ, which confirmed the specificity of the antibodies. Our results show that the expression of alt-EJ components correlates with the development of precursor lesions of pancreatic ductal adenocarcinoma in the presence of oncogenic KRAS and functions independently of the c-NHEJ pathway activity.

A

3-month-old mice | 6-month-old mice

Control | qKO | KC | qKC | KC | qKC

Polθ, PARP1, Mre11, Ku70

100μm

B
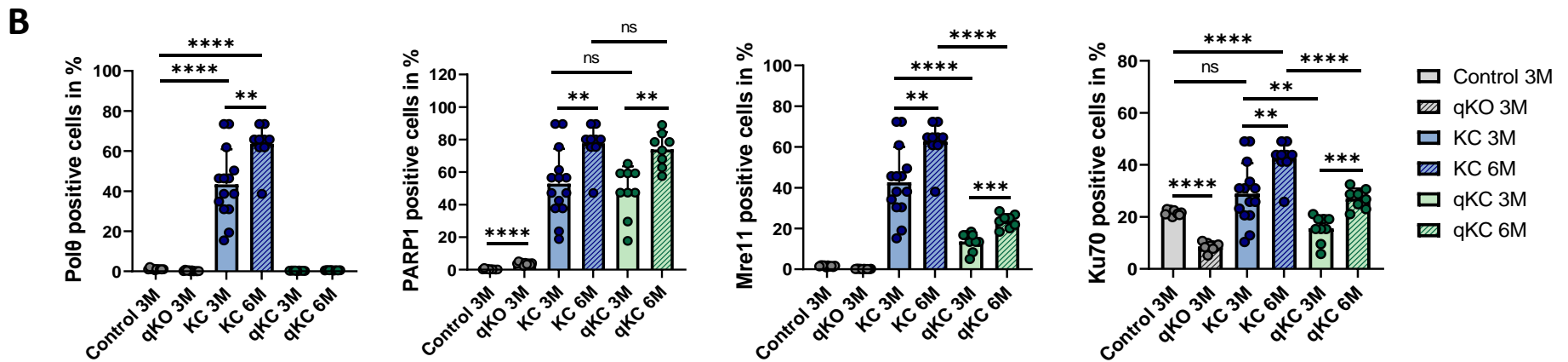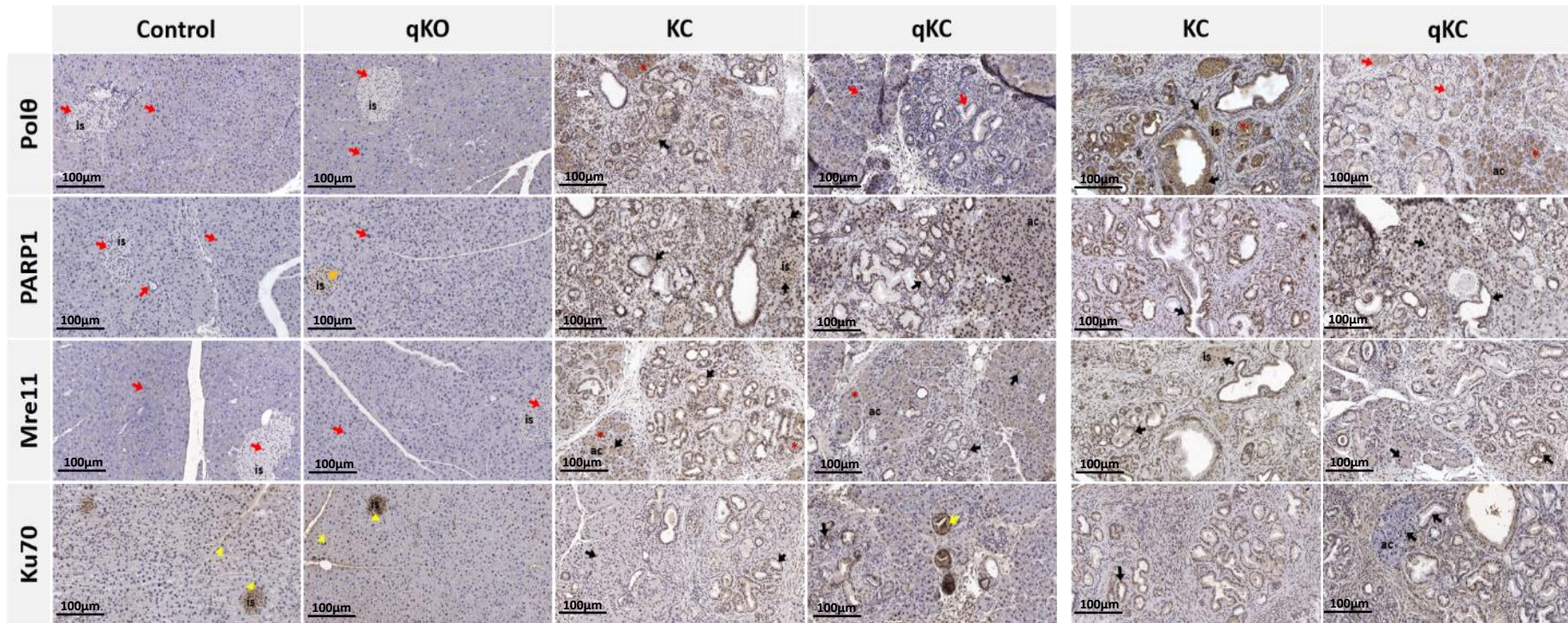
Figure 23. Impact of oncogenic KrasG12D on the expression levels of major alt-EJ and c-NHEJ components in KC and qKC mice. (A) Representative immunohistochemical (IHC) staining images for Polθ, PARP1, Mre11 and Ku70 in the pancreas of control (WT), qKO, KC and qKC mice at 3 months of age and 6-month-old KC and qKC mice. Nuclear expression of PARP1, Mre11 and Ku70 detected in PanINs, acini (ac) and islets (is) in 3- and 6-month-old KC and qKC mice (black arrows). High expression of Ku70 seen in the cytoplasm of low-grade PanINs in 3-month-old qKC mice (yellow arrow). Polθ expression is seen only in 3- and 6-month-old KC mice (black arrows). Absence of PARP1 expression in normal ducts, acini and islets (red arrows) but visible positive staining in islets of qKO mice (orange arrows). Ku70 nuclear and cytoplasmic staining detected in islets and acini of WT and qKO mice (yellow arrowheads). Absence of Polθ and Mre11 immunoreactivity in normal ducts, acini and islets of WT and qKO mice (red arrows). Nonspecific cytoplasmic staining for Polθ and Mre11 noted in KC and qKC mice (red asterisks). Scale bars represent 100 μm. (B) Histological score of Polθ, PARP1, Mre11 and Ku70 positive cells in pancreas of experimental mice groups (control mice, n=10; qKO mice, n=10; KC mice of age 3 months, n=14, 6 months, n=9; qKC mice of age 3 months, n=9, 6 months, n=8). Error bars represent mean ± SD; *$P < 0.05$, **$P < 0.01$, ***$P = 0.0001$, ****$P < 0.0001$ (Student's t-test).

Next, we performed the immunohistochemical staining in normal human pancreas and pancreatic ductal adenocarcinoma (PDAC) to investigate the expression level of above-mentioned alt-EJ and c-NHEJ components. According to the mouse IHC analysis, we observed high expression levels of Polθ, PARP1, Mre11, and Ku70 in human PDAC tissue. In addition, positive IHC staining for Polθ, PARP1 and Mre11 was not detected in ducts, acini and islets of normal pancreas. As expected, visible Ku70 immunoreactivity was found in the same normal pancreatic tissue (Figure 24). These findings clearly indicate pathological relevance of alt-EJ in human pancreatic cancer.
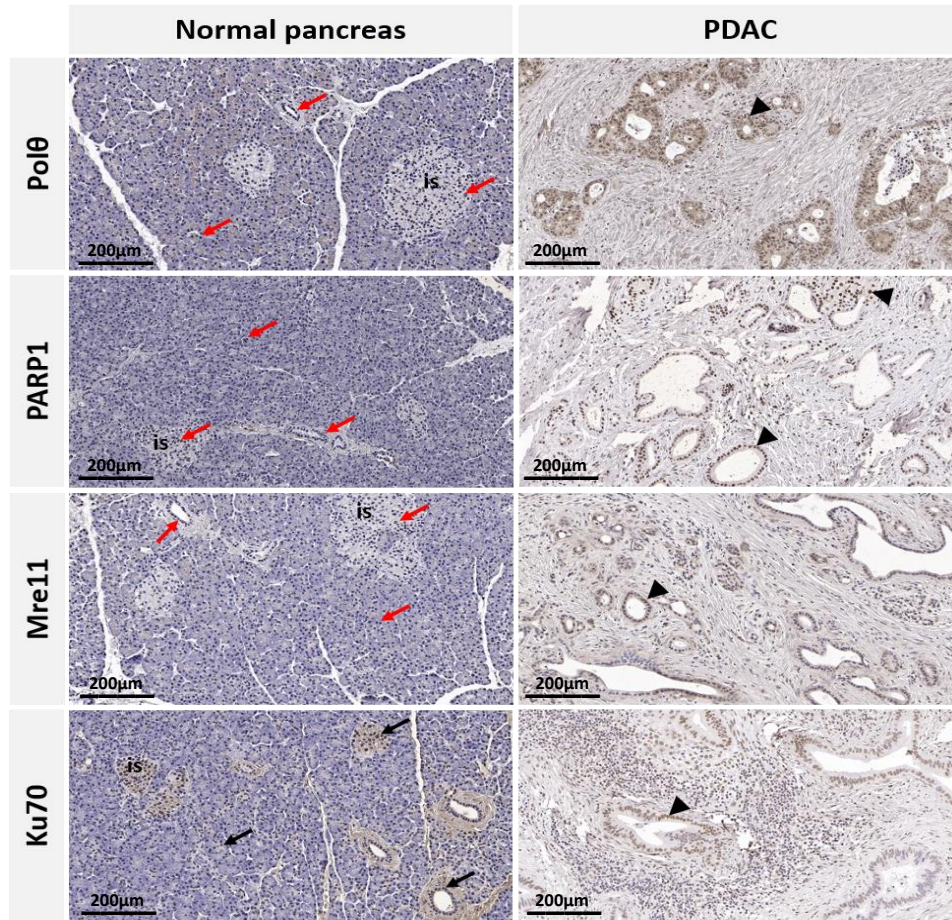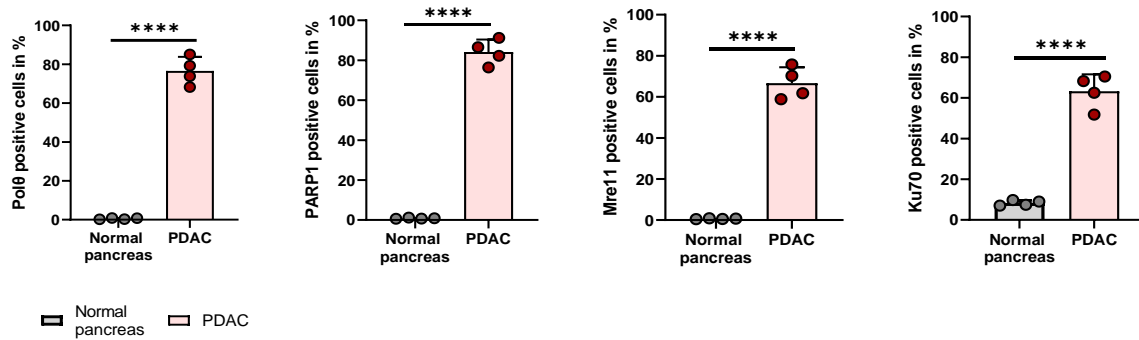
Figure 24. Oncogenic KrasG12D promotes alt-EJ and c-NHEJ activity in human pancreatic ductal adenocarcinoma. (A) Representative immunohistochemical (IHC) images for Polθ, PARP1, Mre11, and Ku70 in normal human pancreas and PDAC. Absence of Polθ, PARP1 and Mre11 immunoreactivity in normal ducts, acini and islets (is) (red arrows). Positive immunohistochemical staining of Ku70 noted in normal ducts, acini and islets (black arrows). High nuclear expression of Polθ, PARP1, Mre11 and Ku70 detected in PDAC (black arrowheads). Scale bars represent 200 μm. (B) Histological score of Polθ, PARP1, Mre11 and Ku70 positive cells in normal pancreas (n=4) and PDAC (n=4). Error bars represent mean ± SD; ****P < 0.0001, (Student's t-test).

5. DISCUSSION

In this study, we aimed to shed some light on the current knowledge of the role of Polθ in pancreatic cancer. For this purpose, the study has been divided into two main parts. In the first part, we evaluated the impact of oncogenic KRAS on the activity of alt-EJ DSB repair pathway in vitro with a panel of murine and human pancreatic cancer cell lines. Afterwards, we determined the effect of KRAS status on the proliferation rate and cell cycle profile of these cells, and finally examined which DNA repair mechanism predominates in analyzed pancreatic cancer cells. In the second part of the thesis, we focused on estimating the effect of alt-EJ inactivation by Polθ deletion on the development of pancreatic intraepithelial neoplasia (PanINs) and their malignant transformation into pancreatic cancer in genetically engineered mouse models (GEMMs). Additionally, going further, we investigated whether the absence of Polθ would affect the activity of the other two DSB DNA repair mechanisms, HR and c-NHEJ in selected transgenic mouse models and in human pancreatic cancer.

5.1 The alt-EJ pathway proteins are upregulated in pancreatic cancer cells expressing oncogenic KRAS G12D

Activating KRAS mutations are among the most common changes in human malignancies. In epithelial tumors, KRAS mutations are already detected in pre-neoplastic lesions, suggesting that oncogenic KRAS is involved in initiating cell transformation. However, additional/sequential genetic events such as the inactivation of tumor suppressor gene pathways are required to ultimately lead to tumorigenesis [201]. Accordingly, oncogenic KRAS alone or together with other genetic events can deregulate double-strand break (DSB) repair and affect DNA repair pathways, causing abnormal repair and accumulation of genomic changes [23, 202]. There are three main DSB repair mechanisms in higher eukaryotes, homologous recombination (HR), canonical non-homologous end joining (c-NHEJ) and alternative end joining (alt-EJ) [88-90]. HR is considered an error-free repair pathway that uses a homologous sister chromatid as a template to faithfully repair the DSB [92, 203]. The other main repair pathway is error-prone C-NHEJ which seals the two broken DNA ends with little or no sequence homology, frequently causing the appearance of small indels or chromosomal translocations [117]. Finally, the alt-EJ is a mutagenic mechanism which uses microhomologies that flanking the DNA ends, always resulting in large deletions and other sequence alterations at the repair junctions [92,95].

Interestingly, studies in several KRAS-mutated leukemic cell lines and in primary T-ALL cells have shown that activation of mutagenic KRAS is associated with increased expression of alt-EJ proteins [204]. Haensel and colleagues observed enhanced expression levels of Lig3, PARP1, and XRCC1. In contrast, Ku70, Ku86, and Lig4, components of the c-NHEJ, were not altered in KRASmut-expressing cells. Increased activity of alt-EJ proteins in DSB repair has been also demonstrated in BCR-ABL– positive chronic myeloid leukemia cells [205]. These findings prompted us to investigate DNA repair pathways in murine and human pancreatic cancer cell lines with the KRAS G12D point mutation, the most common KRAS mutation in PDAC. Performed immunoblot analysis has shown that the expression of oncogenic KRAS is associated with the increased expression levels of Polθ, PARP1, Lig3, and Mre11, key components of the alt-EJ pathway, in both mouse Panc02 and human BxPC3 cell line. In line, protein level expression of c-NHEJ elements (Lig4, Ku80 and Ku70) was not altered in these cell lines. To our surprise, a mouse cell line bearing wild-type KRAS has also showed increased expression of the alt-EJ factors which may indicate species specific properties or increased activity of KRAS wild-type accounted to overexpression. Previous studies have shown the occurrence of KRAS amplification in cancer and that overexpression of wild-type KRAS transformed NIH-3T3 cells, suggesting that wild-type KRAS amplification is an alternative way to activate this oncoprotein in cancer [206]. Notably, recent studies by Wong et al. revealed that wild-type KRAS amplification is associated with enhanced Kras protein expression and poor survival in gastric cancer [207]. Thus, it is very likely that increased amounts of normal proto-oncogene proteins may alter the basic regulatory controls of cell proliferation which is consistent with our results that demonstrated an increased proliferation rate in murine Panc02 cells harboring KRAS wild-type compare to control and KRASmut-expressing cells. On the other hand, we did not observe this effect in human BxPC3 cells which may be species depended. However, for *RAS* genes, low levels of a mutated protein appear to confer more malignant properties than the combined effects of multiple copies of the normal proto-oncogene [206, 208, 209] which may explain why RAS genes are more frequently activated by point mutations than by gene amplification.

In contrast to leukemic cell lines, we did not observe upregulation of core components of the alt-EJ at the transcriptional level. Conducted microarray analysis and qPCR of mouse Panc02 and human BxPC3 PDAC cell lines expressing either exogenous KrasWT or oncogenic KrasG12D did not reveal any alterations in the gene expression of the alt-EJ (Polθ, PARP1, Lig3 and

Mre11) and c-NHEJ (Lig4, Ku80 and Ku70) elements. Although it has been widely assumed that changes in specific mRNA levels are always accompanied by commensurate changes in the encoded proteins and vice versa, there are multiple factors and processes occurring between transcription and translation that provide various different regulatory opportunities [210]. We should also mention the important role of miRNAs and other translation regulators, such as RNA-binding proteins that can regulate protein levels [211, 212]. In addition, comparative studies have shown that correlations between mRNA and protein levels in different model organisms can be relatively weak and uncertain or moderately positive, and that they also could vary between both experiments and organisms [213].

We further investigated DNA repair pathways in a pancreatic ductal adenocarcinoma mouse model, KC and human PDAC. Immunohistological analysis also revealed high expression levels of Polθ, PARP1, and Mre11 as a result of KRAS mutagenic effects, confirming the correlation of alt-EJ components with activating KRAS mutation G12D. Ku70 was also expressed in mouse KC and human PDAC, but to a lesser extent compared with alt-EJ elements. Of note, elevated levels of Ku70 expression were also observed in low- and high-grade human bladder cancer [214]. These findings are consistent with the assumptions that alt-EJ mechanism is highly regulated and functions independently even when c-NHEJ is available [215, 100, 216].

Taken together, our results have shown that expression of oncogenic KRAS contributes to the activation of alt-EJ pathway only at post-transcriptional level in pancreatic cancer cells which points to the need for a broader investigation of the role of factors and processes occurring between transcription and translation in these malignancies.

5.2 Repair of DNA double-strand breaks by alt-EJ pathway in pancreatic cancer cells harboring oncogenic KRAS G12D

DNA double-strand breaks (DSBs) are one of the most harmful and potentially lethal types of DNA damage in cells. Even a single unrepaired or incorrectly repaired DSB can result in various mutations that can lead to genomic instability and tumorigenesis [152]. Accordingly, to ensure genome integrity and cell homeostasis, cells have evolved three major DSB repair pathways mentioned above, HR, c-NHEJ and alt-EJ [88-90].

Choice of DSB repair pathway depends on many regulatory mechanisms such as cell cycle status, post-translational modifications and chromatin effects [217, 218]. However, a key

determinant of the repair mechanism may be the cell-division cycle as DSB repair pathways operate at different phases of the cell cycle and at different rates. For instance, c-NHEJ is active throughout the cell cycle but dominates in G1, whereas HR and alt-EJ operate in S and G2 phases of the cell cycle [88-90].

The fact that KRAS plays an important role in the regulation of cell proliferation and cell cycle, and that KRAS is able to increase the S phase cell population [219], prompted us to formulate hypothesis that oncogenic KRAS can activate the alt-EJ mechanism which is preferred to repair arise DSBs in pancreatic cancer cells. First, the cell cycle analysis in Panc02 and BxPC3 cells revealed an increased number of cells in S/G2-M phase only in murine and human cells expressing oncogenic KrasG12D which may indicate the activity of either of the two DBS repair mechanisms, HR or alt-EJ. The activity of HR and alt-EJ pathway in S and G2 phase is compatible with previous work suggesting that mutagenic alt-EJ pathways may share the resection stage with HR [220]. However, given that alt-EJ is an error-prone mechanism and its presence is often associated with genomic instability characteristic of cancer cells [221, 95, 124], we assumed that alt-EJ may outweigh the other DSB repair mechanism in the presented studies. In support of this, we employed the Traffic Light Reporter (TLR) assay to measure and validate the mutagenic alt-EJ repair activity in murine and human pancreatic cancer cell lines. We found that in both mouse and human cells expressing oncogenic KRAS, alt-EJ was selected as the repair pathway as evidenced by the increased fraction of events accounted for mutagenic alt-EJ pathway. Increased mutNHEJ pathway events was also noted in Kras WT Panc02 cells. These observations are consistent with our results showing increased level of alt-EJ proteins in these cells. On the other hand, several studies have shown that defective DNA repair by HR results in the accumulation of chromatid breaks and cells that cannot repair chromatid breaks by HR become more dependent on other alternative repair pathways [222-224]. As expected high HR capacity was observed in control Panc02 and BxPC3 cells, and BxPC3 expressing KRAS wild-type, which may indicate the absence of pathological changes in these cells through the accurate repair of DSBs using this mechanism, commonly considered to be an error-free pathway when sister chromatid is used as a template [225].

In conclusion, our findings clearly indicate that expression of oncogenic KRAS shifts the balance of DSB repair toward the highly error-prone alt-EJ pathway and highlights the mutagenic properties of alt-EJ making it the preferred DNA repair pathway in pancreatic cancer.

5.3 Depletion of polymerase theta delays pancreatic cancer progression in KrasG12D-driven mouse model

DNA polymerase theta (Polθ) also known as PolQ is a key component of the alt-EJ pathway [167]. Expression of PolQ is generally repressed in normal tissue but is upregulated in several types of cancer [170-172]. In addition, high levels of Polθ is associated with poor prognosis and shorter relapse-free survival of patients with breast and lung cancers [172, 173]. In contrast, molecular studies in mammalian cells demonstrated that knockout of PolQ suppresses alt-EJ pathway [151, 167]. Moreover, research by Shima et al. showed that mice deficient in ATM, a key kinase in DNA damage response, succumb to thymic lymphoma. However, mice deficient in both ATM and PolQ delayed the onset of thymic lymphoma, which significantly extended their lifespan [176]. These reports led us to examine the effect of polymerase theta depletion in a well-established KrasG12D-driven mouse model of pancreatic cancer known as KC. Our study is the first attempt to demonstrate the role of polymerase theta in PDAC progression using Polq knockout in mice with the KC background. We found that loss of Polθ results in slower tumorigenesis and PDAC progression. In line, less PanIN lesions were observed in qKC mice which were especially visible in younger animals. A higher amount of low-grade PanINs were also noted in these mice. Accordingly, performed Alcian blue staining revealed less mucin-rich PanIN lesions in qKC relative to KC mice, confirming delayed cancer progression caused by polymerase theta deletion [188-191]. As expected, the overall survival of qKC mice was significantly increased compared to KC mice, highlighting the critical role of polymerase theta in pancreatic cancer progression. This work is supported by performed survival analysis of TCGA PDAC patients which showed that low POLQ expression correlates with higher survival rates regardless of KRAS status compared to high POLQ expression in PDAC patients. Our findings are in agreement with the study by Shima et al. that demonstrated increased survival of mice deficient for both ATM and polymerase theta in thymic lymphoma [176]. Other studies on PARP inhibitor treatment of patients with metastatic PDAC and BRCA mutation revealed a significant progression-free survival benefit and no progression with platinum-based chemotherapy [226]. To our surprise, more qKC mice developed full-blown pancreatic tumors than KC mice despite extended survival. In addition, qKC animals showed progression to liver and lung metastases, as well as the presence of sarcomatoid which can be found in KPC mice, a more aggressive KrasG12D-driven mouse model of PDAC. Moreover, abdominal distention was observed in two qKC males which is also

common in KPC mice [69]. These findings may suggest that polymerase theta deficiency may on the one hand prolong the survival of experimental animals, but on the other hand lead to the activation of other repair pathway factors or molecular processes, resulting in an even more severe disease course. Intriguingly, studies on PARP1, another a-EJ component, in colorectal cancer have shown that PARP-1 also acts as a double-edged sword that protects against colorectal tumor induction but promotes inflammation-driven tumor progression [227].

5.4 Deficiency of polymerase theta dampens cell proliferation, migration and invasion in KrasG12D-driven mouse model of PDAC

Given the well-known mechanistic role of KRAS in PDAC growth, we decided to explore the proliferation and invasion status under PolQ deficiency. Uncontrolled proliferation is one of characteristic features of neoplasm [228]. One of the indexes of cell proliferation can be Ki67 protein present in all phases, except G0 of the cell cycle and found in multiplying cells, both normal and cancerous [192]. In our study, expression of Ki67 was performed and a statistically significant correlation was proven between this protein expression and mice age. Ki67 expression was observed to be upregulated in older qKC mice that exhibited more low- and high-grade PanINs compared with younger animals. Experimental work from Klein et al. and Zinczuk et al. on human pancreatic tissues showed that enhanced Ki67 expression increases with progressive stage of pancreatic intraepithelial neoplasia, implying intensified proliferation within the pancreatic duct epithelium [229, 195]. Importantly, Ki67 expression was significantly lower in 9-month-old qKC mice compared with KC mice of the same age, suggesting that PolQ deficiency may reduce the proliferation rate in the mouse model of PDAC.

Another protein whose expression is caused by intense cell proliferation is PCNA. Overexpression of PCNA has also been observed in various types of cancer, including pancreatic cancer, and is enhanced during the DNA synthesis phase of the cell cycle. [194]. Clinical research on PCNA expression in pancreatic cancer patients have shown that increased PCNA expression is associated with histological tumor progression [195, 230]. In our studies, immunohistochemical analysis of PCNA performed on PolQ-deficient KC mice showed, similar to the Ki67 protein, an increase in expression with animal age resulting from intense cellular proliferation. However, we did not observe reduced PCNA expression in qKC mice compared

with KC mice, as was seen for Ki67 expression. Because both Ki67 and PCNA are proliferation markers, we expected that PCNA expression in qKC mice would also be lower than in KC mice. In Zinczuk's study [195] describing Ki67 and PCNA expression in pancreatic cancer, direct correlations between these proteins were demonstrated, revealing that an increase in expression of one protein resulted in an increase in expression of the other. In contrast, studies on breast cancer have shown that expression of PCNA poorly correlate with Ki67 expression suggesting that usefulness of PCNA as a marker of proliferative activity, appears to be limited [231, 232]. Moreover, PCNA expression in Polq knock-out mice was also increased compared with control mice indicating that depletion of polymerase theta might already affect molecular processes in the cell cycle.

The negative regulator of the cell cycle for PCNA is cyclin D1, usually located in the cell nucleus, from which it disappears in S phase. The interaction of cyclin D1 with PCNA may prevent the binding of cell proliferation antigen to the replication complex. Overexpression of this protein is common in cancer and can be caused by chromosome translocation [233]. Overexpression of cyclin D1 has been identified in many types of cancer [195, 234, 235]. In our mouse model of PDAC lacking PolQ, we demonstrated that cyclin D1 expression increases with cancer progression characterized by increased presence of high-grade PanINs in older animals. The same trend was observed in KC mice where expression of this protein was significantly higher compared to qKC mice presenting a higher degree of proliferation in this mouse model. Our findings are consistent with observations made in patients with various pancreatic diseases such as ductal adenocarcinoma, cysts, pancreatitis where a progressive increase in cyclin D1 expression was observed in correlation with PanIN staging [195]. On the other hand, Biankin et al. [233] and Al-Aynati et al. [235] found that D1 protein expression did not show correlation with the staging of pancreatic intraepithelial neoplasia suggesting that this protein did not play an important role in precursor lesions in pancreatic cancer. However, cyclin D1 overexpression shortens the transition time from G1 to S phase, promoting cell progression and proliferation, which is one of the features of neoplastic transformation. The fact that cyclin D1 expression is induced by an activated RAS oncogene is evidence supporting the association of this protein with tumorigenesis [236].

Activated oncogenic KRAS is associated with increased phospho-extracellular signal-regulated kinase (ERK) which plays a crucial role in the proliferation, survival and development of tumor

cells [192]. Previous studies have shown that upregulation in phospho-ERK is associated with reduced survival in pancreatic cancer [237]. The present study examined the expression of phosphorylated ERK (p-ERK) as a hallmark of ERK activation in KrasG12D-driven mouse model of PDAC lacking PolQ. Here, we demonstrated that increased expression of p-ERK enhances with age, consistent with PanIN progression in both qKC and KC mice. However, we did not observe the difference in p-ERK expression between qKC and KC mouse model. These results suggest that the absence of PolQ might have no direct effect on the ERK signaling pathway whose activation promotes cancer-stromal interaction in PanIN cells due to oncogenic KRAS. In PDAC progression, interaction between cancer cells and stromal cells is a key regulator of ERK1/2 activation [238]. Moreover, qKO mice also showed slightly higher expression of p-ERK compared with control mice, suggesting that loss of PolQ in these mice may affect the MAPK/ERK pathway. Nevertheless, these mice do not develop cancer and this effect is likely KRAS-independent.

We further investigated whether deficiency of polymerase theta in KrasG12D-driven mouse model of PDAC could affect inflammation. Cyclooxygenase-2 (COX-2) is an important enzyme that synthesize the proinflammatory mediators, prostaglandins which play a key role in the generation of the inflammatory response. Its expression is usually absent in most normal cells and tissues but is highly induced in response to several cytokines, growth factors, and tumor promoters [239]. COX-2 has been shown to be induced and overexpressed in many tumors, including pancreatic cancer, suggesting its role in carcinogenesis [195, 240-246]. In addition, COX-2 as an important antigen that promotes tumor angiogenesis and cell proliferation may affects the prognosis of breast cancer patients [247]. Our study showed positive expression of COX-2 in both qKC and KC pancreas compared to healthy and qKO pancreas. Moreover, COX-2 expression in older animals with an increased number of high-grade PanIN lesions was significantly higher than that in young mice with a predominant number of low-grade PanINs in both qKC and KC. These results are compatible with the Maitra et al. study showing that expression of COX-2 was significantly higher in high-grade PanIN lesions and poorly differentiated adenocarcinomas than in low-grade PanINs and moderately differentiated adenocarcinomas [200]. Overall, COX-2 expression in the pancreas increased with age and progression from normal ducts to low- and high-grade PanINs. In contrast, breast cancer studies did not show a correalation between COX-2 expression and age in cancer patients [232] which may suggest a dependence on cancer model or tissue type. Furthermore, we

observed that COX-2 expression was significantly higher in older qKC mice than in KC mice. Several lines of evidence indicate that COX-2 is not only a critical player in tumor development but also promotes dissemination of cancer cells to other organs [232, 248-251]. Our finding demonstrates that lack of PolQ can increase the expression of COX-2 in a mouse model of PDAC which would explain the presence of an increased number of liver and lung metastases in these mice compared to KC mice.

In conclusion, our results on the effect of the absence of PolQ in PDAC mouse model provide direct evidence that loss of one of the alt-EJ components can delay PanIN lesion development and pancreatic cancer progression. These findings therefore reveal the high potential of polymerase theta as a novel therapeutic candidate for cancer treatment. On the other hand, deficiency of Polθ in KC mice resulted, despite prolonged survival, in the eventual development of full-blown PDAC, metastasize to other organs. This may indicate that the absence of polymerase theta is insufficient to fully inhibit cancer development and combined inhibition of PolQ with another alt-EJ component is probably needed. Hence, we believe that it is necessary to fully understand all alt-EJ factors and their involvement in DSB repair and tumorigenesis.

6. SUMMARY

Pancreatic ductal adenocarcinoma (PDAC), due to its genomic heterogeneity and lack of development of effective therapies, will become the second leading cause of cancer-related death within 10 years. Therefore, identifying novel targets that can predict response to specific treatments is a key goal to personalize pancreatic cancer therapy and improve survival. Given that the occurrence of oncogenic KRAS mutations is a characteristic event in PDAC leading to genome instability, a better understanding of the role of DNA repair mechanisms in this process is desirable. The aim of our study was to investigate the role of the error-prone DNA double strand breaks (DSBs) repair pathway, alt-EJ in the presence of KRAS G12D mutation in pancreatic cancer formation. Our findings showed that oncogenic KRAS contributes to the activation of the alt-EJ mechanism by increasing the expression of Polθ, Lig3 and Mre11, key components of alt-EJ in both mouse and human PDAC models. In addition, we demonstrated that alt-EJ has increased activity in DNA DSBs repair pathway in a mouse and human model of PDAC bearing KRAS G12D mutation. We further focused on estimating the impact of alt-EJ inactivation by polymerase theta (Polθ) deletion on pancreatic cancer development and survival in genetically engineered mouse models (GEMMs). Here, we described that although deficiency of Polθ resulted in delayed cancer progression and prolonged survival of experimental mice, it can lead to full-blown PDAC. Our study showed that disabling one component of the alt-EJ may be insufficient to fully suppress pancreatic cancer progression and a complete understanding of all alt-EJ factors and their involvement in DSB repair and oncogenesis is required.

7. ZUSAMMENFASSUNG

Das duktale Adenokarzinom des Pankreas (PDAC) wird aufgrund seiner genomischen Heterogenität und fehlender Entwicklung effektiver Therapien innerhalb von 10 Jahren zur zweithäufigsten krebsbedingten Todesursache werden. Daher ist die Identifizierung neuer Zielmoleküle, die das Ansprechen auf bestimmte Therapien vorhersagen können, ein wesentliches Ziel, um die Behandlung des Pankreaskarzinoms zu personalisieren und die Überlebenschancen zu verbessern. Da das Auftreten von onkogenen KRAS-Mutationen ein charakteristisches Ereignis beim PDAC ist, welches zu Genominstabilität führt, ist ein besseres Verständnis der Rolle der DNA-Reparaturmechanismen in diesem Prozess wünschenswert. Ziel unserer Studie war es, die Rolle des fehlerbehafteten DNA-Doppelstrangbrüche (DSBs)-Reparaturwegs, alt-EJ, in Gegenwart einer KRAS G12D-Mutation bei der Pankreaskarzinomentstehung zu untersuchen. Unsere Ergebnisse zeigten, dass onkogenes KRAS zur Aktivierung des alt-EJ-Mechanismus beiträgt, indem es die Expression von Polθ, Lig3 und Mre11, Schlüsselkomponenten von alt-EJ, sowohl in murinen als auch humanen PDAC-Modellen erhöht. Zusätzlich haben wir gezeigt, dass alt-EJ eine erhöhte Aktivität im DNA-DSBs-Reparaturweg in einem murinen und humanen PDAC-Modell, welches eine KRAS G12D-Mutation trägt, aufweist. Weiterhin haben wir uns darauf konzentriert, die Auswirkungen einer alt-EJ-Inaktivierung durch Deletion der Polymerase Theta (Polθ) auf die Entwicklung von Pankreaskarzinomen und das Überleben bei genetisch veränderten Mausmodellen (GEMMs) abzuschätzen. Hier haben wir beschrieben, dass ein Fehlen der Polθ zwar das Fortschreiten des Krebses verzögert und das Überleben von Versuchsmäusen verlängert, aber dennoch zu einem voll ausgebildeten PDAC führen kann. Unsere Studie hat gezeigt, dass die Deaktivierung einer Komponente des alt-EJ möglicherweise unzureichend ist, um das Fortschreiten des Pankreaskarzinoms vollständig zu unterdrücken, und dass ein vollständiges Verständnis aller alt-EJ-Faktoren und ihrer Beteiligung an der DSB-Reparatur und Onkogenese erforderlich ist.

8. REFERENCES

1. Rahib, L. et al. Projecting cancer incidence and deaths to 2030: the unexpected burden of thyroid, liver, and pancreas cancers in the United States. Cancer Res. 74, 2913–2921 (2014).

2. Are, C. et al. Predictive global trends in the incidence and mortality of pancreatic cancer based on geographic location, socio- economic status, and demographic shift. J. Surg. Oncol. 114, 736–742 (2016).

3. Bouvier, A.M. et al. Focus on an unusual rise in pancreatic cancer incidence in France. Int. J. Epidemiol 46, 1764–1772 (2017).

4. Ryan, D.P. et al. Pancreatic adenocarcinoma. N. Engl. J. Med. 371, 1039–1049 (2014).

5. Hidalgo, M. et al. Addressing the challenges of pancreatic cancer: future directions for improving outcomes. Pancreatology 15, 8 –18 (2015).

6. Lai, E. et al. New therapeutic targets in pancreatic cancer, Cancer Treatment Reviews (2019).

7. McGuigan, A. et al. Pancreatic cancer: A review of clinical diagnosis, epidemiology, treatment and outcomes. World J Gastroenterol (2018).

8. Ducreux, M. et al. Treatment of advanced pancreatic cancer. Semin. Oncol. 34, 25–30 (2007).

9. Neoptolemos, J.P. et al. Therapeutic developments in pancreatic cancer: current and future perspectives. Nat. Rev. Gastroenterol. Hepatol. 15, 333–348 (2018).

10. Conroy, T. et al. FOLFIRINOX or gemcitabine as adjuvant therapy for pancreatic cancer. N. Engl. J. Med. 379, 2395–2406 (2018).

11. Karanikas, M. et al. Pancreatic Cancer from Molecular Pathways to Treatment Opinion. J Cancer (2016).

12. Pereira, N.P. & Corrêa, J.R. Pancreatic cancer: treatment approaches and trends. Journal of Cancer Metastasis and Treatment. 4(6), 30 (2018).

13. Hezel, A.F. et al. Genetics and biology of pancreatic ductal adenocarcinoma. Genes Dev. 20, 1218–1249 (2006).

14. Tanaka, M. Thirty years of experience with intraductal papillary mucinous neoplasm of the pancreas: from discovery to international consensus. Digestion. 90, 265–272 (2014).

15. Ren, B. et al. Pancreatic Ductal Adenocarcinoma and Its Precursor Lesions. Am. J. Pathol. 189, 9–21 (2019).

16. Hruban, R.H. et al. Pancreatic intraepithelial neoplasia: a new nomenclature and classification system for pancreatic duct lesions. Am J Surg Pathol (2001).

17. Basturk, O. et al. A Revised Classification System and Recommendations From the Baltimore Consensus Meeting for Neoplastic Precursor Lesions in the Pancreas. Am. J. Surg. Pathol. 39, 1730–1741 (2015).

18. Gill, A.J. et al. Tumours of the pancreas. In WHO Classification of Tumours of the Digestive System, 5th ed. World Health Organization: Geneva, Switzerland, 295–340 (2019).

19. Wilentz, R.E. et al. Loss of expression of Dpc4 in pancreatic intraepithelial neoplasia: Evidence that DPC4 inactivation occurs late in neoplastic progression. Cancer Res. 60, 2002–2006 (2000).

20. Sagami, R. et al. Pre-Operative Imaging and Pathological Diagnosis of Localized High-Grade Pancreatic Intra-Epithelial Neoplasia without Invasive Carcinoma. Cancers. 13, 945 (2021).

21. Zhang, Q. et al. Pancreatic Cancer Epidemiology, Detection, and Management. Gastroenterol Res Pract (2016).

22. Jones, S. et al. Core signaling pathways in human pancreatic cancers revealed by global genomic analyses. Science. 321, 1801–1806 (2008).

23. Waddell, N. et al. Whole genomes redefine the mutational landscape of pancreatic cancer. Nature. 518, 495–501 (2015).

24. Maitra, A. & Hruban, R.H. Pancreatic cancer. Annu Rev Pathol. 3, 157-88 (2008).

25. Yachida, S. et al. Distant metastasis occurs late during the genetic evolution of pancreatic cancer. Nature. 28, 467(7319), 1114-1117 (2010).

26. Biankin, A.V. et al. Pancreatic cancer genomes reveal aberrations in axon guidance pathway genes. Nature. 491, 399–405 (2012).

27. Murphy, S.J. et al. Genetic alterations associated with progression from pancreatic intraepithelial neoplasia to invasive pancreatic tumor. Gastroenterology. 145, 1098-1109 (2013).

28. Kanda, M. et al. Presence of somatic mutations in most early-stage pancreatic intraepithelial neoplasia. Gastroenterology. 142(4), 730-733 (2012).

29. Hong, S.M. et al. Telomeres are shortened in acinar-to-ductal metaplasia lesions associated with pancreatic intraepithelial neoplasia but not in isolated acinar-to-ductal metaplasias. Mod Pathol. 24, 256–266 (2011).

30. Van Heek, N.T. et al. Telomere shortening is nearly universal in pancreatic intraepithelial neoplasia. Am J Pathol (2002).

31. Collins, M.A. & Pasca di Magliano, M. Kras as a key oncogene and therapeutic target in pancreatic cancer. Front Physiol. 4, 407 (2014).

32. Matsuda, Y. et al. Gradual Telomere Shortening and Increasing Chromosomal Instability among PanIN Grades and Normal Ductal Epithelia with and without Cancer in the Pancreas. PLoS One. 10(2): e0117575 (2015)

33. Gil, J. & Peters, G. Regulation of the INK4b-ARF-INK4a tumour suppressor locus: all for one or one for all, Nat. Rev. Mol. Cell Biol. 7, 667-677 (2006).

34. Wang, X. et al. P300 plays a role in p16(INK4a) expression and cell cycle arrest. Oncogene. 27, 1894-1904 (2008).

35. Wilentz, R.E. et al. Inactivation of the p16 (INK4A) tumor-suppressor gene in pancreatic duct lesions: loss of intranuclear expression. Cancer Res. 58(20), 4740–4744 (1998).

36. Rosty, C. et al. p16 Inactivation in pancreatic intraepithelial neoplasias (PanINs) arising in patients with chronic pancreatitis. Am J Surg Pathol. 27(12), 1495–1501 (2003).

37. Toufektchan, E. & Toledo, F. The Guardian of the Genome Revisited: p53 Downregulates Genes Required for Telomere Maintenance, DNA Repair, and Centromere Structure. Cancers (Basel). 10(5), 135 (2018).

38. Shioda, T. et al. Transcriptional activating activity of Smad4: roles of SMAD hetero-oligomerization and enhancement by an associating transactivator. Proc. Nat. Acad. Sci. 95, 9785-9790 (1998).

39. Kubiczkova, L. et al. TGF-β – an excellent servant but a bad master. J Transl Med. 10, 183 (2012).

40. Hruban, R.H. et al. Progression model for pancreatic cancer. Clin Cancer Res. 6, 2969-2972 (2000).

41. Maitra, A. et al. Multicomponent analysis of the pancreatic adenocarcinoma progression model using a pancreatic intraepithelial neoplasia tissue microarray. Mod Pathol. 16, 902–912 (2003).

42. Milburn, M.V. et al. Molecular switch for signal transduction: structural differences between active and inactive forms of protooncogenic ras proteins. Science. 247, 939-945 (1990).

43. Vigil, D. et al. Ras superfamily GEFs and GAPs: validated and tractable targets for cancer therapy? Nat. Rev. Cancer. 10, 842–857 (2010).

44. Buscail, L. et al. Role of oncogenic KRAS in the diagnosis, prognosis and treatment of pancreatic cancer. Nat Rev Gastroenterol Hepatol. 17(3), 153-168 (2020).

45. Lu, S. et al. Ras Conformational Ensembles, Allostery, and Signaling. Chem Rev. 116, 6607–6665 (2016).

46. Jonckheere, N. et al. The cornerstone K-RAS mutation in pancreatic adenocarcinoma: from cell signaling network, target genes, biological processes to therapeutic targeting. Crit. Rev. Oncol. Hembuscailatol. 111, 7–19 (2017).

47. Singh, H. et al. Improving Prospects for Targeting RAS. J Clin Oncol. 33(31), 3650-3659 (2015).

48. Liu, P. et al. Targeting the untargetable KRAS in cancer therapy. Acta Pharm Sin B. 9(5), 871-879 (2019).

49. Cox, A.D. et al. Drugging the undruggable RAS: mission possible? Nat Rev Drug Discov. 13(11), 828–851 (2014).

50. Qian, Z.R. et al. Association of alterations in main driver genes with outcomes of patients with resected pancreatic ductal adenocarcinoma. JAMA Oncol. 4:e173420 (2018).

51. Yan, L. et al. Molecular analysis to detect pancreatic ductal adenocarcinoma in high-risk groups. Gastroenterology. 128, 2124–2130 (2005).

52. Lu, X. et al. Detecting K-ras and p53 gene mutation from stool and pancreatic juice for diagnosis of early pancreatic cancer. Chin Med J (Engl). 115, 1632–1636 (2002).

53. Parsons, B.L. & Meng, F. K-RAS mutation in the screening, prognosis and treatment of cancer. Biomark Med. 3, 757–769 (2009).

54. Yakubovskaya, M.S. et al. High frequency of K-ras mutations in normal appearing lung tissues and sputum of patients with lung cancer. Int J Cancer. 63, 810–814 (1995).

55. Bardeesy, N. et al. Smad4 is dispensable for normal pancreas development yet critical in progression and tumor biology of pancreas cancer. Genes Dev. 20(22), 3130–3146 (2006).

56. Guerra, C. et al. Chronic Pancreatitis Is Essential for Induction of Pancreatic Ductal Adenocarcinoma by K-Ras Oncogenes in Adult Mice. Cancer Cell. 11, 291–302 (2007).

57. Daniluk, J. et al. An NF-kappaB pathway-mediated positive feedback loop amplifies Ras activity to pathological levels in mice. J. Clin. Investig. 122, 1519–152 (2012).

58. Zhang, Z. et al. Wildtype kras2 can inhibit lung carcinogenesis in mice. Nat. Genet. 29, 25-33 (2001).

59. To, M.D. et al. A functional switch from lung cancer resistance to susceptibility at the pas1 locus in kras2la2 mice. Nat. Genet. 38, 926–930 (2006).

60. To, M.D. et al. Interactions between wild-type and mutant ras genes in lung and skin carcinogenesis. Oncogene. 32, 4028–4033 (2013).

61. Bentley, C. et al. A requirement for wild-type ras isoforms in mutant kras-driven signalling and transformation. Biochem. J. 452, 313–320 (2013).

62. Westcott, P.M. et al. The mutational landscapes of genetic and chemical models of KRAS-driven lung cancer. Nature. 517, 489–492 (2015).

63. Burgess, M.R. et al. KRAS allelic imbalance enhances fitness and modulates map kinase dependence in cancer. Cebentleyll. 168, 817–829 (2017).

64. Hegi, M.E. et al. Allelotype analysis of mouse long carcinomas reveals frequent allelic losses on chromosome 4 and an association between allelic imbalances on chromosome 6 and K-ras activation. Cancer Research. 54 (23), 6257–6264 (1994).

65. Qiu, W. et al. Disruption of p16 and activation of Kras in pancreas increase ductal adenocarcinoma formation and metastasis in vivo. Oncotarget. 2(11), 862-873 (2011).

66. Herreros-Villanueva, M. et al. Mouse models of pancreatic cancer. World J Gastroenterol. 18, 1286-1294 (2012).

67. Hingorani, S.R. et al. Preinvasive and invasive ductal pancreatic cancer and its early detection in the mouse. Cancer Cell. 4, 437–450 (2003).

68. Kleeff, J. Pancreatic cancer. Nat Rev Dis Primers (2016).

69. Hingorani, S.R. et al. Trp53R172H and KrasG12D cooperate to promote chromosomal instability and widely metastatic pancreatic ductal adenocarcinoma in mice. Cancer Cell. 7(5), 469-83 (2005).

70. Kojima, K. et al. Inactivation of Smad4 accelerates Kras (G12D)-mediated pancreatic neoplasia. Cancer Res. 1, 67(17), 8121-8130 (2007).

71. Mann, K.M. et al. KRAS-related proteins in pancreatic cancer. Pharmacol Ther. 168, 29-42 (2016).

72. Lee, A.Y.L. et al. Cell of origin affects tumour development and phenotype in pancreatic ductal adenocarcinoma. Gut. 68, 487–498 (2019).

73. Pinho, A.V. et al. Chronic pancreatitis: a path to pancreatic cancer. Cancer Lett. 345, 203-209 (2014).

74. Mehrotra, S. & Mittra, I. Origin of Genome Instability and Determinants of Mutational Landscape in Cancer Cells. Genes (Basel). 21, 11(9), 1101 (2020).

75. Ferguson, L.R. et al. Genomic instability in human cancer: Molecular insights and opportunities for therapeutic attack and prevention through diet and nutrition. Semin Cancer Biol. 35, 5-24 (2015).

76. Yao, Y. & Dai, W. Genomic Instability and Cancer. J Carcinog Mutagen. 5:1000165 (2014).

77. Hoeijmakers, J.H. Genome maintenance mechanisms for preventing cancer. Nature. 411(6835), 366-374 (2001).

78. Shrivastav, M. et al. Regulation of DNA Double-Strand 299 Break Repair Pathway Choice. Cell Res. 18, 134–147 (2008).

79. Jackson, S.P. Sensing and repairing DNA double-strand breaks. Carcinogenesis. 23(5), 687-696 (2002).

80. Kinner, A. et al. Gamma-H2AX in Recognition and Signaling of DNA Double-Strand Breaks in the Context of Chromatin. Nucleic Acids Res. 36, 5678–5694 (2008).

81. Vilenchik, M.M. & Knudson, A.G. Endogenous DNA Double-Strand Breaks: Production, Fidelity of Repair, and Induction of Cancer. Proc. Natl. Acad. Sci. U. S. A. 100, 12871-12876 (2003).

82. Lieber, M.R. The Mechanism of Double-Strand DNA Break Repair by the Nonhomologous DNA End-Joining Pathway. Annu. Rev. Biochem. 79, 181– 211 (2010).

83. Saintigny, Y. et al. Characterization of homologous recombination induced by replication inhibition in mammalian cells. EMBO J. 16, 20(14), 3861-3870 (2001).

84. Khanna, K.K. et al. ATM, a central controller of cellular responses to DNA damage. Cell Death Differ. 8(11), 1052-1065 (2001).

85. Fugmann, S.D. et al. The RAG proteins and V(D)J recombination: complexes, ends and transposition. Annu. Rev. Immunol. 18, 495 –527 (2000).

86. Soulas-Sprauel, P. et al. V(D)J and immunoglobulin class switch recombinations: a paradigm to study the regulation of DNA end-joining. Oncogene. 10, 26(56), 7780-7791 (2007).

87. Mehta, A. & Haber, J.E. Sources of DNA double-strand breaks and models of recombinational DNA repair. Cold Spring Harb Perspect Biol. 6(9):a016428 (2014).

88. Chang, H.H.Y. et al. Non-homologous DNA end joining and alternative pathways to double-strand break repair. Nat. Rev. Mol. Cell Biol. 18, 495–506 (2017).

89. Carvajal-Garcia, J. et al. Mechanistic basis for microhomology identification and genome scarring by polymerase theta. Proc Natl Acad Sci U S A (2020).

90. Schrempf, A. et al. Targeting the DNA Repair Enzyme Polymerase θ in Cancer Therapy. Trends Cancer. 7(2), 98-111 (2021).

91. Patterson-Fortin, J. & D'Andrea, A.D. Exploiting the Microhomology-Mediated End-Joining Pathway in Cancer Therapy. Cancer Res. 1, 80(21), 4593-4600 (2020).

92. Brambati, A. et al. DNA polymerase theta (Polθ) - an error-prone polymerase necessary for genome stability. Curr Opin Genet Dev. 60, 119-126 (2020).

93. Heyer, W.D. et al. Regulation of homologous recombination in eukaryotes. Annu. Rev. Genet. 44, 113–139 (2010).

94. Chapman, J.R. et al. Playing the end game: DNA double-strand break repair pathway choice. Mol. Cell. 47, 497–510 (2012).

95. Dueva, R. & Iliakis, G. Alternative pathways of non-homologous end joining (NHEJ) in genomic instability and cancer. Transl Cancer Res. 2(3), 163-177 (2013).

96. Guirouilh-Barbat, J. et al. S-phase progression stimulates both the mutagenic KU-independent pathway and mutagenic processing of KU-dependent intermediates, for nonhomologous end joining. Oncogene. 27, 1726-1736 (2008).

97. Wu, W. et al. Repair of radiation induced DNA double strand breaks by backup NHEJ is enhanced in G2. DNA Repair (Amst). 7, 329-338 (2008).

98. Sallmyr, A. & Tomkinson, A.E. Repair of DNA double-strand breaks by mammalian alternative end-joining pathways. J Biol Chem. 6, 293(27), 10536-10546 (2018).

99. Yanik, M. et al. Development of a Reporter System to Explore MMEJ in the Context of Replacing Large Genomic Fragments. Mol Ther Nucleic Acids. 1, 11, 407-415 (2018).

100. Truong, L.N. et al. Microhomology-mediated end joining and homologous recombination share the initial end resection step to repair DNA double-strand breaks in mammalian cells. Proc Natl Acad Sci U S A. 110, 7720-7725 (2013).

101. Wang, H. & Xu, X. Microhomology-mediated end joining: new players join the team. Cell Biosci. 7, 6 (2017).

102. Wang, H. et al. DNA ligase III as a candidate component of backup pathways of nonhomologous end joining. Cancer Res. 15, 65(10), 4020-4030 (2005).

103. Mladenov, E. & Iliakis, G. Induction and repair of DNA double strand breaks: the increasing spectrum of non-homologous end joining pathways. Mutat Res. 711, 61-72 (2011).

104. Thyme, S.B. & Schier, A.F. Polq-mediated end joining is essential for surviving DNA double-strand breaks during early zebrafish development. Cell Rep. 15, 707-714 (2016).

105. Corneo, B. et al. Rag mutations reveal robust alternative end joining. Nature. 449, 483-486 (2007).

106. Helleday, T. et al. DNA repair pathways as targets for cancer therapy. Nat Rev Cancer. 8(3), 193-204 (2008).

107. Sishc, B.J. & Davis, A.J. The Role of the Core Non-Homologous End Joining Factors in Carcinogenesis and Cancer. Cancers (Basel). 9(7), 81 (2017).

108. Anand, R. et al. Phosphorylated CtIP Functions as a Co-factor of the MRE11-RAD50-NBS1 Endonuclease in DNA End Resection. Mol Cell. 64(5), 940–950 (2016).

109. Blackford, A.N & Jackson, S.P. ATM, ATR, and DNA-PK: The Trinity at the Heart of the DNA Damage Response. Molecular Cell. 801–817 (2017).

110. Hudson, J.J.R. et al. DNA-PKcs-dependent signaling of DNA damage in Dictyostelium discoideum. Curr Biol. 15(20), 1880–1885 (2005)

111. Kirchgessner, C.U. et al. DNA-dependent kinase (p350) as a candidate gene for the murine SCID defect. Science. 267(5201), 1178-1183 (1995).

112. Pitcher, R.S. et al. New insights into NHEJ repair processes in prokaryotes. Cell Cycle. 4(5), 675–678 (2005).

113. Aravind, L. & Koonin, E.V. Prokaryotic homologs of the eukaryotic DNA-end-binding protein Ku, novel domains in the Ku protein and prediction of a prokaryotic double-strand break repair system. Genome Res. 11(8), 1365–1374 (2001).

114. Lee, J.W. et al. Implication of DNA Polymerase λ in Alignment-based Gap Filling for Nonhomologous DNA End Joining in Human Nuclear Extracts. J Biol Chem. 279(1), 805-811 (2004).

115. Mahajan, K.N. et al. Association of DNA polymerase μ (pol μ) with Ku and ligase IV: role for pol mu in end-joining double-strand break repair. Mol Cell Biol. 22(14), 5194-5202 (2002).

116. Lieber, M.R. & Wilson, T.E. SnapShot: Nonhomologous DNA end joining (NHEJ). Cell. 142(3), 496-496 (2010).

117. Moynahan, M.E. & Jasin, M. Mitotic homologous recombination maintains genomic stability and suppresses tumorigenesis. Nat Rev Mol Cell Biol. 11(3), 196-207 (2010).

118. Aguilera, A. & García-Muse, T. Causes of Genome Instability. Annu Rev Genet. 47(1), 1-32 (2013).

119. Bétermier, M. et al. Is non-homologous end-joining really an inherently error-prone process?. PLoS Genet. 10(1) (2014).

120. Fraczek, M.G. et al. History of genome editing in yeast. Yeast. 35(5), 361-368 (2018).

121. Toone, W.M. et al. Getting started: regulating the initiation of DNA replication in yeast. Annu Rev Microbiol. 51, 125–149 (1997).

122. Truong, L.N. et al. Homologous recombination is a primary pathway to repair DNA double-strand breaks generated during DNA replication. J Biol Chem. 289(42), 28910-28923 (2014).

123. Symington, L.S. Mechanism and regulation of DNA end resection in eukaryotes. Crit. Rev. Biochem. Mol. Biol. 51, 195–212 (2016).

124. Ceccaldi, R. et al. Repair Pathway Choices and Consequences at the Double-Strand Break. Trends Cell Biol. 26(1), 52-64 (2016).

125. Paull, T.T. & Gellert, M. The 3' to 5' exonuclease activity of Mre 11 facilitates repair of DNA double-strand breaks. Mol. Cell. 1, 969–979 (1998).

126. Liao, S. et al. Analysis of MRE11's function in the 5"-->3" processing of DNA double-strand breaks. Nucleic Acids Res. 40, 4496–4506 (2012).

127. Shibata, A. et al. DNA double-strand break repair pathway choice is directed by distinct MRE11 nuclease activities. Mol. Cell 53, 7–18 (2014).

128. Limbo, O. et al. Ctp1 is a cell-cycle-regulated protein that functions with Mre11 complex to control double-strand break repair by homologous recombination. Mol. Cell 28, 134-146 (2007).

129. Sartori, A.A. et al. Human CtIP promotes DNA end resection. Nature. 450, 509–514 (2007).

130. Prakash, R. et al. Homologous Recombination and Human Health. Perspect Biol. 1–29 (2015).

131. Chen, C.C. et al. Homology-Directed Repair and the Role of BRCA1, BRCA2, and Related Proteins in Genome Integrity and Cancer. Annu Rev Cancer Biol (2018).

132. Nimonkar, A.V. et al. BLM-DNA2-RPA-MRN and EXO1-BLM-RPA-MRN constitute two DNA end resection machineries for human DNA break repair. Genes Dev. 25, 350–362 (2011).

133. Mimitou, E.P. & Symington, L.S. Sae2, Exo1 and Sgs1 collaborate in DNA double-strand break processing. Nature. 455, 770–774 (2008).

134. Cejka, P. et al. DNA end resection by Dna2-Sgs1-RPA and its stimulation by Top3-Rmi1 and Mre11-Rad50-Xrs2. Nature. 467(7311), 112-116 (2010).

135. Niu, H. et al. Mechanism of the ATP-dependent DNA end-resection machinery from Saccharomyces cerevisiae. Nature. 467, 108–111 (2010).

136. Ferretti, L.P. et al. Controlling DNA-end resection: a new task for CDKs. Front Genet. 4, 99 (2013).

137. Daley, J.M. et al. Enhancement of BLM-DNA2-mediated long-range DNA end resection by CtIP. Cell Rep. 21, 324–332 (2017).

138. Scully, R. et al. DNA double-strand break repair-pathway choice in somatic mammalian cells. Nat Rev Mol Cell Biol. 20(11), 698-714 (2019).

139. Davies, A.A. et al. Role of BRCA2 in control of the RAD51 recombination and DNA repair protein. Mol. Cell. 7, 273–282 (2001).

140. Shivji, M.K.K. et al. A region of human BRCA2 containing multiple BRC repeats promotes RAD51-mediated strand exchange. Nucleic Acids Res. 34, 4000–4011 (2006).

141. Carreira, A. et al. The BRC repeats of BRCA2 modulate the DNA-binding selectivity of RAD51. Cell. 136, 1032–1043 (2009).

142. Wright, W.D. et al. Homologous recombination and the repair of DNA double-strand breaks. J Biol Chem. 293 (2018).

143. Boulton, S.J. & Jackson, S.P. Saccharomyces cerevisiae Ku70 potentiates illegitimate DNA double-strand break repair and serves as a barrier to error-prone DNA repair pathways. EMBO J. 15, 5093-5103 (1996).

144. Aniukwu, J. et al. The pathways and outcomes of mycobacterial NHEJ depend on the structure of the broken DNA ends. Genes Dev. 22, 512-527 (2008).

145. Chayot, R. et al. An end-joining repair mechanism in Escherichia coli. Proc Natl Acad Sci U S A. 107, 2141-2146 (2010).

146. Chan, S.H. et al. Dual roles for DNA polymerase theta in alternative end-joining repair of double-strand breaks in Drosophila. PLoS Genet. 6, 1-16 (2010).

147. Koole, W. et al. A polymerase theta-dependent repair pathway suppresses extensive genomic instability at endogenous G4 DNA sites. Nat Commun. 5, 1-10 (2014).

148. Van Kregten, M. et al. T-DNA integration in plants results from polymerase-u-mediated DNA repair. Nat Plants. 2 (2016).

149. Yan, C.T. et al. IgH class switching and translocations use a robust non-classical end-joining pathway. Nature. 449, 478-482 (2007).

150. Audebert, M. et al. Involvement of poly(ADP-ribose) polymerase-1 and XRCC1/DNA ligase III in an alternative route for DNA double-strand breaks rejoining. The Journal of Biological Chemistry. 279(53), 55117–55126 (2004).

151. Kent, T. et al. Mechanism of microhomology-mediated end-joining promoted by human DNA polymerase theta. Nature Structural & Molecular Biology. 22(3), 230–237 (2015).

152. Han, J. & Huang, J. DNA double-strand break repair pathway choice: the fork in the road. Genome Instab. Dis. 1, 10–19 (2020).

153. Lu, G. et al. Ligase I and Ligase III Mediate the DNA Double-Strand Break Ligation in Alternative End-Joining. Proc. Natl. Acad. Sci. 113, 1256–1260 (2016).

154. Zou, G.M. & Maitra, A. Small-molecule inhibitor of the AP endonuclease 1/REF-1 E3330 inhibits pancreatic cancer cell growth and migration. Mol Cancer Ther. 7, 2012–2021 (2008).

155. Higgins, G.S. & Boulton, S.J. Beyond PARP-POLθ as an anticancer target. Science. 359, 1217-1218 (2018).

156. Wood, R.D. & Doublie, S. DNA polymerase θ (POLQ), double-strand break repair, and cancer. DNA Repair (Amst.) 44, 22–32 (2016).

157. Lange S.S. et al. DNA polymerases and cancer. Nat. Rev. Cancer. 11, 96–110 (2011).

158. de Lima, L.P. et al. Ortholog of the polymerase theta helicase domain modulates DNA replication in Trypanosoma cruzi. Sci Rep. 9, 2888 (2019).

159. Beagan, K. et al. Drosophila DNA polymerase theta utilizes both helicase-like and polymerase domains during microhomology-mediated end joining and interstrand crosslink repair. PLoS Genet, 13 (2017).

160. Mateos-Gomez, P.A. et al. The helicase domain of Polθ counteracts RPA to promote alt-NHEJ. Nat Struct Mol Biol. 23, 1116-1123 (2017).

161. Boyd, J.B. et al. Mus308 mutants of Drosophila exhibit hypersensitivity to DNA cross-linking agents and are defective in a deoxyribonuclease. Genetics. 125(4), 813-819 (1990).

162. Beagan, K. & McVey, M. Linking DNA polymerase theta structure and function in health and disease. Cell Mol Life Sci. 73(3), 603-615 (2016).

163. Mateos-Gomez, P.A. et al. Mammalian polymerase theta promotes alternative NHEJ and suppresses recombination. Nature. 518, 254–257 (2015).

164. Ceccaldi, R. et al. Homologous-recombination-deficient tumours are dependent on Poltheta-mediated repair. Nature. 518, 258–262 (2015).

165. Goff, J.P. et al. Lack of DNA polymerase Q radiosensitizes bone marrow stromal cells in vitro and increases reticulocyte micronuclei after total-body irradiaton. Radiat Res. 172, 165-174 (2009).

166. Yousefzadeh, M.J. et al. Mechanism of suppression of chromosomal instability by DNA polymerase POLQ. PLoS Genet. 10 (2014).

167. Wyatt, D.W. et al. Essential Roles for Polymerase θ-Mediated End Joining in the Repair of Chromosome Breaks. Mol. Cell. 63, 662–673 (2016).

168. Saito, S. et al. Dual loss of human POLQ and LIG4 abolishes random integration. Nat Commun. 8, 16112 (2017).

169. Zelensky, A.N. et al. Inactivation of Polu and C-NHEJ eliminates off-target integration of exogenous DNA. Nat Commun. 8, 1-7 (2017).

170. Kawamura, K. et al. DNA polymerase θ is preferentially expressed in lymphoid tissues and upregulated in human cancers. Int J Cancer. 109(1), 9–16 (2004).

171. Lemée, F. et al. DNA polymerase θ up-regulation is associated with poor survival in breast cancer, perturbs DNA replication, and promotes genetic instability. Proc Natl Acad Sci USA. 107(30), 13390–13395 (2010).

172. Allera-Moreau, C. et al. DNA replication stress response involving PLK1, CDC6, POLQ, RAD51 and CLASPIN upregula-tion prognoses the outcome of early/mid-stage non-small cell lung cancer patients. Oncogenesis. 1, 1–10 (2012) .

173. Higgins, G.S. et al. Overexpression of POLQ confers a poor prognosis in early breast cancer patients. Oncotarget. 1, 175–184 (2010).

174. Nik-Zainal, S. et al. Landscape of somatic mutations in 560 breast cancer whole-genome sequences. Nature. 534, 47–54 (2016).

175. Alexandrov, L.B. et al. Signatures of mutational processes in human cancer. Nature 500, 415–421 (2013).

176. Shima, N. et al. The Mouse Genomic Instability Mutation chaos1 Is an Allele of Polq That Exhibits Genetic Interaction with Atm. Mol. Cell. Biol. 24, 10381–10389 (2004).

177. Helleday, T. The underlying mechanism for the PARP and BRCA synthetic lethality: Clearing up the misunderstandings. Mol Oncol. 5(4), 387–393 (2011).

178. Brown, J.S. et al. Targeting DNA Repair in Cancer: Beyond PARP Inhibitors. Cancer Discov. 7(1), 20–37 (2017).

179. Hoppe, M.M. et al. Biomarkers for Homologous Recombination Deficiency in Cancer. JNCI Natl Cancer Inst. 110(7), 704–713 (2018).

180. Villanueva, M.T. et al. DNA repair: A new tool to target DNA repair. Nat Rev Cancer. 15(3), 136–136 (2015).

181. Kumar, R.J. et al. Hyperactive end joining repair mediates resistance to DNA damaging therapy in p53-deficient cells. BioRxiv 2020.

182. Ozaki, T. & Nakagawara, A. Role of p53 in Cell Death and Human Cancers. Cancers (Basel). 3(1), 994-1013 (2011).

183. Powell, E. et al. Contribution of p53 to metastasis. Cancer Discov. 4(4), 405-414 (2014).

184. Jinesh, G.G., et al. Molecular genetics and cellular events of K-Ras-driven tumorigenesis. Oncogene 37, 839–846 (2018).

185. Evan, G. & Vousden, K. Proliferation, cell cycle and apoptosis in cancer. Nature 411, 342-348 (2001).

186. Feitelson, M.A. et al. Sustained proliferation in cancer: Mechanisms and novel therapeutic targets. Seminars in cancer biology. 35, 25-54 (2015).

187. Certo, M.T. et al. Tracking genome engineering outcome at individual DNA breakpoints. Nat Methods. 8(8), 671-676 (2011).

188. Kopp, J.L. et al. Identification of Sox9-dependent acinar-to-ductal reprogramming as the principal mechanism for initiation of pancreatic ductal adenocarcinoma. Cancer Cell. 22, 737–750 (2012)

189. Krah, N.M. et al. The acinar differentiation determinant PTF1A inhibits initiation of pancreatic ductal adenocarcinoma. Elife. 4:e07125 2015.

190. Lee, A.Y.L. et al. Cell of origin affects tumour development and phenotype in pancreatic ductal adenocarcinoma. Gut (2018)

191. Johnson, B.L. et al. Desmoplasia and oncogene driven acinar-to-ductal metaplasia are concurrent events during acinar cell-derived pancreatic cancer initiation in young adult mice. PLoS One. 14(9):e0221810 (2019)

192. Scholzen, T. & Gerdes, J. The Ki67 protein: from the known and the unknown. J Cell Physiol. 182, 311–322 (2000).

193. Wang, S.C. PCNA: a silent housekeeper or a potential therapeutic target? Trends Pharmacol Sci. 35, 178–186 (2014).

194. Maga, G. & Hubscher, U. Proliferating cell nuclear antigen (PCNA): a dancer with many partners. J Cell Sci. 116, 3051–3060 (2003).

195. Zinczuk, J. et al. Expression of chosen cell cycle and proliferation markers in pancreatic intraepithelial neoplasia. Prz. Gastroenterol. 13(2), 118-126 (2018).

196. Fusté, N.P. et al. Characterization of cytoplasmic cyclin D1 as a marker of invasiveness in cancer. Oncotarget. 7, 26979-26991 (2016).

197. Principe, D. et al. TGFβ engages MEK/ERK to differentially regulate benign and malignant pancreas cell function. Oncogene. 36, 4336–4348 (2017).

198. Cagnol, S. & Chambard, J.C . ERK and cell death: mechanisms of ERK-induced cell death-apoptosis, autophagy and senescence. FEBS J. 277, 2–21 (2010).

199. Dubois, R.N. et al. Cyclooxygenase in biology and disease. FASEB J. 12, 1063–1073 (2010).

200. Maitra, A. et al Cyclooxygenase 2 expression in pancreatic adenocarcinoma and pancreatic intraepithelial neoplasia: an immunohistochemical analysis with automated cellular imaging. Am J Clin Pathol. 118(2), 194-201 (2002).

201. Mueller, S. et al. Evolutionary routes and KRAS dosage define pancreatic cancer phenotypes. Nature 554, 62–68 (2018).

202. Rowley, M. et al. Inactivation of BRCA2 promotes Trp53-associated but inhibits KrasG12D-dependent pancreatic cancer development in mice. Gastroenterology. 140, 1303–1313 (2011).

203. Sebesta, M. & Krejci, L. Mechanism of Homologous Recombination. In: Hanaoka, F. & Sugasawa, K. (eds) DNA Replication, Recombination, and Repair. Springer, Tokyo (2016).

204. Hähnel, P.S. et al. Targeting components of the alternative NHEJ pathway sensitizes KRAS mutant leukemic cells to chemotherapy. Blood. 123(15), 2355-2366 (2014).

205. Sallmyr, A. et al. Up-regulation of WRN and DNA ligase IIIalpha in chronic myeloid leukemia: consequences for the repair of DNA double-strand breaks. Blood. 112(4), 1413-1423 (2008).

206. Pulciani, S. et al. Ras gene amplification and malignant transformation. Mol. Cell. Biol. 5, 2836–2841 (1985).

207. Wong, G.S. et al. Targeting wild-type KRAS-amplified gastroesophageal cancer through combined MEK and SHP2 inhibition. Nat Med. 24, 968–977 (2018).

208. Chang, E.H. et al. Tumorigenic transformation of mammalian cells induced by a normal human gene homologous to the oncogene of Harvey murine sarcoma virus. Nature (London). 297, 479-483 (1982).

209. Spandidos, D.A. & Wilkie, N.M. Malignant transformation of early passage rodent cells by single mutated human oncogene. Nature (London). 310, 469-475 (1984).

210. Taylor, R. et al. Steady State Analysis of Integrated Proteomics and Transcriptomics Data Shows Changes in Translational Efficiency a Dominant Regulatory Mechanism in the Environmental Response of Bacteria, Integrative Biology 5(11), 1393-1406 (2013).

211. Oliveto, S. et al. Role of microRNAs in translation regulation and cancer. World J Biol Chem. 8(1), 45-56 (2017).

212. Harvey R.F. et al. Trans-acting translational regulatory RNA binding proteins. Wiley Interdiscip Rev RNA. 9(3):e1465 (2018).

213. Vogel, C. & Marcotte, E. M. Insights into the regulation of protein abundance from proteomic and transcriptomic analyses. Nat Rev Genet. 13, 227–232 (2012).

214. He, S. et al. Down-regulation of GP130 signaling sensitizes bladder cancer to cisplatin by impairing Ku70 DNA repair signaling and promoting apoptosis. Cell Signal. 81, 109931 (2021).

215. Deriano, L. & Roth, D.B. Modernizing the Nonhomologous End-Joining Repertoire: Alternative and Classical NHEJ Share the Stage. Annu. Rev. Genet. 47, 433–455 (2013).

216. Hanscom, T. & McVey, M. Regulation of Error-Prone DNA Double-Strand Break Repair and Its Impact on Genome Evolution. Cells. 9(7), 1657 (2020).

217. Branzei, D. & Foiani, M. Regulation of DNA repair throughout the cell cycle. Nat Rev Mol Cell Biol. 9, 297–308 (2008).

218. Her, J. & Bunting S.F. How cells ensure correct repair of DNA double-strand breaks. J Biol Chem. 293, 10502-10511 (2018).

219. Agbunag, C. & Bar-Sagi, D. Oncogenic K-ras drives cell cycle progression and phenotypic conversion of primary pancreatic duct epithelial cells. Cancer Res. 64, 5659–5663 (2004).

220. Bennardo, N. et al. Limiting the persistence of a chromosome break diminishes its mutagenic potential. PLoS Genet. 5:e1000683 (2009).

221. Bentley, J. et al. DNA double strand break repair in human bladder cancer is error prone and involves microhomology-associated end-joining. Nucleic Acids Res. 32, 5249-5259 (2004).

222. Andreassen, P.R. et al. DNA damage responses and their many interactions with the replication fork. Carcinogenesis. 27, 883–892 (2006).

223. Sonoda, E. et al. Sister chromatid exchanges are mediated by homologous recombination in vertebrate cells. Molecular and cellular biology. 19, 5166–5169 (1999).

224. Bunting S.F. et al. 53BP1 inhibits homologous recombination in Brca1-deficient cells by blocking resection of DNA breaks. Cell. 141(2), 243-254 (2010).

225. Jimeno, S. et al. Controlling the balance between chromosome break repair pathways. Advances in protein chemistry and structural biology. 115, 95-134 (2019).

226. Golan, T. et al. Maintenance Olaparib for germline BRCA -mutated metastatic pancreatic cancer. N Engl J Med. 381(4), 317–27 (2019).

227. Dorsam, B. et al. PARP-1 protects against colorectal tumor induction, but promotes inflammation-driven colorectal tumor progression. Proc. Natl Acad. Sci. USA. 115, 4061–4070 (2018).

228. King, T.C. Neoplasia. Elsevier's Integrated Pathology. 1(5), 111-143 (2007).

229. Klein, W.M. et al. Direct correlation between proliferative activity and dysplasia in pancreatic intraepithelial neoplasia (PanIN): additional evidence for a recently proposed model of progression. Mod Pathol. 15, 441–447 (2002).

230. Dang, C.X. et al. Clinical significance of expression of p21 and p53 proteins and proliferating cell nuclear antigen in pancreatic cancer. Hepatobiliary Pancreat Dis Int. 1, 302–305 (2002).

231. Sullivan, R.P. et al. Cell proliferation in breast tumours: analysis of histological parameters Ki67 and PCNA expression. Ir J Med Sci. 162(9), 343-347 (1993).

232. Qiu, X. et al. Correlation analysis between expression of PCNA, Ki67 and COX-2 and X-ray features in mammography in breast cancer. Oncology Letters. 14, 2912-2918 (2017).

233. Biankin, A.V. et al. Pancreatic intraepithelial neoplasia in association with intraductal papillary mucinous neoplasms of the pancreas: implications for disease progression and recurrence. Am J Surg Pathol. 28, 1184–1192 (2004).

234. Yang, K. et al. Variations in cyclin D1 levels through the cell cycle determine the proliferative fate of a cell. Cell Div. 1, 32 (2006).

235. Al-Aynati, M.M. et al. Overexpression of G1-S cyclins and cyclin-dependent kinases during multistage human pancreatic duct cell carcinogenesis. Clin Cancer Res. 10, 598-605 (2004).

236. Hitomi, M. & Stacey, D.W. Cyclin D1 production in cycling cells depends on ras in a cell-cycle-specific manner. Curr Biol. 9(19), 1075-1084 (1999).

237. Javle, M.M. et al. Epithelial-mesenchymal transition (EMT) and activated extracellular signal-regulated kinase (p-Erk) in surgically resected pancreatic cancer. Ann Surg Oncol. 14(12), 3527-3533 (2007).

238. Yan, Z. et al. Inhibition of ERK1/2 in cancer-associated pancreatic stellate cells suppresses cancer–stromal interaction and metastasis. J Exp Clin Cancer Res. 38, 221 (2019).

239. Wang, D. & Dubois, R.N. Prostaglandins and cancer. Gut. 55(1), 115-122 (2006).

240. Wolff H. et al. Expression of cyclooxygenase-2 in human lung carcinoma. Cancer Res. 58, 4997-5001 (1998).

241. Morris, C.D. et al. Cyclooxygenase-2 expression in the Barrett's metaplasia-dysplasia adenocarcinoma sequence. Am J Gastroenterol. 96, 990- 996 (2001).

242. Hwang, D. et al. Expression of cyclooxygenase-1 and cyclooxygenase-2 in human breast cancer. J Natl Cancer Inst. 90, 455-460 (1998).

243. Komhoff, M. et al. Enhanced expression of cyclooxygenase-2 in high grade human transitional cell bladder carcinomas. Am J Pathol. 157, 29-35 (2000).

244. Lee, L.M. et al. Expression of cyclooxygenase-2 in prostate adenocarcinoma and benign prostatic hyperplasia. Anticancer Res. 21, 1291-1294 (2001).

245. Colby, J.K. et al. Progressive metaplastic and dysplastic changes in mouse pancreas induced by cyclooxygenase-2 overexpression. Neoplasia. 10, 782-796 (2008).

246. Hill, R. et al. Cell intrinsic role of COX-2 in pancreatic cancer development. Mol Cancer Ther. 11, 2127-2137 (2012).

247. Mansourian, M. et al. Statins use and risk of breast cancer recurrence and death: A systematic review and meta-analysis of observational studies. J Pharm Pharm Sci. 19, 72-81 (2016).

248. Gupta, G.P. et al. Mediators of vascular remodelling co-opted for sequential steps in lung metastasis. Nature. 446, 765-770 (2007).

249. Greenhough, A. et al. The COX-2/PGE2 pathway: key roles in the hallmarks of cancer and adaptation to the tumour microenvironment, Carcinogenesis. 30(3), 377–386 (2009).

250. Yu, J.R. et al. Expression of cyclooxygenase-2 in gastric cancer and its relation to liver metastasis and long-term prognosis. World J. Gastroenterol. 11, 4908–4911 (2005).

251. Ghasemi, M. et al. The role of immunohistochemistry expression of COX-2 in differentiating pigmented benign and malignant skin neoplasms. Medical Journal of the Islamic Republic of Iran. 33, 75 (2019).

Eidesstattliche Erklärung

Hiermit erkläre ich, dass ich die vorliegende Dissertation selbständig verfasst und keine anderen als die angegebenen Hilfsmittel benutzt habe.

Die Dissertation ist bisher keiner anderen Fakultät, keiner anderen wissenschaftlichen Einrichtung vorgelegt worden.

Ich erkläre, dass ich bisher kein Promotionsverfahren erfolglos beendet habe und dass eine Aberkennung eines bereits erworbenen Doktorgrades nicht vorliegt.

Datum   Unterschrift

Curriculum Vitae

Personal information

Surname/First name(s)	**Smolińska Agnieszka Anna**
Family Name	Opasińska
Nationality	Polish
Date of birth	02/07/1989
Gender	Female

Publications

Smolinska A, Singer K, Golchert J, Smyczynska U, Fendler W, Sendler M, van den Brandt J, Singer S, Homuth G, Lerch MM, Moskwa P. DNA Polymerase Theta Plays a Critical Role in Pancreatic Cancer Development and Metastasis. Cancers. 2022; 14(17):4077.

Smolinska A, Swoboda J, Fendler W, Lerch MM, Sendler M, Moskwa P. MiR-502 is the first reported miRNA simultaneously targeting two components of the classical non-homologous end joining (C-NHEJ) in pancreatic cell lines. Heliyon. 2020; 6(1):e03187.

Dziewulska A, Dobosz AM, Dobrzyn A, **Smolinska A**, Kolczynska K, Ntambi JM, et al. SCD1 regulates the AMPK/SIRT1 pathway and histone acetylation through changes in adenine nucleotide metabolism in skeletal muscle. J Cell Physiol. 2020; 235:1129–40.

Smolinska A, Swoboda J, Fendler W, Lerch MM, Sendler M, Moskwa P. MiR-502 is the first reported miRNA targeting simultaneously classical non-homologous end joining (NHEJ) and the cell cycle response. Pancreatology 18(4):119. June 2018. *Conference paper*.

Smolinska A, Swoboda J, Lerch MM, Moskwa P. MiR-502 regulates non-homologous end joining (NHEJ) and reduces radioresistance in human pancreatic cancer cell line. Pancreatology 17(3):24-25. July 2017. *Conference paper*.

Bednarski T, Olichwier A, **Opasinska A**, et al. Stearoyl-CoA desaturase 1 deficiency reduces lipid accumulation in the heart by activating lipolysis independently of peroxisome proliferator-activated receptor α. Biochim Biophys Acta. 2016; 1861(12):2029-2037.

Bednarski T, Pyrkowska A, **Opasińska A**, Dobrzyń P. Regulation of cardiac metabolism and function by lipogenic factors. Postepy Hig Med Dosw (Online). 2016; 70(0):644-653.

Bednarski T, Olichwier A, **Opasinska A**, Dobrzyn P. Hypertension-induced heart steatosis is not associated with increased cardiac lipogenesis. Acta biochimica Polonica 61(1):229. September 2014. *Conference paper*.

Bednarski T, **Opasinska A**, Olichwier A, Dobrzyn P. Role of cardiac lipid metabolism in the development of hypertension – induced heart steatosis. FEBS Journal. 2014; 281(1):597.

Conferences

EPC 2018 - 50th Meeting of European Pancreatic Club in Berlin, Germany – abstract "MiR-502 is the first reported miRNA targeting simultaneously classical non-homologous end joining (NHEJ) and the cell cycle response" (June 2018)

3rd DNA Replication/Repair Structures and Cancer Conference in Cancun, Mexico – abstract "MiR-502 is the first reported miRNA targeting simultaneously classical non-homologous end joining (NHEJ) and the cell cycle response" (February 2018)

EPC 2017 - 49th Meeting of European Pancreatic Club in Budapest, Hungary – abstract "MiR-502 regulates non-homologous end joining (NHEJ) and reduces radioresistance in human pancreatic cancer cell line" (June 2017). *Travel Grant Award*

37th Annual Meeting of the German Pancreatic Club e.V in Greifswald, Germany – abstract "MiR-502 synchronizes cell cycle with DNA repair in pancreatic cell lines" (January 2017)

36th Annual Meeting of the German Pancreatic Club e.V in Freising, Germany – abstract "Mutation of Kras in pancreatic intraepithelial neoplasis (PanINs) activates alternative non-homologous end joining and leads to accumulation of mutation causing malignant transformation" (February 2016)

1st Congress of the Polish Biochemistry, Cell Biology, Biophysics and Bioinformatics "BIO 2014" in Warsaw, Poland – abstract "Hypertension-induced heart steatosis is not associated with increased cardiac lipogenesis" (September 2014)

FEBS EMBO in Paris, France – abstract "Role of cardiac lipid metabolism in the development of hypertension-induced heart steatosis" (August/September 2014)

XLII MSKN in Olsztyn, Poland – abstract „PNA – future of the treatment of bacterial infections". *Best Poster Award: Third Place* (May 2013)
XLII MSKN in Olsztyn, Poland – abstract „The prokaryotic defense system" (May 2013)

II Copernican Symposium of Natural Science Students in Toruń, Poland – abstract "RNA interference as a defense mechanism of cultivated plants against root-knot nematodes" (March 2012)

XLI MSKN in Olsztyn, Poland – abstract "Small cerers and their role in the formation and treatments like cataract surgery" (May 2012)

I MSB "Symbioza" in Warsaw, Poland – abstract "Synthesis of nanoparticles using plant extracts" (May 2012)

Acknowledgement

As we express our gratitude, we must never forget that the highest appreciation is not to utter words, but to live by them.

- John F. Kennedy